Honours thesis

BIOMASS-POWERED ZERO LIQUID DISCHARGE DESALINATION OF BRACKISH WATER

Grant Harper
Bachelor of Environmental Engineering (Honours)
School of Engineering & I.T.
Murdoch University
2018

Declaration

The thesis herein is the student's own account of his research and he acknowledges that it is based on Intellectual Property owned by Enerbi Pty Ltd.

Word count: 17,208

ABSTRACT

Desalination is accepted as being a necessary technology to support the livelihood of communities. However, to prevent the harmful environmental impacts of brine, desalination needs to be designed with zero liquid discharge being the process rather than an afterthought. Existing approaches are often found to be inadequate and significant amounts of research into ways to prevent liquid waste are currently in place. The challenge is that the technology must be able to treat post-RO salinities (usually with high amounts of thermal energy) to be able to overcome the low heat capacities and high boiling points of saline solutions >70,000 mg/L.

This research honours project investigates a proposal developed by Enerbi Pty Ltd that incorporates heat, mechanical and electrical energy into a desalination unit that is powered by Biomass and produces a Zero Liquid Discharge product. The system was modeled in Excel and ChemCad and found to successfully produce a dry product with moderate quantities of biomass. The proposal was then modelled to treat 60ML per year under various scenarios using two particular types of Biomass, Plantation Waste, and Oil Mallee crops. These scenarios included high-value agricultural and horticultural crop scenarios using desalinated water for irrigation and salinity, with salinity problems on site being amended via saline water uptake and intervention crop planting.

The design was carried further to a Pilot Plant configuration specified using 'off the shelf' products, and the Pilot Plant design included upgrading the power configuration to allow for additional equipment. The Pilot Plant configuration was tested up to salinities of 85,000mg/L. It was found to successfully cope with this salinity, the most likely upper limit due to heat requirements of evaporation of hyper-saline solutions. A final concept 3D model was created to assist with placement and configuration.

Table of Contents

TABLE OF FIGURES

TABLE OF TABLES

TABLE OF ABBREVIATIONS

Abbreviation	Description
BWRO	Brackish Water Reverse Osmosis
CHP	Combined Heat & Power
CSG	Coal Seam Gas
ED	Electrodialysis
EDR	Electrodialysis Reversal
ERD	Energy Recovery Device
FO	Forward Osmosis
HDH	Humidification/Dehumidification
H/X	Heat Exchanger
ISD	In Situ Desalination
kPa	Kilopascals
kW	KiloWatt
kWh	KiloWatt Hour
LPM	Litres Per Minute
LNG	Liquid Natural Gas
MBR	Membrane Bioreactor
MD	Membrane Distillation
MED	Multi Effect Distillation
MENA	Middle East & North Africa
MJ	MegaJoule
ML	MegaLitre
MSF	Multiple Stage Flash
MVC	Mechanical Vapour Compression
nm	Nanometer
pH	Acidity
PWT	Phoenix Water Technology
RO	Reverse Osmosis
SEC	Specific Energy Consumption
SSH	Selective Solids Harvesting
SWRO	Seawater Reverse Osmosis
TDS	Total Disolved Solids
TVC	Thermal Vapour Compression
WA	Western Australia
WAIV	Wind-Aided Intensified Evaporation
ZLD	Zero Liquid (Waste) Discharge

ACKNOWLEDGEMENT

This research was done at the request and under the guidance of Enerbi Pty Ltd as an Industry Project and sincere thanks to Dr Karne De Boer for providing me with the main concept as well as the information needed to create this report. Enerbi Pty Ltd remains the owner of the Intellectual Property in this report.

Chapter 1 Introduction

The provision of fresh water via desalination is increasingly becoming attractive for inland communities given the maturity of desalination technology. This allows for easily available, well-tested products with the knowledge-base of expertise, especially in Reverse Osmosis. The problem is the liquid brine waste product. Along the coastline, with Seawater Reverse Osmosis (SWRO) this waste product is effectively dumped back in the ocean. With inland desalination using brackish water, this opportunity does not exist. The liquid waste products that are highly saline will do a lot of damage if they are mobilised into water tables or waterways. Transporting the waste product is expensive, large evaporation ponds can cost up to 50% of the capital cost of the project and if they fail there are expensive consequences. Desalination projects often fail to be 'green-lighted' if there are no waste treatment options available. So more and more desalination systems are being designed to be Zero Liquid Waste Discharge (ZLD), which creates a dry inert waste product which can be disposed of safely & cheaply.

HYPOTHESIS

It is possible to design a brackish water desalination system for remote inland areas powered by biomass, that has a ~85% recovery rate and no liquid discharge.

AIM

The aim of this thesis is to examine the Zero Liquid Waste Discharge desalination plant concept provided by Enerbi Pty Ltd to see if it is viable alternative to existing brackish water desalination plants.

OBJECTIVES

- Literature review to ascertain the issues surrounding the availability and adoption of zero liquid waste discharge desalination technology.
- Examine the existing zero liquid discharge technology available for adoption.
- Model the zero liquid discharge concept provided by Enerbi Pty Ltd.
- Apply the zero liquid discharge concept provided by Enerbi Pty Ltd to 'real world' scenarios at 60ML production levels.
- Design the Pilot Plant of the zero liquid discharge concept provided by Enerbi Pty Ltd so that it generates power solely from biomass input.
- Examine future options for the proposed technology, in particular scenarios where there is no cost for fuel.

LITERATURE REVIEW

Brackish groundwater is the water located under the Earth's surface that is characterized by a higher salinity than that of fresh groundwater (Mike Mickley 2001). As a resource for fresh water, desalination of brackish water has some significant differences to seawater desalination. Water quality of brackish water tends to be quite variable in composition and concentration (see Figure 1). This variability in composition impacts the process of desalination in that pretreatment needs to be tailored to the type. Ionic components such as calcium, magnesium, carbonate, sulphate, phosphate, and silicate, and components such as soluble silica if not treated, can limit water recovery in membrane desalination (Sanciolo et al. 2014).

Brackish Water is water having a concentration of Total Dissolved Solids (TDS) between 1000-15,000 mg/L (El-Manharawy and Hafez 2001), however, further classification by Watson, Morin, and Henthorne (2003) is shown in Table 1 on the next page. The benchmark level used in this report based on field data from Wagin groundwater sampling is 11,000 mg/L TDS.

Typical TDS Levels of Different Water Sources	
Type	TDS (mg/L)
Drinking water	≤500
Fresh water	<1000
Mildly brackish water	1000–5000
Moderately brackish water	5000–15,000
Heavily brackish water	15,000–35,000
Seawater	≥35,000

Table 1: Typical TDS levels of Different Water Sources
Watson, Morin, and Henthorne (2003*)*

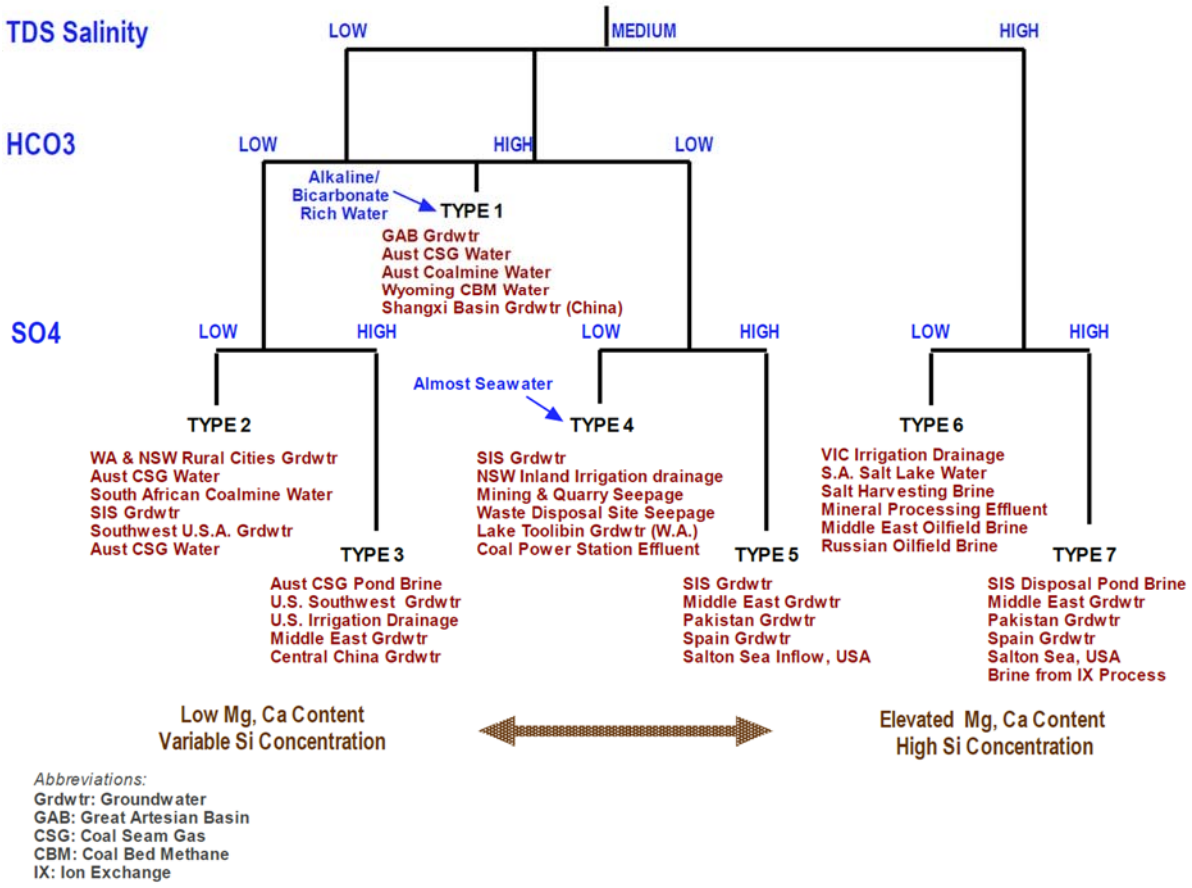

Figure 1: Classification of saline waters into water types according to molar ratios of Cl/HCO3 and Cl/2SO4 (Geo-Processors Pty Ltd 2008)

The need for brackish water desalination Australia-wide has been most pertinent around remote towns especially mining towns, as well as island communities and tourist resorts. Volume reduction of wastewater in mining operations has also been a significant brackish water desalination industry. An example is coal seam gas (CSG) and the associated liquid natural gas (LNG) industries in inland Queensland (Arakel and Mickley 2011). Brackish Water Reverse Osmosis has increasingly become a necessity as a way to control urban salinity due to a history of dewatering. Salt intrusion to inland waterways (e.g. Murray River) or as a way to protect coastal fresh groundwater resources from sea-water intrusion where seawater desalination was not economical (Geo-Processors Pty Ltd 2008).

Current State of Desalination Overview

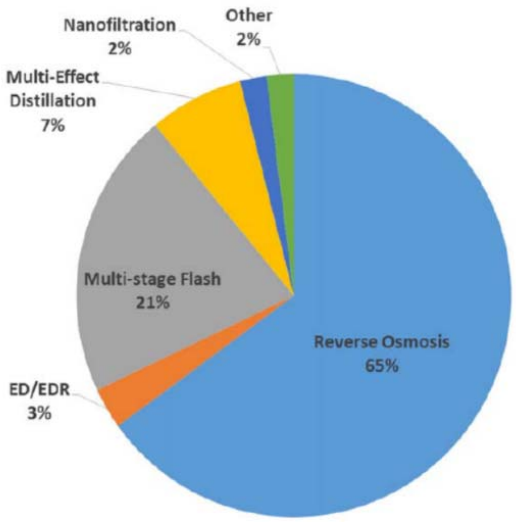

Figure 2: Desalination Technologies 2017 (Cohen, Semiat, and Rahardianto 2017)

Desalination currently produces 1% of the world's drinking water. In 2015 there were 18,426 plants with a total capacity of 86.5 million m^3/day (VirgiliPankratz and Gasson 2016).

Reverse Osmosis is known as the 'workhorse' of desalination. It is presently the fastest growing desalination technique (Amy et al. 2017) as well as the most well represented. Multiple-stage flash (MSF) is very well represented as it is the principal production technique in the Middle East (Semiat 2008). Thermal desalination like MSF is higher in energy consumption however it tolerates higher salinities and produces higher quality water (Fritzmann et al. 2007). Examining Figure 2, ED/EDR in refers to electrodialysis & electrodialysis reversal; Other 2% refers to technology including vapour compression, forward osmosis and membrane distillation (Cohen, Semiat, and Rahardianto 2017).

This report refers to large-scale and small-scale desalination plants, especially in reference to the types of technology they employ. Whilst some cross-over does exist (i.e. small-scale plants can be permanent), the delineation essentially means:

1. Large-scale or municipal scale provision of drinking/household water.
   Almost always Sea Water Reverse Osmosis (SWRO) systems like many of the large coastal desalination plants around the world. The one major difference is the prevalence of MED and MSF plants in the Middle East. Regardless of the technology, their primary purpose is to provide water security in the case of drought.
2. Small-scale plants, also known as desalination package plants or modular desalination plants usually need to provide a more environmentally sensitive and cost-effective way to create fresh water for temporary locations, remote coastal settlements and also process water for industry (e.g. mine sites). The demand is usually smaller and thus the units are often transportable and modular and almost all brackish water desalination plants fit this category (Veolia Water Technologies 2017).

Desalination brine management

While there are many factors that determine whether a desalination plant goes ahead, a major hurdle that often is the make-or-break factor (especially in brackish water desalination) is what waste disposal options are available. Brine management is inherently site-specific given the salinity and composition of the feedwater as well as the disposal options available.

Environmental Impact

The potential for coastal disposal of brine does not necessarily guarantee a viable brine disposal option. The environmental impact of concentrate discharge into marine environments is a key issue for coastal desalination plants (Clark et al. 2018). Social concerns can also have an impact, with community backlash about brine dumping preventing the go-ahead of many desalination plants (e.g. Denmark, W.A.).

Characteristics of brine that may have environmental impacts apart from salinity include temperature, pH, discharge flow rate & volume, dissolved oxygen, chemicals added pre, during and post Reverse Osmosis (including but not limited to anti-scalants, coagulants, biocides, cleaning chemicals), heavy metals and nutrients which can accumulate in sediments around outfalls (Clark et al. 2018; RPS Environment and Planning 2009). Nutrient levels limit the potential for freshwater disposal due to the impact on algal populations & subsequent deoxygenation. Salinity in itself has detrimental impacts on many plants & animals, and changes in salinity can impact on nutrient spiralling/recycling and energy flows (Khan et al. 2009).

Terrestrial disposal has many of the issues that marine disposal does due to water movement into waterways and groundwater tables. Additionally, salinity impacts on soil structure and productivity. The most common form of site treatment of brine is evaporation ponds. There is much experience & know-how of this approach in Australia. This method is used for salinity control in the Murray-Darling Basin by pumping saline water into some 180 evaporation ponds, thus lowering the saline groundwater table (Khan et al. 2009).

Evaporation ponds are relatively cheap to construct and often only require a pump for operation. They require large areas of land if evaporation rates are not very high, can leak, need to be cleaned out without being damaged and can be impacted by wind if they are large. This can lead to structural damage of levees (Khan et al. 2009). Other types of disposal such as sewer disposal and deep well injection are equally problematic and are therefore rarely permitted by environmental authorities.

Zero Liquid Discharge

Zero liquid discharge is defined as ‘no liquid discharge beyond the plant boundary’. Initially, this was to prevent power plants disposing of their waste into US rivers (Mike Mickley 2010). The technology used was either thermal crystallizers, evaporators or spray dryers depending on the volume or evaporation ponds if space was available but within the plant boundary. This

is still the case with large-scale desalination operations. There are actually very few of these plants with a ZLD status that don't use either crystallizers, evaporators or evaporation ponds of some kind.

Economics is another driving force increasing the demand for ZLD. The cost of using evaporators or crystallizers for volume reduction is usually too expensive for fresh water production for small-scale plants as the capital and operating costs often exceeding the cost of the desalting facility (Martinetti, Childress, and Cath 2009). The trend is thus to concentrate salinity to as close as possible to the technical limit and then evaporate the remaining slurry as cheaply and as safely as possible so that a dry product results. This can then be sold if valuable or disposed of in landfill (Arakel and Mickley 2s011; Khan et al. 2009).

Enerbi Zero Liquid Discharge Concept

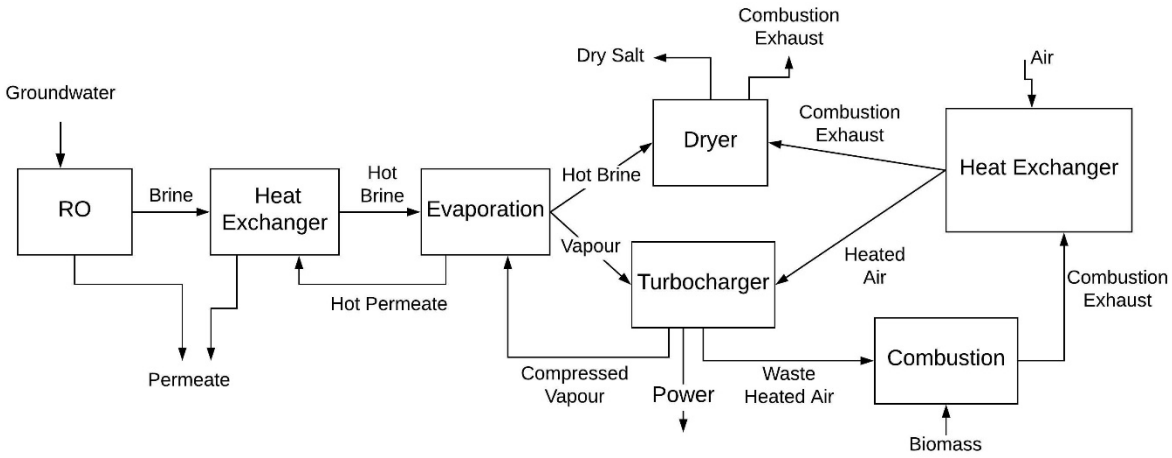

Figure 3: Enerbi Zero Liquid Discharge Concept

The concept proposed by Enerbi Pty Ltd is a Reverse Osmosis System followed by a Mechanical Vapour Compression (MVC) evaporation process followed by a final spray drying process to achieve ZLD. The system runs from the energy derived from a combined heat & power (CHP) system:

- Power is generated from heat generated from biomass combustion using a turbocharger which generates mechanical shaft power to run the MVC. This turbocharger also generates power for the various pumps required for the Reverse Osmosis system as well as other process control components.
- Heat is used directly to evaporate brine in the spray dryer. Heat is recovered where possible in two different heat exchangers, thereby reducing the overall energy consumption of the system.
- The waste heat from the turbines is recycled (shown as waste heated air). This reduces the amount of biomass consumption.

Enerbi Concept Component Overview

Reverse Osmosis

This technology is readily used as it is well-established and easily modular and scalable. It is constructed using long 200nm-thick semi-permeable polymer sheets, separated by spacers and spirally wound about a tube (Gray et al. 2011). They are extremely permeable for water and much less so for dissolved substances, preventing their movement across the membrane. Pressure is used to push water through the polymer membrane. For brackish water RO pressure ranges normally from 145 to 218 psi (Rao et al. 2016) although this can be as high as 600 for some waters (Li 2012). By comparison, SWRO pressures get up to 1200 psi. The global minimum for RO without an Energy Recovery Device (ERD) & assuming constant pump efficiency is at a recovery of 50% (Cohen, Semiat, and Rahardianto 2017). As a rule, plants are designed to be operated near their thermodynamic limit (i.e. the applied pressure is slightly above the concentrate osmotic pressure). This reduces the specific energy consumption (Song et al. 2003), thus reducing cost.

The energy cost for Brackish Water Reverse Osmosis (BWRO) is lower than seawater, becoming increasingly more expensive the more saline or contaminated the water. It is generally in the range of 20 -30% of the total cost (Gray et al. 2011; Semiat and Hasson 2010), as opposed to 38% for a large SWRO plant (Gray et al. 2011; Rao et al. 2016). For inland developments the cost of pumping coastal desalinated water can become prohibitive, making BWRO attractive. However, this needs to be balanced against the cost of brine management, which can be as much as 0.4-1.78 $US/m^3 (Cohen, Semiat, and Rahardianto 2017). This is often being 50% of the total cost (McCool et al. 2013). Pre-treatment is usually also a requirement, involving the removal of particulate matter and addition of chemicals to prevent scaling and fouling (Fritzmann et al. 2007). The most commonly used technology used is Membrane Bioreactor technology (MBR) (Joo and Tansel 2015).

Pre-treatment is a condition of all desalination systems due to scaling as the precipitation of sulphates and carbonates at high temperatures limits upper brine temperatures in distillation systems (Joo and Tansel 2015). The issue of fouling is considerable given the levels of contaminants commonly found in brackish water. These contaminants can quickly compromise the efficacy of a system once concentrated at higher levels; this is more so with Reverse Osmosis if they are put through a two-stage system. Limestone, organics, colloidal species (silt, clay etc.) and microorganisms must be removed from the feed usually in mechanical pre-filtration and chemical dosing (Ning and Troyer 2009).

Mechanical Vapor Compression

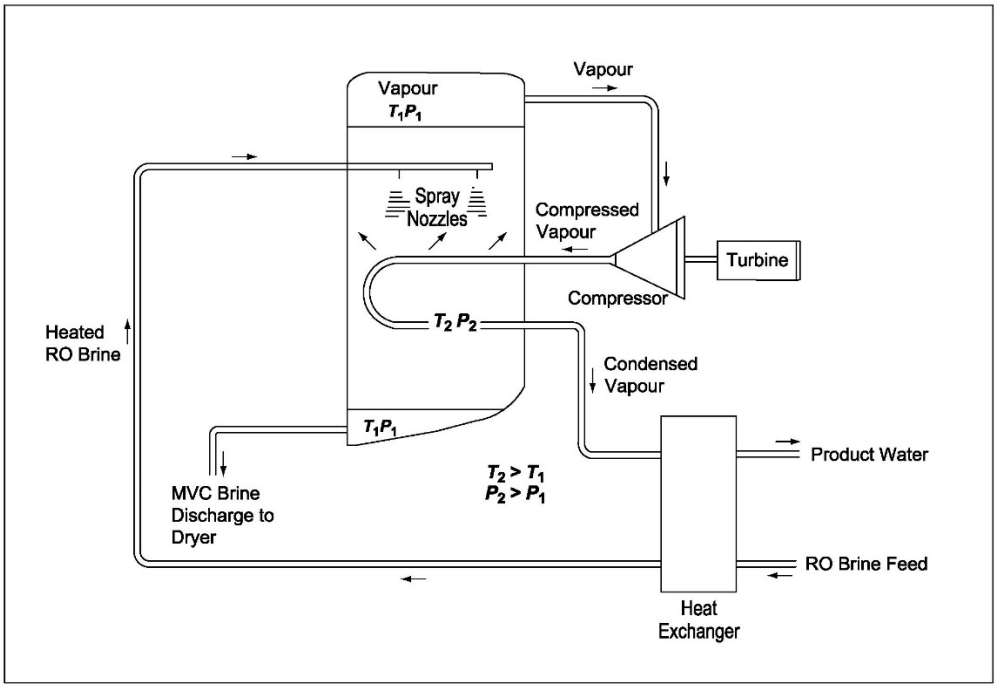

Figure 4: Mechanical Vapour Compression Concept
Derived from Al-Karaghouli and Kazmerski (2013)

Distillation systems use energy to heat saline water, turning it into vapour, which is then condensed and turned into fresh water. To do this in an economical fashion these systems are designed to operate by reducing the vapour pressure of water within the unit to permit boiling to occur at lower temperatures. Preferably without the use of additional heat (Da Franca and

Dos Anjos 1998). Likewise, these systems are usually designed to interchange the heat of condensation and heat of vaporization to reduce costs.

Mechanical vapour compression is the simplest and cheapest option of the distillation types as the heat for vaporization to the feedwater is provided mechanically and the distillation product provides the heat for evaporation. The feedwater is typically preheated by heat exchangers utilizing the heat from the distillate product water as well as (typically) the brine discharge. It is preheated as close to boiling point as possible. In Figure 4 this mixing is shown with the recirculating brine and this is done to increase the distillation volume if required.

This brine is sprayed inside the evaporation chamber via spray nozzles onto the pipes containing the compressed vapour as shown. The spray forms a falling film over multiple tube rows. Many tubes are needed to meet the surface area requirement that is calculated from the various thermodynamic inputs. Formation of the thin film enhances the heat transfer rate and makes the evaporation process more efficient.

Water vapour is drawn from the evaporation chamber and compressed by a vapour compressor. This increases its pressure and temperature and then is sent back into the same chamber. The feedwater gets condensed on the inside of the tube(s) as shown in Figure 4, and the heat of enthalpy provides the heat that evaporates the feedwater water.

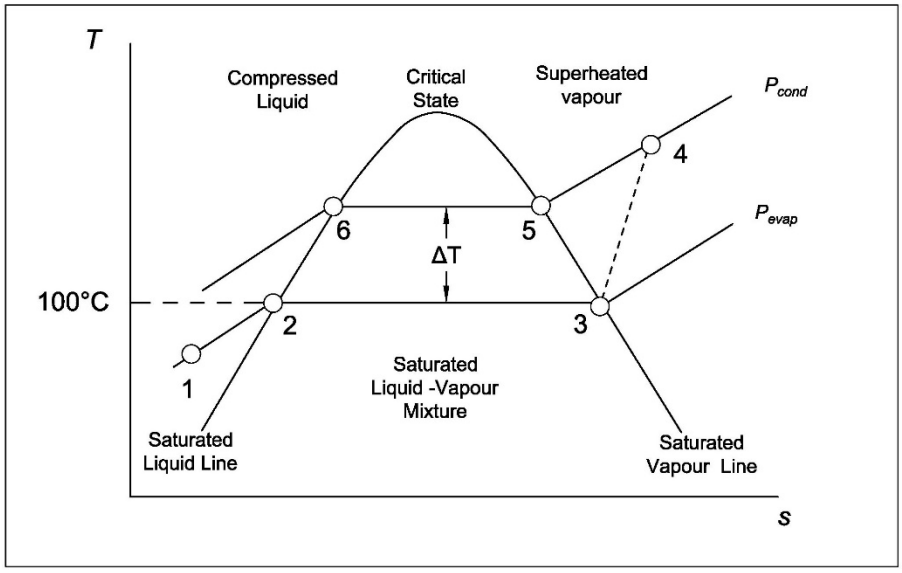

Figure 5: Temperature - Entropy Diagram for MVC (Aquaback Pty Ltd 2018)

Using the temperature-entropy diagram (Figure 5) the incoming feedwater (state 1) is heated in a heat exchanger to near boiling point (state 2). The product to be concentrated is partially evaporated (state 2 transition to state 3). The compressor extracts the vapour created, compresses it from state 3 to state 4, as increasing the pressure of the saturated vapour increases the temperature at which the steam condenses. Its boiling point is shown as the dotted line between the constant pressure lines ($P_{evap} \rightarrow P_{cond}$). This increases the enthalpy of the vapor, and this enthalpy is used as the heat source for evaporation at state 2. This occurs as the vapor is sent back through the evaporator (state 5) and it condenses back into a liquid (state 6).

A valid alternative is Thermal Vapour Compression (TVC). Generally, MVC has higher levels of output and it has a simpler more robust design. TVC requires low-temperature steam for the thermal compressor as well as electricity to drive the pumps, and thus has a higher power consumption ~16 kWh/m^3 compared to 7–12 kWh/m^3 for MVC (Al-Karaghouli and Kazmerski 2013)

While it consumes more energy than RO, MVC doesn't need membrane replacement and offers a better product, tolerating much higher salinities (García-Rodríguez 2003). These units are usually built with capacities of less than 100 m^3/day and are often used at resorts and industrial sites (Da Franca and Dos Anjos 1998) as well as oil field brines, power plant Flue Gas Desulphurisation (FGD) wastewater, and RO system reject (Mishra 2018). They are considered highly reliable and hold a clear advantage when dealing with harsh feeds and remote locations (Jamil and Zubair 2017).

Specific Energy Consumption

The energy per volume of desalted water product becomes problematic to ascertain due to differences in source water salinity, plant size, pump, and other system components efficiencies, product water recovery (i.e. product volume/feed volume), and heat quality (for thermal desalination processes). In some cases the inclusion of intake and discharge pumping energy must be taken into account (Cohen, Semiat, and Rahardianto 2017). General SEC values are shown in Table 2 below:

Desal Tech	Electrical SEC	Thermal SEC	Total SEC
RO	0.3-3	-	0.3-3
ED	7-15	-	7-15
MED	4–20.2	1.5–2.5	5.5–22.7
MVC	7–12	-	7–12

Table 2: Reported SEC (kWh/m^3) for Brackish Water >15,000 mg/L TDS

(Brandhuber et al. 2014; Cohen, Semiat, and Rahardianto 2017; Gray et al. 2011; Mickley 2007; Rao et al. 2016; Semiat 2000; Semiat 2008; Zhu, Christofides, and Cohen 2009).

The energy requirements for brackish water desalination (BWRO) are lower than seawater reverse osmosis (SWRO), accounting for 11% of total costs, compared to 44% for SWRO desalination (Foundation 2010). BRWO via EDR (Electrodialysis reversible) of brackish water is comparable to RO depending on the initial salinity of the feedwater (Miller, Shemer, and Semiat 2014). Heat and osmotically driven desalination (e.g. Forward-osmosis) appear to be only really cost-effective if a low-cost source of heat is available (e.g. waste heat from a power plant) (Semiat 2000; Semiat, Sapoznik, and Hasson 2010).

BRINE MANAGEMENT

Spray dryer technology is used to achieve the final dry product; the other main option is thermal crystallizer. The energy to use either dryers or crystallizers is high, ~17 kWh per litre of feedwater for crystallizers. They are generally only more cost-effective than spray dryers for feedwater streams above 40 LPM (Michael Mickley 2008). The specific energy consumption for spray drying (assuming an RO-MVC system where brine is created at 100°C) assuming 10L/hr flow rate of brine the energy for drying is 6.39 kWh. This assumes a 24hr process which equates to ~150 kWh per day.

POWER GENERATION

Comprehensive power modelling is outside the scope of this paper, however it is necessary to discuss biomass as an energy source as it plays a major role in the implementation of the design, especially siting considerations. Biomass is generally not considered an option in the renewable desalination literature because the logic is that where there is biomass production there is available fresh water. However, the system being specified in this paper is to be operated to address soil salinity rather than aridity, so it is not necessarily the case that biomass will not be available (it also means that the water only needs to be desalinated rather than rendered potable). It turns out that in the south west of WA there are two broad groups of

biomass feedstock potential around lands affected by salinity: agricultural waste and forestry waste (Dunin 2002).

Energy and material flows	LPG	Woodchips	Wheat straw
Thermal power	5.00MW$_{th}$	5.00MW$_{th}$	5.00MW$_{th}$
Thermal efficiency	0.8	0.8	0.8
Heating value	26MJ/L	14MJ/kg	13MJ/kg
Flow rate	865L/h	1 607kg/h	1 731kg/h
Operating costs			
Operating time	10h/d	10h/d	10h/d
Unit fuel cost	$0.80/L	$0.09/kg	$0.095/kg
Unit energy cost	$0.111/kWh	$0.023/kWh	$0.026/kWh
Consumption	8 654L/d	16 071kg/d	17 308kg/d
Daily cost	$6 923	$1 446	$1 644
Annual cost	$1 661 538	$347 143	$394 615
Additional operating costs	$0	$100000	$100000
Total annual operating cost	$1 661 538	$447 143	$494 615
Annual savings	$0	$1 214 396	$1 166 923

Table 3: Economic comparison of three systems for delivering process heat in Regional Western Australia (Brooksbank et al. 2014)

The other parameter to be taken into account is that the potential for reducing soil salinity comes about not just through the removal of groundwater that has accumulated in discharge areas. It also needs recharge control, something to use the water at or near where it infiltrates the soil and enters groundwater systems (John Bartle et al. 2002). It is widely accepted that perennial tree crops or revegetation are the way to achieve this. So the system being specified treats the soil for salinity (discharge control) by removing excess water, desalinating it and irrigating with it thereby making it suitable for tree planting (recharge control). The irrigation system is then used to grow these trees, which in turn can then be used as a biomass stock for energy production (John Bartle et al. 2002), most likely through sustainable harvesting like coppicing (Bartle et al. 2002; Turner and Ward 2002).

Another argument for this position is the cost (and environmental benefit) of having a fuel source on-site as opposed to having a fuel driven to the site for use. Woodchips also have a slight advantage over wheat straw as shown in Table 3, the main agricultural waste product available in the south west of WA, both in terms of heating value (MJ/kg), cost of supply of fuel (prior to the fuel crop being grown) and operating cost (Brooksbank et al. 2014).

TURBOCHARGERS

A key component of this design is turbochargers which are being used to generate all of the mechanical and electrical power. These systems are usually used to capture the waste heat from Internal Combustion Engines, especially long-haul trucks. Waste exhaust is converted to mechanical or electrical energy either by connecting a turbine in the exhaust stream to a crankshaft to provide mechanical power or this crankshaft is connected to a generator which provides electrical energy (Briggs 2012). Commercial turbochargers do exist within desalination plants, typically these are Energy Recovery Devices (ERD) used to recover the pressure from the brine stream in Seawater Reverse Osmosis plants, reducing the cost of power inputs required to get the high pressures needed to operate.

In contrast BWRO plants tend to operate at smaller scales and lower pressures and thus tend not to employ ERD technology (Martin and Eisberg 2007). Additionally, BWRO plants often operate using variable frequency drives to compensate for variations in concentrate pressure and flow, which is a concern for turbochargers as they have bell-shaped efficiency curves and lower peak efficiencies compared to other types of ERD (Martin and Eisberg 2007). A design consideration to take into account when using turbochargers is that for optimum performance the flows on the turbine and compressor sides of the turbocharger must be matched. In Reverse Osmosis systems the flow rates of the Permeate and Retentate streams can vary significantly and thus reduce efficiency (Martin and Eisberg 2007).

The use of turbochargers in the system proposed in this paper avoids the issues associated with optimum performance of turbochargers as the rates of flow proposed are not variable, or are variable within a narrow a range as feasible.

SYSTEM CONFIGURATION ASSESSMENT

The aim of this section is to give a disinterested appraisal of the Enerbi concept. Given the low feed rate (100L/hr or 0.1m^3/hr) Reverse Osmosis is justified because of its low power consumption. In addition, it's established position in the marketplace makes construction, operation and maintenance streamlined & practical. A two-pass RO system to get the level of salt removal required to make ZLD economical is expensive. It also requires a higher level of management expertise to avoid fouling and the pretreatment necessary to remove potential scalants to enable a two-stage RO treatment is considerable. This is especially true in high-hardness waters where softening is necessary, as lime softening requires large amounts of chemicals and produce large amounts of solids (Michael Mickley 2008).

The practical solution becomes a hybrid system, with the second component being able to manage high TDS of the RO brine product for which distillation systems are best. The cheapest distillation options are MED and MVC, the smallest power consumer of these being MVC. These systems are the most economical for low volume systems and by using this option the potential for renewable power is also greatly increased. MVC is also the simplest and best suited for remote systems that could be turned on and left to run. Another significant reason to use MVC is that after RO, MVC has the highest second law efficiency (Swaminathan, Nayar, and Lienhard V 2016). The result is a system that runs on a low power configuration that also needs no thermal inputs, as RO runs off of electricity and MVC runs off electrical or shaft power.

The combined SEC for this type of system as shown in Table 2 would be 7.3 – 15 kWh/m^3 for Brackish Water >15,000 mg/L TDS. Assuming the system desalination system in this report was to run 24 hours a day, this would be the equivalent of 2.4m^3 desalinated. Total SEC would be in the range of 17.5 – 36 kWh/Day. Added to this is the energy demand for spray drying and averaging and the SEC demand is ~180 kWh.

Chapter 2: Current ZLD technology

The system proposed in this report is only viable if it offers a better outcome than the current zero-liquid discharge desalination systems available. The proposed system works as a CHP system maximizing brine concentration as efficiently as possible and then uses available waste heat to treat the last ~10% to achieve ZLD.

An important part of evaluating the existing technology is that it needs to be cost effective and it needs to be able to be scaled up to large production in the context of brackish water desalination. The example in this report is 60ML per year. Desalination technology of a similar nature that are commercially available include the following.

PWT

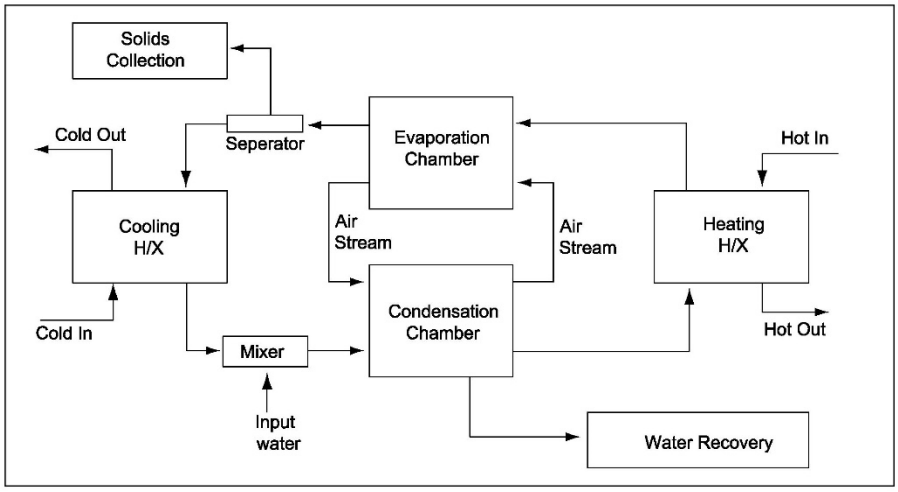

Figure 6: Single Stage PWT Model
Derived from Connell, Wakim, and Wakim (2011)

PWT is Phoenix Water Technology, a process designed by Phoenix Water, the simple version shows contaminated water (shown in blue in Figure 6) flowing in a continuous loop through a heating heat exchanger (heating H/X) to a humidification chamber. From this the flow is separated then cooled in a heat-exchanger (Cooling H-X). The cool product is combined with the input water in a mixer and then piped to a water recovery chamber and back to the heating heat exchanger. (Connell, Wakim, and Wakim 2011). Solids are gradually collected as they precipitate out, and the resulting slurry contains only enough water to allow the movement of

the salt precipitate. This slurry is treated and dried in an evaporative process, which is driven by low temperatures and can thus be operated using solar or waste heat.

The efficiency of this system becomes reduced when multiple passes are required in order to achieve high recovery rates, by comparison with MVC working on single pass process. Limited information was available on this process, however like other Humidification/Dehumidification HDH processes, energy consumption would be high ~200 kWh/m^3 without an ERD (Xu et al. 2013).

Membrane Distillation (MD)

Membrane Distillation is a hybrid separation process that involves phase-change thermal distillation and microporous hydrophobic membrane separation (Duong et al. 2015). Figure 7 illustrates the process of hot brine traversing a hydrophobic membrane which allows for the transport of water vapour but prevents the movement of brine. The temperature difference between the hot and cold faces causes a vapour pressure gradient. The vapour formed then accumulates on the face that is cooled, creating clean distillate.

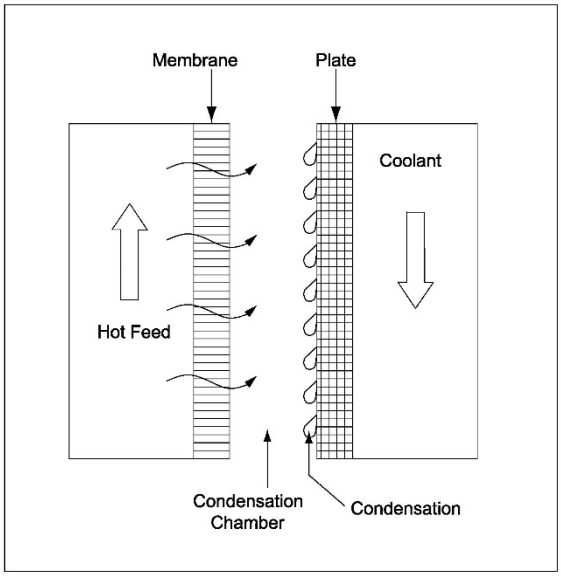

Figure 7: Air gap configured membrane distillation Derived from Ghalavand, Hatamipour, and Rahimi (2015)

The advantages of this system include it has a low power consumption - specific heat consumption below 60kWh/m^3 is technically feasible; operating temps between 50-90°C; no pressure is necessary; limited issues with scaling due to flow movement & membrane design; manages high salinities well, produces a very clean product, can handle low and normal desalination capacities and has multiple design configurations (Zhani et al. 2016). The efficiency of this system becomes reduced when multiple passes are required to achieve high

recovery rates, by comparison with MVC working on single pass process. In fact, conventional MD is thermodynamically limited to less than 5% per pass (Foster, Burgoyne, and Vahdati 2001). Whilst this technology is seen as the 'next big thing", it is currently still effectively at research stage (Zaragoza 2018).

Dew-vaporation

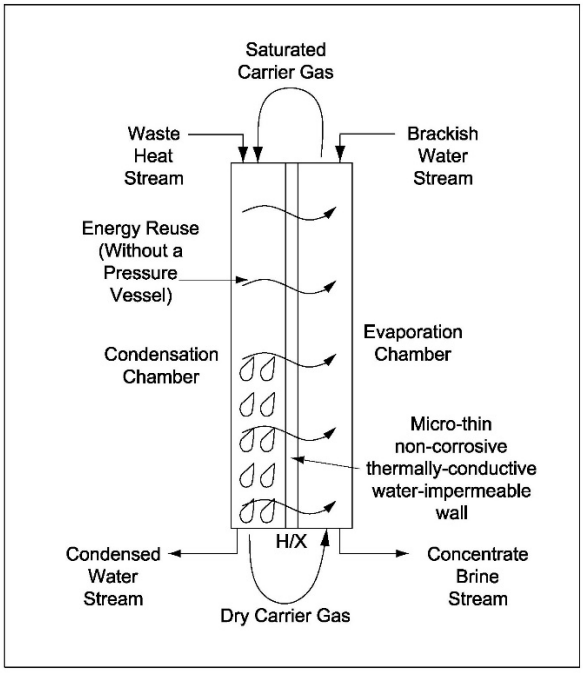

Figure 8: Schematic diagram of AltelaRain process
Derived from Igunnu and Chen (2014)

Dew-vaporation is a humidification-dehumidification (HDH) process. It is marketed as AltelaRain℠ and it is a process that evaporates brine concentrate using heated air. This evaporation provides heat causing fresh water to condense on the face of a heat transfer wall shown in Figure 8. Some benefits include that the process operates at atmospheric pressure and low temperatures; evaporation occurs at a liquid-air interface so scaling is minimal and much of the energy is provided by vapour formation. The big cost is the energy required, as the heat needed for distillate production would be ~200 kWh/m^3 without an ERD (Xu et al. 2013).

Salt Recovery

Salt solidification and sequestration (also known as stabilization or inerting) is the process of rendering the brine slurry into a solid by adding an inert low-cost product like cement or lime. This product can also be achieved with a dry waste product (e.g. sewage sludge). The purpose is to finish drying the product chemically then disposing of it to landfill. Typically, 0.8 and 2 litres of binder per litre of liquid waste or paste is required and would be done in a mixer or in a batch process.

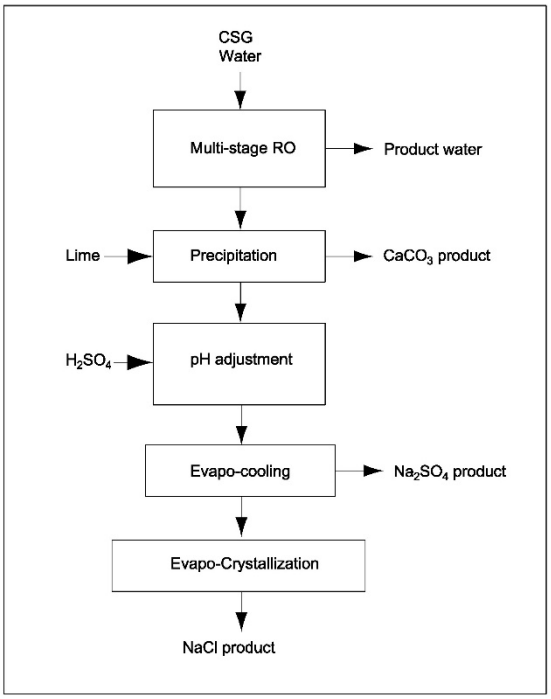

Figure 9: Application of SAL-PROC™ technology to CSG produced water
Derived from Rioyo et al. (2017)

This process can be made more viable by Selective Solids Harvesting (SSH) which consists of precipitating salts of an economic value using the SAL-PROC™ process which produces salts such as magnesium hydroxide, gypsum and calcium chloride (NSW Public Works 2011). This system tends to have high capital costs to maintain the purity of the product (e.g. additional cyclones and drying equipment). (Rioyo et al. 2017). Generally, this process is not viable for Brackish desalination plants due to the cost of further treatment and remoteness of the sites from potential product markets (Arakel and Mickley 2011).

In situ desalination (ISD)

This technology is currently running commercially at Glenkara Winery in Victoria, Australia. The essence of this technology is putting the RO unit & the bore pump into a single unit, which is inserted down a borehole into an aquifer. The desalination occurs down the well, with the permeate being pumped to the surface and the retentate remaining in the aquifer. The system is

optimized to prevent "dipole flow" of retentate fluid back into the feed stream, utilizing any aquifer stratification that may exist as well as the density contrast between natural groundwater and the saline retentate. The unit at Glenkara is producing approximately 4KL/hour (100KL/day) of high-quality water with Total Dissolved Solids (TDS) of 100mg/L from an aquifer containing brackish groundwater with 3200mg/L TDS. This unit can produce up to 35 megalitres (ML) a year (desaln8 2018).

Other trials include:

- Katanning site is treating brackish water with 10,000mg/L TDS and producing 400L/hour with less than 500mg/L TDS.
- Swan Valley, WA around 500L/hour of 150mg/L TDS water produced from water with a salinity of 3500mg/L TDS. (desaln8 2018).

The benefits of this system include that its capital and operating costs are smaller than standard desalination plants and its negligible footprint. Depending on groundwater movement and aquifer recharge, a concentration or cluster of salt could get created around the unit and increase the salinity of the ISD feed. Thus the salinity of the permeate will gradually increase with time. This can cause additional problems if there are toxic components like arsenic or radioactive elements (NSW Public Works 2011). Other downsides to this system are its lack of mobility and the lack of control over salinity of the water coming out of the bore.

Wind-aided intensified evaporation (WAIV)

This process uses evaporation however brine is applied to vertical hanging fabric to maximize exposure to wind. This creates a very small footprint compared to evaporation ponds, increasing the evaporative area by a factor of 10 – 33 depending on the design. This system has very low energy cost and is well suited for climates with high natural evaporation (where

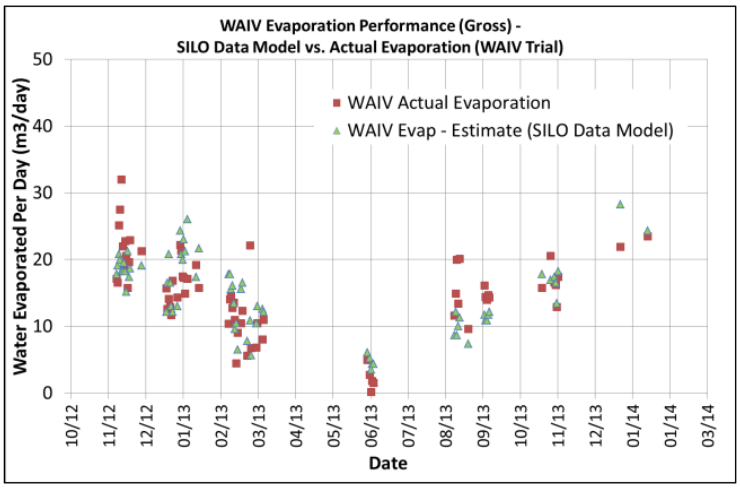

Figure 10: WAIV Evaporation Performance – Model (Empirical) vs. Actual (Murray, Mcminn, and Gilron 2015)

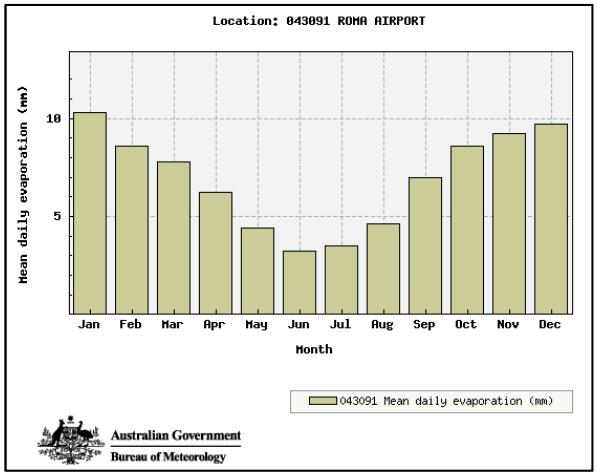

Figure 11: Mean Daily Pan Evaporation Roma Airport BOM (Bureau of Meteorology 2018)

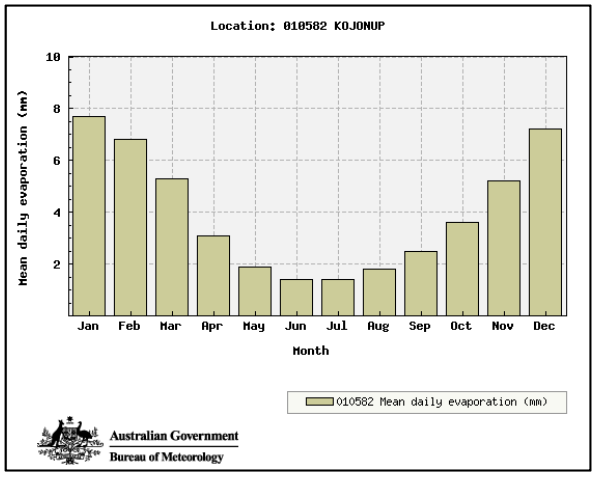

Figure 12:Mean Daily Pan Evaporation Kojunup BOM (Bureau of Meteorology 2018)

desalination is more prevalent). The fabric used can also be selected to provide more sites for salt precipitation. Limitations include the need for constant warm/hot air, which in turn creates problems in cold weather.

This is illustrated shown in WAIV trials run by Murray, Mcminn, and Gilron (2015) in Roma, Queensland in 2013. Figure 10 shows evaporation results illustrating the drop in evaporation rates in winter, and Figure 11 shows Bureau of Meteorology pan evaporation data at the closest weather station from 1992 – 2008 as a reference (Bureau of Meteorology 2018).

By comparison Figure 12 is evaporation data from Kojunup from 1975 – 1997, this being the closest weather station to Wagin with evaporation data (Bureau of Meteorology 2018). This station is some 60km SSW of Wagin. Evaporation is even lower than that in Roma, giving a clear idea of how poor evaporation performance would be in winter.

The other concern is that an evaporation pond is still needed for overflows and buffering. Low evaporation rates in winter would mean larger ponds to store desalination brine if the desalination plant was to keep operating throughout the year. This goes back to issues of cost, land area and groundwater pollution if it leaks.

Spray Irrigation

The premise of this approach is to spray the brine into the open air in such a way that the water is evaporated and the dry salt product falls to the ground, is collected and disposed. The argument against WAIV technology holds for this form of treatment too. This approach is suitable in dry arid environments like MENA, however it is limited to summer periods and would also be limited to open desert areas due to drift. This technique is often coupled with evaporative ponds to prevent too much groundwater contamination. A commercial example is the Landshark Wastewater Evaporator (Landshark 2018).

Conclusion

Existing ZLD technology generally relies on power to produce a dry product or relies on environmental techniques like evaporation ponds. The desire in much of the review literature is to move away from ponding as it is too risky in the event of pond lining perforation and leaking into the groundwater table. This leaves techniques like crystallization which is generally too costly if it is not allied to a value-added produce e.g. Oil & Gas. Waste heat scenarios are generally suited to CHP allied to large industrial complexes producing high volumes and usually are for seawater desalination which then gets used by the industry in question.

Zero Liquid Discharge for brackish water desalination really only occurs in very small setups e.g. Solar Distillation or at great cost e.g. Membrane Distillation. And even in most of these cases ponding is still used. No technology alternatives currently exist that meet the criteria of no ponding, economic and are feasible for scaling up to large quantities.

Chapter 3: Model Development

100L/HR PILOT PLANT

Two programs were used to examine the 100L/h Pilot Plant design of the proposed system. Initially modelling with Excel proceeded by referencing literature running similar scenarios and adjusting the calculations to fit the Enerbi concept. Much of the MVC literature discussed operating evaporators at below atmospheric pressure (Al-Juwayhel, El-Dessouky, and Ettouney 1997; Aly and El-Fiqi 2003; El-Feky 2016; Ettouney 2006; Veza 1995) to reduce the boiling temperature of the feedwater and hence reducing the energy input costs. Proceeding with this approach ran afoul with the turbocharger which needs to run at atmospheric pressure or above so this approach was discarded. Excel was used to optimize scenarios with the use of the forecast tool in Data Analysis, in particular Goal Seek in the What-If-Analysis.

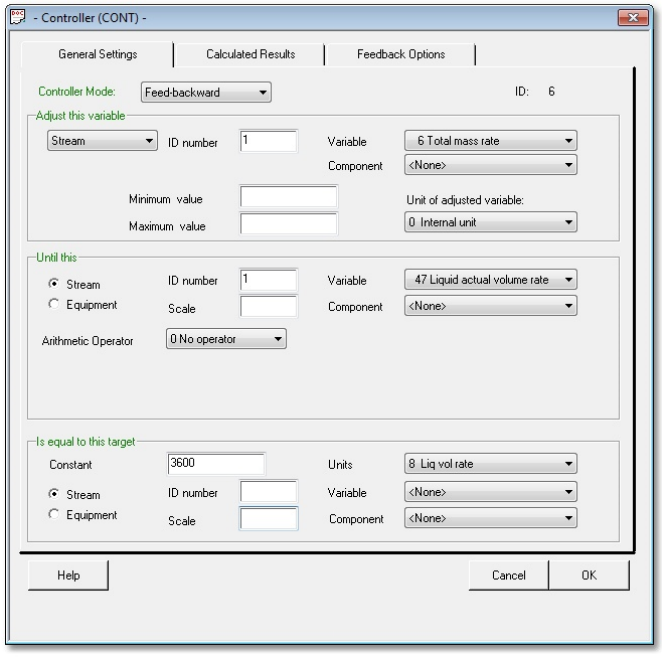

Figure 13: ChemCad Controller Settings (Silverstein 2016)

Adjusting the model to operate at atmospheric pressures created a scenario that worked, and these calculations then became the inputs into ChemCad (Chemstations 2018). This is a process simulator for modeling steady state and unsteady state process systems and was used to fault-find the Excel calculations and to fine-tune the process model to optimize production.

Optimization in ChemCad is a stand-alone feature that acts like Goal Seek, with Feed-backward and Feed-Forward functions. Figure 13 shows the Feed-Backward settings box; this was the function mostly used, being particularly useful in minimizing heat loss from the dryer (Silverstein 2016).

Using Excel and ChemCad the four 'corners' of the optimization process are thus minimizing the volume of biomass required to treat the volume of water; minimizing the amount of heat lost to the environment through the dryer exhaust; minimizing the area of the heat exchangers and minimizing the area of the evaporator.

Assumptions

Reverse Osmosis was specified at a 55% recovery rate. This is based on known production values given groundwater salinity levels at Wagin of 11000 mg/L, so with a 55% RO recovery this means that brine concentration out of the RO system which was the feed salinity into the MVC was ~24,444 mg/L at 45kg/hr. MVC was set at a 30% recovery rate which meets with literature values (Swaminathan, Nayar, and Lienhard V 2016; Warsinger et al. 2015). The output from the dryer was set at 100% vapour to attain a ZLD product.

Flow Charts & Tables

The following page is the overall flowchart, labelled as Figure 14. In each section this chart is broken down into smaller images and labelled as either Excel or ChemCad. The Excel Modelling is shown as the equations that were used to do the calculations. The Raw Data used is appended as Appendix A. ChemCad modelling is demonstrated by filling in the stream data on the image and the two sets of modelling are then reviewed. Table 4 follows this flowchart and this is a summary of the data for clarity.

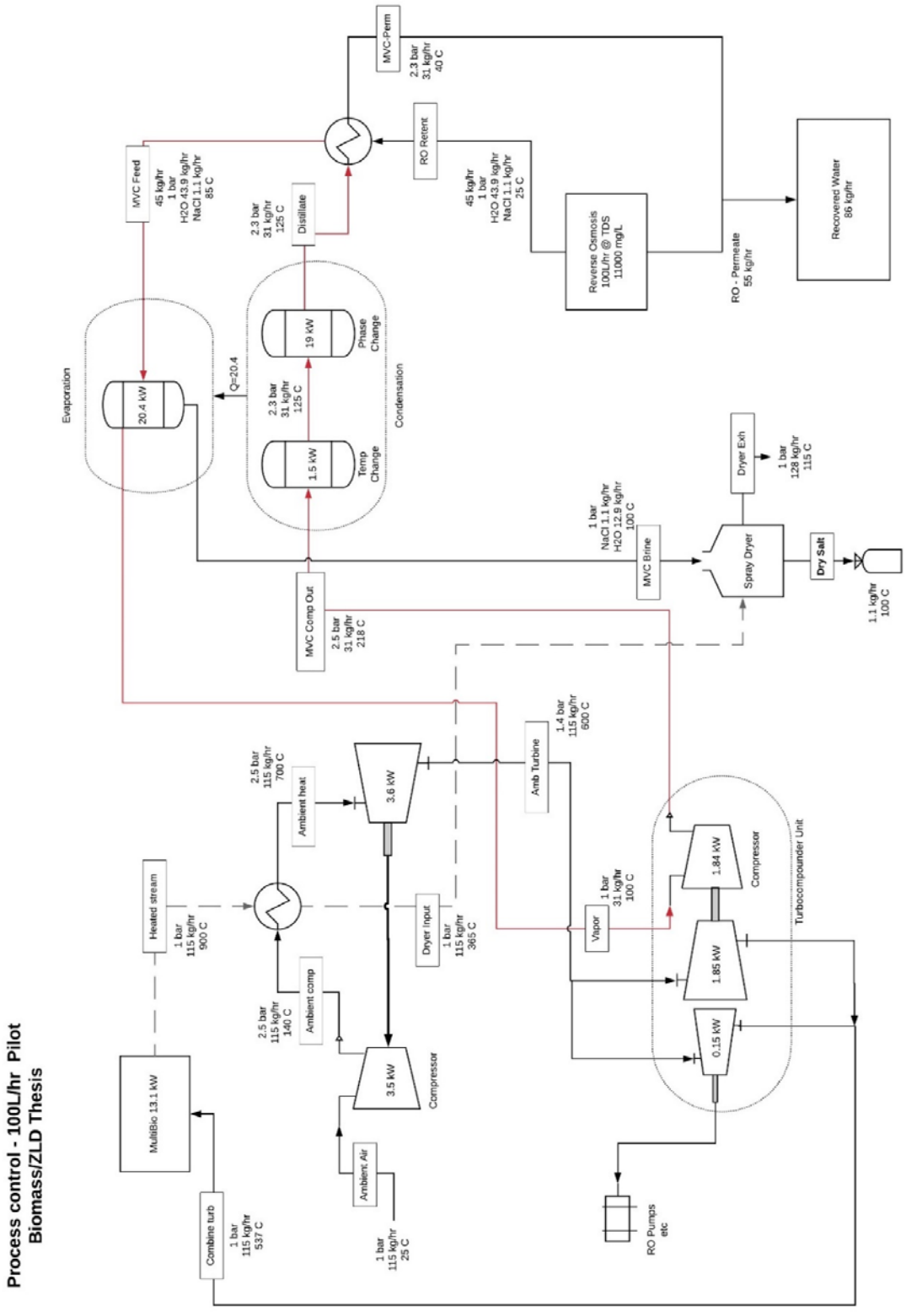

Figure 14: Process Control Flow Diagram 100L/h Pilot Plant

Table 4: Pilot Plant Process Modelling Overview

Stream name	Description	Excel value	Chemcad value	Comment
Stage 1	**Brine heat exchanger**	Area = 0.55m^2	Area = 0.32m^2	
RO Retent	Stream from RO into heat exchanger	25°C, 1 bar 45 kg/hr	25°C, 1 bar 45 kg/hr	
MVC Feed	Stream from heat exchanger into MVC	80°C, 1 bar 45 kg/hr	85°C, 1 bar 45 kg/hr	1.1kg salt/hr
Distillate	Distilled product from MVC	116°C, 2.4 bar 31kg/hr	125°C, 2.3 bar 31kg/hr	
MVC Perm	Final MVC fresh water product	35°C, 2.4 bar 31kg/hr	40°C, 2.3 bar 31kg/hr	
Stage 2	**Distillation Process**	Q = 20.45 kW	Q = 20.4 kW	
Vapor	Evaporate that leaves the reaction vessel	100°C, 1 bar 31 kg/hr	100°C, 1 bar 31 kg/hr	70% recovery
MVC Comp Out	Compressed vapour returning to the reaction vessel	213°C, 2.4 bar 31 kg/hr	218°C, 2.5 bar 31 kg/hr	
MVC Brine	Brine product from reaction vessel	100°C, 1 bar 14 kg/hr	100°C, 1 bar 14 kg/hr	30% retained
Distillate	Distilled product from MVC	116°C, 2.4 bar 31kg/hr	125°C, 2.3 bar 31kg/hr	
Stage 3	**Drying Process**	$Q_{evap} = 7.54$ kW	$Q_{evap} = 8.05$ kW	
Dryer Input	Combustion exhaust heat stream from Heat Exchanger	338.3°C, 1 bar 115 kg/hr	365°C, 1 bar 115 kg/hr	
Dryer Exh	Exhaust from dryer containing water vapour & combustion exhaust	115°C, 1 bar 128 kg/hr	115°C, 1 bar 128 kg/hr	Vapor fraction = 1
Dry Salt	Dry waste product	100°C, 1.1kg salt/hr	100°C, 1.1kg salt/hr	
Stage 4	**Water Vapour Compression**	$\dot{W} = -1.76$ kW	$\dot{W} = -1.84$ kW	
	Water Vapour Turbine	$\dot{W} = 1.81$ kW	$\dot{W} = 1.85$ kW	Total turbine $\dot{W} = 2$kW
	Power turbine	$\dot{W} = 0.19$ kW	$\dot{W} = 0.15$ kW	
Amb Turbine	Stream from the air turbine	660°C, 1.43 bar 115 kg/hr	600°C, 1.4 bar 115 kg/hr	
Stream name	Description	Excel value	Chemcad value	Comment

Combine turb	Combined turbine exhaust streams that are re-routed as heat & air supply back into the combustor	604.7°C, 1 bar 115 kg/hr	537°C, 1 bar 115 kg/hr	
Stage 5	**Air Compressor**	$\dot{W} = -3.54$ kW	$\dot{W} = -3.5$ kW	
Ambient Air	Air Compressor inlet stream	25°C, 1 bar 115 kg/hr	25°C, 1 bar 115 kg/hr	
Ambient Comp	Air Compressor outlet stream	136.5°C, 2.5 bar 115 kg/hr	140°C, 2.5 bar 115 kg/hr	
	Combustor	$Q = 10.5$ kW Volume of Biomass required 3.6 kg/hr	$Q = 13.1$ kW	
Combine turb	Combined turbine exhaust streams that are re-routed as heat & air supply back into the combustor	604.7°C, 1 bar 115 kg/hr	537°C, 1 bar 115 kg/hr	
Heated Air stream	Heated exhaust coming out of the combustor	900°C, 1 bar 115 kg/hr	900°C, 1 bar 115 kg/hr	
	Air Heat Exchanger	Area = 0.03m^2	Area = 0.08m^2	
Ambient Heat	Heated clean air coming out of the heat exchanger	758.1°C, 2.5 bar 115 kg/hr	700°C, 2.5 bar 115 kg/hr	
Dryer Input	Combustion exhaust heat stream from Heat Exchanger	338.3°C, 1 bar 115 kg/hr	365°C, 1 bar 115 kg/hr	
	Air Turbine	$\dot{W} = 3.59$ kW	$\dot{W} = 3.6$ kW	
Amb Turbine	Stream from the air turbine	660°C, 1.43 bar 115 kg/hr	600°C, 1.4 bar 115 kg/hr	

See Appendix A for Raw Excel Tables

Modelling Stages

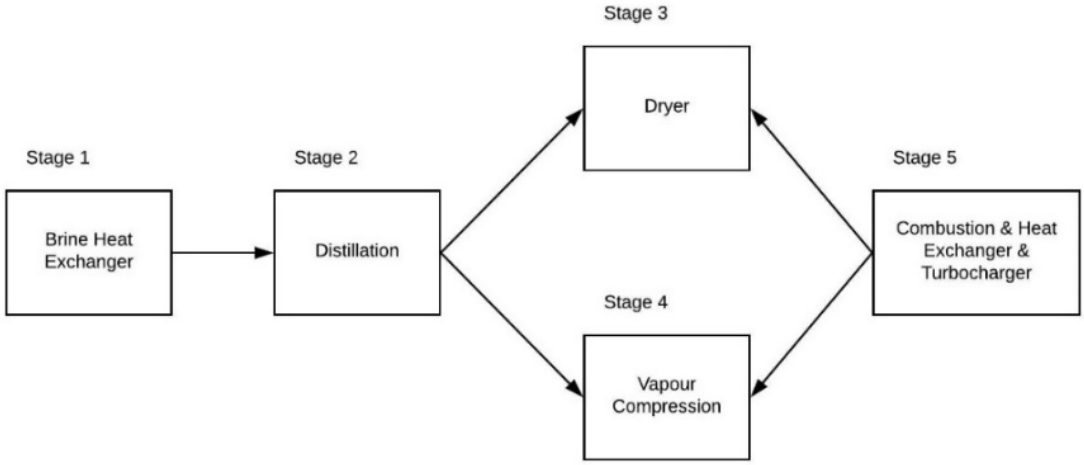

Figure 15: Enerbi Concept Modelling Stages

Stage 1: Brine Heat Exchanger

Model Stream Descriptions

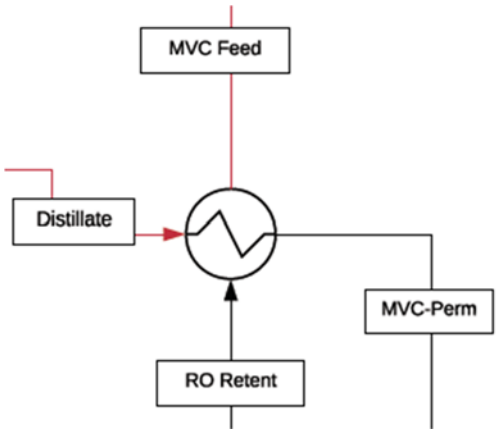

Figure 16: MVC Heat Exchanger

RO Retent is the stream coming out of the Reverse Osmosis process (see Figure 16) and into the heat exchanger prior to MVC. The brine from Reverse Osmosis is assumed to be at atmospheric pressure to provide the lowest feasible evaporation temperature. It is assumed to be at 25°C.

MVC Feed refers to the stream coming out of the cold stream outlet of the heat exchanger with increased heat. Its initial temperature coming out of heat exchanger was nominally set at 80°C as evaporation occurs at 100°C inside evaporator given the evaporator was designed to operate at atmospheric pressure.

Distillate is the product stream from the MVC process, this is the hot inlet stream that donates most of its heat to **MVC Feed**.

MVC Perm is the permeate stream coming out of the cold outlet of the heat exchanger with decreased heat, i.e. the MVC product stream. To calculate Log Mean Temperature Difference

(LMTD) (needed to determine the temperature driving force & calculate exchanger area) the hot stream outlet (**MVC-Perm**) temperature needs to be higher than cold stream inlet (**RO Retent**) temperature. This was designated at 35°C.

Heat exchanger heat flow equation.

$$\dot{m}_{distillate}\, C_P(T_{distillate} - T_{mvc\ perm}) = \dot{m}_{ro\ retent}\, C_P(T_{mvc\ feed} - T_{ro\ retent})$$

$$30\ kg/hr * C_P(T_{distillate} - 35) = 45\ kg/hr * 4.18\ \text{kJ/kg°C} * (80 - 25)$$

$$C_P(T_{distillate} - 35) = 344.85$$

$T_{distillate} \approx 116$°C (Derived from Excel, see Appendix A, Table A.3)

$\dot{Q}_{heat} = 344.85\ \text{kJ/hr} = 0.1\ \text{kW}$

Heat Exchanger Heat Transfer Area

$$A_{heat-ex} = \frac{\dot{m}_{distillate}\, C_P(T_{distillate} - T_{mvc-perm})}{U_{heat-ex}(LMTD)_{heat-ex}} = \frac{\dot{m}_{feed}\, C_{P_f}(T_{mvc\ feed} - T_{ro\ retent})}{U_{heat-ex}(LMTD)_{heat-ex}}$$

Where $U_{heat-ex}$ is the overall heat transfer coefficient in the heat exchanger

Logarithmic Mean Temperature Difference

$$(LMTD)_{heat-ex} = \frac{(T_{distillate} - T_{mvc\ feed}) - (T_{mvc-perm} - T_{ro\ retent})}{\ln \frac{(T_{distillate} - T_{mvc\ feed})}{(T_{mvc-perm} - T_{ro\ retent})}}$$

$$(LMTD)_{heat-ex} = \frac{(T_{distillate} - T_{mvc\ feed}) - (T_{mvc-perm} - T_{ro\ retent})}{\ln \frac{(T_{distillate} - T_{mvc\ feed})}{(T_{mvc-perm} - T_{ro\ retent})}}$$

Assumption: Heat exchanger heat transfer coefficient $U_{heat-ex} = 0.37\ \text{kW/m}^2\text{°C}$

Calculations from Appendix A, Table A.4:

$(LMTD)_{heat-ex} = 20.3$

Area of heat exchanger $= 0.55\text{m}^2$

Chemcad Modelling

Modelling the heat exchangers heat balance uses the following formulas:

$$Q = U \cdot A \cdot LMTD; Q = H_{out,process} - H_{in,process}$$

$$Q = H_{out,utility} - H_{in,utility}$$

U was provided using the values for the previous heat exchanger calculations, the area was calculated accordingly.

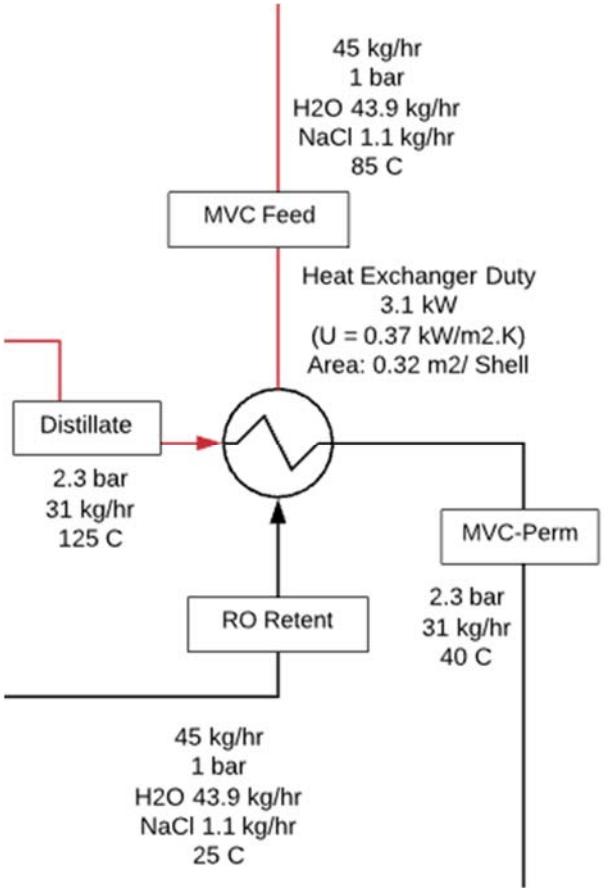

Figure 17: ChemCad MVC Heat Exchanger Outputs

RO Retent was established at 1 bar pressure and 25C; lowest feasible pressure was to keep the boiling temperature of the feed at a minimum to reduce the work required to be inputted into the system via the compressor. This stream would be coming out of the reverse osmosis system at pressures ranging from 5-10 bar depending on the membrane so this pressure could be removed from the stream via a pressure exchanger (referred to as an ERD - energy recovery device).

MVC-Perm was specified in the program module at 40°C. Excel modelling at 35°C proved to be too low, causing pinch-point alerts in ChemCad meant that 40°C was the lowest temperature this stream could go (see Figure 17). This stream was minimized to prevent as much heat lost to waste as possible. Pressure (2.3 bar) was determined from the compression/condensation process in the evaporator and the pressure loss parameters of the heat exchanger. The **Distillate** stream was specified by the MVC component. **MVC-Feed** this stream was calculated by the

program on the basis of the heat exchanger pressure-loss configuration and the other hot & cold streams.

Overview

RO Retent for both modelling scenarios was kept at 1 bar pressure and 25°C. **MVC-Perm** was estimated at 25°C to establish a baseline with which to test against; ChemCad modelling found it to be better at 40°C; this was independently verified using online heat exchanger software . **Distillate** was determined to be 116°C using excel modelling, 125°C using ChemCad. **MVC-Feed** was estimated at 80°C to establish a baseline with which to test against; ChemCad modelling found it to be better at 85°C. **LMTD** was estimated in excel at 20.3; ChemCad estimated this at 25.4. **Area of heat exchanger** in excel: 0.55m^2; in ChemCad 0.32 m^2

Results:

The aim was to minimize the area of the heat exchanger necessary by keeping the **Distillate** (hot stream inlet) temperature as high as possible so that **MVC-Feed** (cold stream outlet temperature) could receive the maximum amount of heat; this is based on the greater the temperature difference, the quicker the rate of heat transfer (and the smaller heat transfer area required). This was illustrated in the Excel calculations as there was a larger heat exchanger area requirement due to smaller temperature differences between the inlet and outlet streams. Similarly, the larger the LMTD, the more heat is transferred (see Figure 18):

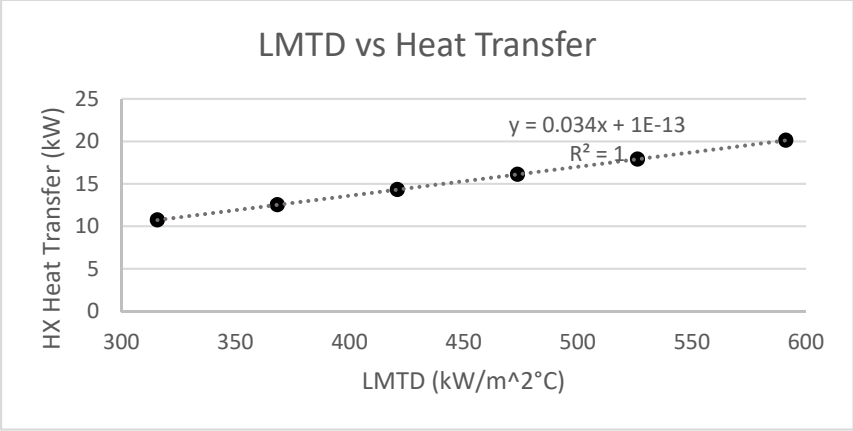

Figure 18: LMTD vs Heat Transfer

Stage 2 Evaporation Process

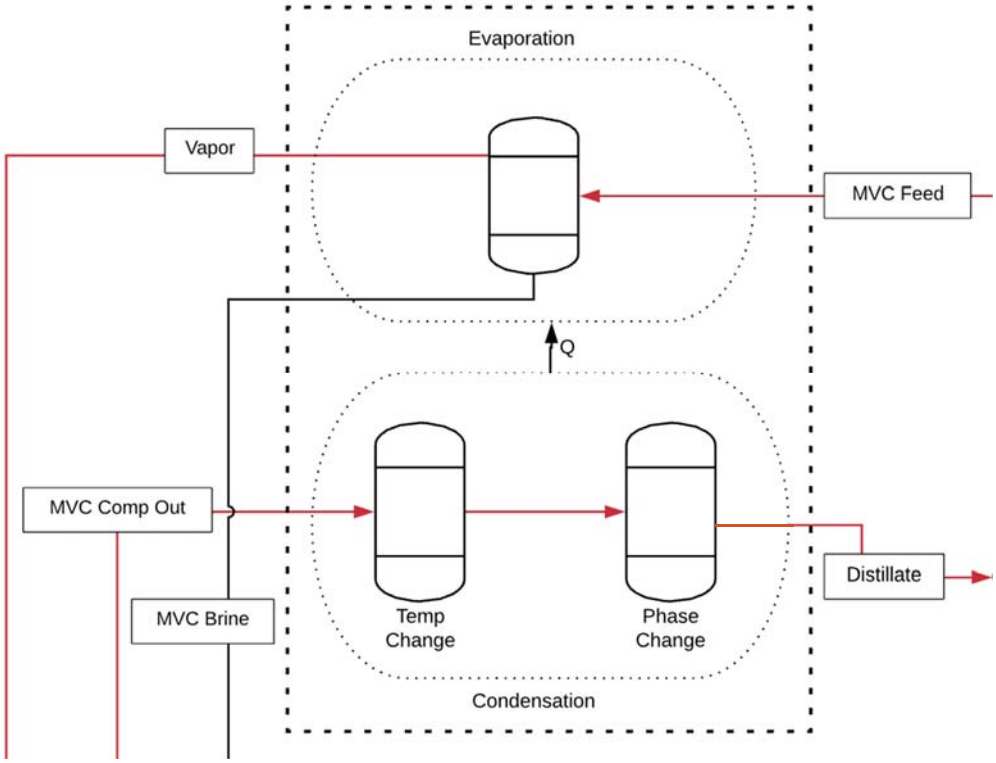

Figure 19: MVC Evaporation

As illustrated in Figure 19, **MVC Feed** is the stream out of the cool outlet of the heat exchanger, providing the water that is to be separated into vapour and brine. **Vapor** is the evaporated water stream that leaves the reaction vessel as a gas to be compressed. **MVC Comp Out** is the vapour stream that has been compressed and is entering back into the evaporator in pipes at a high heat and provides the heat source for the MVC Feed evaporation. **MVC Brine** is the liquid stream from the evaporation process that holds all of the non-vaporized compounds including the salt. **Distillate** is the condensed or precipitated vapour stream.

<u>MVC calculations for 100L/hr Pilot Plant</u>

$\dot{m}_{mvc\,feed} = \dot{m}_{distillate} + \dot{m}_{mvc\,brine}$

$\dot{m}_{mvc\,feed} = 45$ L/hr

Assume a 70% recovery rate from the evaporator

$\dot{m}_{distillate} = 31\ \text{L/hr};\ \dot{m}_{mvc\ brine} = 14\ \text{L/hr}$

$X_{mvc\ feed} = \frac{1.1\ \text{kg/hr}\ salt}{45\ \text{L/hr}} = 0.024444\ \text{kg/L} = 24444\ \text{mg/L}$

$X_{mvc\ brine} = \frac{1.1\ \text{kg/hr}\ salt}{14\ \text{L/hr}} = 0.078571\ \text{kg/L} = 78571\ \text{mg/L}$

Evaporator thermal load (BPE = 0)

Heat required to raise **MVC Feed** from 80°C to 100°C:

$Q = c_p m\Delta T = 4.1 * 45 * (100 - 80) = 3690\ \text{kJ/hr} = 1.025\ \text{kW}$

Latent heat required for evaporation of **MVC Feed**:

$2256\ \text{kJ/kg} * 31\ \text{kg/hr} = 69{,}936\ \text{kJ/hr} = 19.43\ \text{kW}$

Total thermal load required for evaporation process: 20.45 kW

Minimum total thermal output required from condensation process: 20.45 kW

Distillate remains a vapour until boiling point is above 116°C; this happens at 1.8 bar.

At 1.8 bar:

γ (specific heat ratio) $= 1.4$

$\eta = 0.8$

$T_2 = T_1\left(\frac{p_2}{p_1}\right)^{1-\frac{1}{\gamma}} = 373\left(\frac{1.8}{1}\right)^{1-\frac{1}{1.33}} = 431.56\text{K}$

$\eta = 0.8 = \frac{(\text{T}_2 - \text{T}_1)}{(\text{T}_{2'} - \text{T}_{1'})} = \frac{(431.56 - 373)}{(\text{T}_{2'} - 373)} = 446.2\text{K}$

Compressor outlet temperature = 173°C

$Q = c_{p_v} m\Delta T = 2.1037 * 31 * (173 - 116) = 3717.2\ \text{kJ/hr} = 1.03\ \text{kW}$

Latent heat generated:

$2048.1\ \text{kJ/kg} * 31\ \text{kg/hr} = \ 63{,}491\ \text{kJ/hr} = 17.63\ \text{kW}$

Total thermal output =18.66 kW, which is insufficient to provide heat for evaporation

Maximum setting for compressor derived from compressor map:

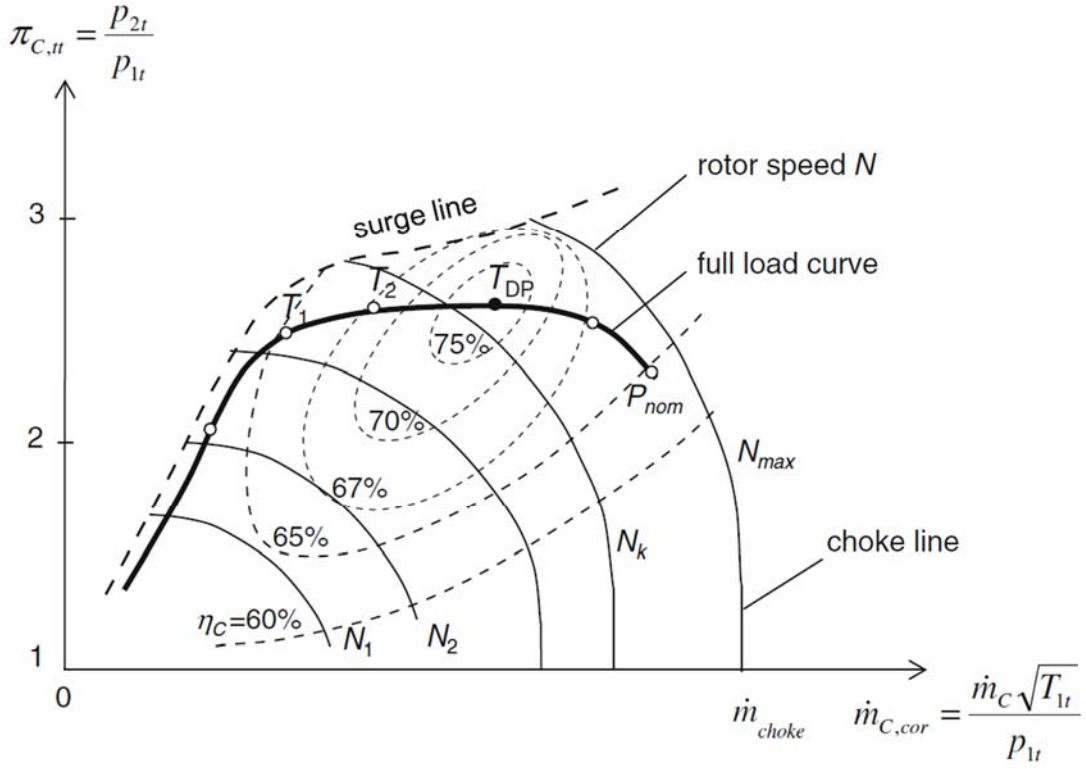

Figure 20: Compressor performance map (Nguyen-Schäfer 2015)

The compressor performance map in Figure 20 shows the compressor ratio π_C versus the corrected mass flow rate.

At 2.4 bar: $T_2 = T_1\left(\frac{p_2}{p_1}\right)^{1-\frac{1}{\gamma}} = 373\left(\frac{2.4}{1}\right)^{1-\frac{1}{1.33}} = 463.5\text{K}$

$$\eta = 0.8 = \frac{(\mathrm{T_2} - \mathrm{T_1})}{(\mathrm{T_{2'}} - \mathrm{T_{1'}})} = \frac{(463.5 - 373)}{(\mathrm{T_{2'}} - 373)} = 486.1\text{K}$$

Compressor outlet temperature = 213°C

$Q = c_{p_v} m\Delta T = 2.1531 * 31 * (213 - 116) = 6474\ \text{kJ/hr} = 1.8\ \text{kW}$

Latent heat generated:

$$2184.9\,\text{kJ/kg} * 31\,\text{kg/hr} = 67{,}732\,\text{kJ/hr} = 18.81\,\text{kW}$$

Total thermal output =20.61 kW, which is sufficient to provide heat for evaporation

Chemcad modelling

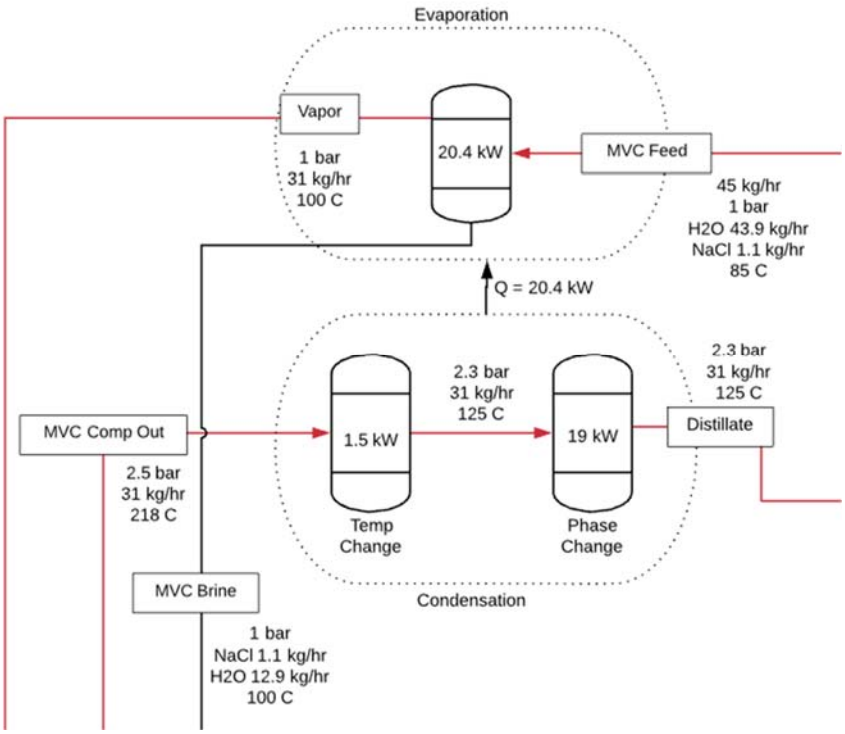

Figure 21: ChemCad MVC Modelling Outputs

The evaporator system was modelled in ChemCad as illustrated in Figure 21. The processes were modelled by separating out the process into three flash components and modelling them individually as follows.

1. The Feed flash evaporation process that produced Water vapour and brine (requiring heat)
2. The rapid temperature change of the liquid distillate inside pipes as a result of the brine contact with the outside of the pipes (producing heat)
3. The phase change of the compressed vapour to liquid distillate (producing heat) when the temperature dropped below the boiling point as set by the pressure created by the

compressor.

The system was calibrated so that the heat produced equalled the heat required, with a small excess of heat to account for the loss of heat to the environment through the evaporator walls.

MVC Feed - ChemCad set this at 85°C opposed to 80°C in Excel. The **Vapour** was set at 1 bar and a temperature of 100°C. **MVC Comp Out** stream settled on 2.5 bar which set this temperature stream slightly higher than the Excel modelling because of the distillate temp being 125°C as opposed to 116°C. **MVC Brine** is the same temperature as the vapour stream, 100°C.

Distillate was set higher @ 125°C; consequently, the pressure was set at 2.5 bar

Results

There was essentially no difference between the two modelling scenarios, as is indicated by the same heat transfer value for the condensation/evaporation process. Excel was optimized to achieve the lowest energy input requirement from the compressor using Goal Seek in a "What If' analysis. ChemCad was modelled to minimize the size of the Heat Exchanger in the previous section with the use of the Controller function so as such temperature streams were higher and compressor inputs (Stage 4) were higher.

Stage 3 Drying Process

Specifying the drying process provides the heat stream information required to specify the combustion heat exchanger. The streams inputs and outputs are illustrated in Figure 22.

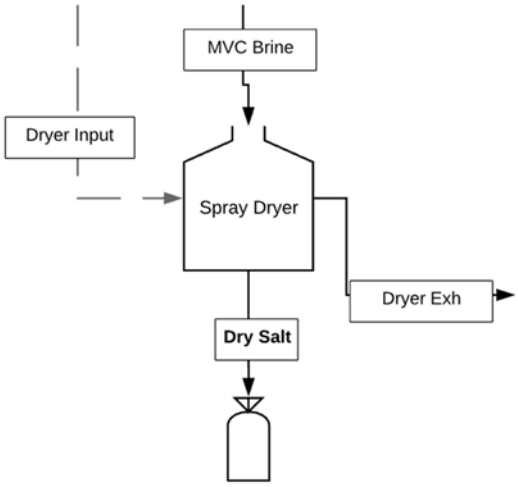

Figure 22: Drying Process Diagram

Dryer Input is the exhaust stream from the combustion process that provides the heat for the brine evaporation

MVC Brine is the residue liquid product from the distillation process that contains all of the salt and 30% of the liquid from the initial MVC feed.

Dry Salt is the bagged waste product with 0% moisture.

Dryer Exhaust is the combined evaporated water and exhaust from the combustion process.

Heat balance of spray dryer

Temperature at the outlet set at 115℃

Heat of evaporation of water:

$$Q_{evap} = \dot{m}_{mvc\ brine} * \left(1 - \frac{TS}{1 - u_{powder}}\right) * \left[\Delta H_{water} + \left(C_{v,dryer\ exh} * \left(t_{dryer\ exh} - t_{mvc\ brine}\right)\right)\right]$$

TS: %solids of brine feed

u_{powder}: salt powder moisture content allowed (set at zero)

ΔH_{water} – latent heat for water evaporation

$C_{v,dryer\ exh}$: specific heat capacity of water vapour at the dryer's outlet temperature

$$Q_{evap} = \dot{m}_{mvc\ brine} * (1 - TS)\left[\Delta H_{water} + (C_{v,dryer\ exh} * (t_{dryer\ exh} - t_{mvc\ brine}))\right]$$

$$= 14 * (1 - 0.0786) * [2076 + 1.87 * (115 - 100)]$$

$$= 27141 \text{ kJ/hr}$$

$$= 7.54 \text{ kW}$$

Heat of dry salt:

$$Q_{powder} = \dot{m}_{mvc\ brine} * \left(\frac{TS}{1 - u_{powder}}\right)\left[C_{powder}(1 - u_{powder}) + C_{water}u_{powder}\right]$$

C_{powder}: specific heat capacity of dry powder

C_{water}: specific heat capacity of water

$$Q_{powder} = \dot{m}_{mvc\ brine} * TS * C_{powder}$$

$$= 14 * 0.0786 * 1.26$$

$$= 1.39 \text{ kJ/hr}$$

$$= negligible$$

Total energy required: $Q_{evap} = 7.54$ kW

ChemCad Modelling

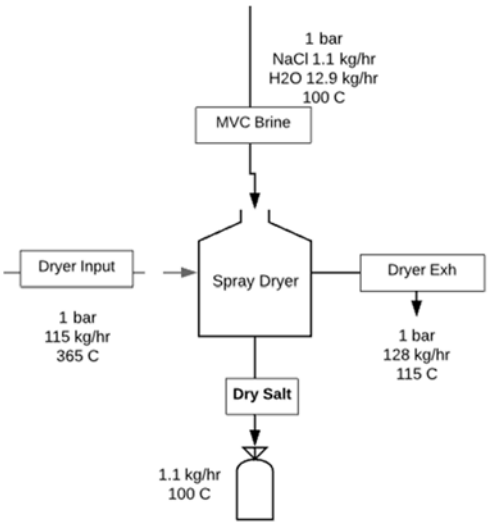

Figure 23: ChemCad Dryer Process model

The DRYR module was used to simulate the spray drying process. A vapour stream was provided from the combustion process via the combustion heat exchanger; the temperature flow in the heat exchanger and flow rate was adjusted so that the Vapour Moisture fraction of the **Dryer Exh** stream was equal to 1 (i.e. 100% Vapour 0% liquid moisture), whilst still providing sufficient heat to the turbines running the vapour compression. The calculations from ChemCad are shown in Figure 23.

Heat from heat exchanger was provided as 115 kg/hr at 365°C:

$$Q = c_p m \Delta T = 1.008 * 115 * (365 - 115)$$

$$= 28,980 \text{ kJ/hr}$$

$$= 8.05 \text{ kW}$$

Results:

Heat load for the two modelling scenarios was roughly similar; the Excel modelling went into more detail; it being based on industrial drying practices where the dry product is a commodity they wish to sell i.e. powdered milk. Very limited information was available as to how ChemCad modelled the Spray Dryer Unit & the only two inputs allowed was air flow in and vapour moisture fraction, which was set to 1, meaning 100% vapour and 0% liquid.

Stage 4 Water Vapor Compression Process

The system is a turbocharger unit with an alternator adapted to attach to the turbine shaft which generates the power required to run pumps & other electrical devices. As there are two turbocharger units in the project this one will be referred to as the Vapor Compressor.

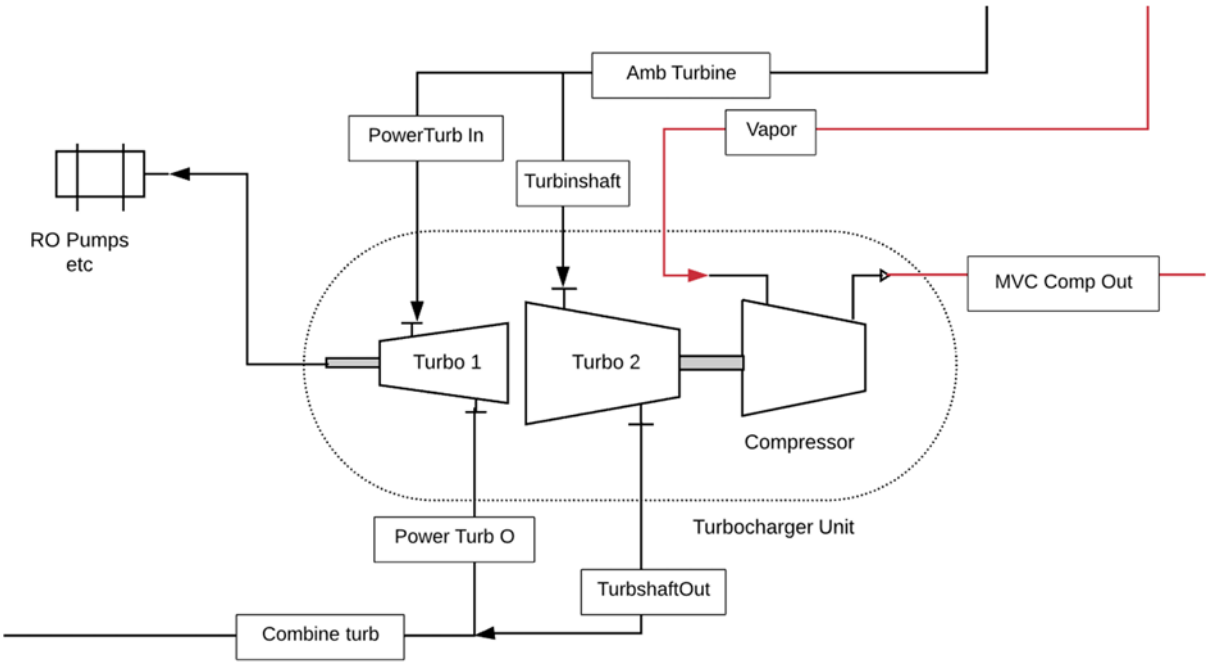

Figure 24: Vapour Turbocharger Process Diagram

Amb Turbine is the stream from the air turbine process. **PowerTurb In** is the stream into the turbine that generates electricity, **PowerTurb O** is the exhaust stream from this. **Turbinshaft** is the stream into the turbine that provides the mechanical shaft power for the vapour compressor. **TurbshaftOut** is the exhaust from this turbine. **Combine turb** is the combined exhaust streams that are re-routed as supply back into the combustion process so the heat is reused. **Vapor** is the stream from the flash evaporation. **MVC Comp Out** is the compressed exhaust from the Compressor unit attached to Turbo 2 as shown in Figure 24.

P_{vapor} is the inlet pressure; $P_{mvc\ comp\ out}$ is the outlet (compressed) pressure. These pressures are equal to the saturation pressures of the formed vapour at T_{brine} and the compressed vapour at $T_{mvc\ comp\ out}$.

$\therefore P_{mvc\ comp\ out} = 2.4$ bar and $P_{vapor} = 1$ bar

Specific Volume of Saturated Steam @ $T_{brine} = 1.67\ \mathrm{m^3/kg}$

γ (specific heat ratio of steam) $= 1.33$

Compressor efficiency $\eta = 0.8$

$$W_{compressor} = \left[\frac{\gamma}{\eta(\gamma-1)}\right] P_{vapor} v_{vapor} \left[\left(\frac{P_{mvc\ comp\ out}}{P_{vapor}}\right)^{\frac{\gamma-1}{\gamma}} - 1\right] \quad \text{(kJ/kg)}$$

$$= \left[\frac{1.33}{0.8(1.33-1)}\right] 100 * 1.67 \left[\left(\frac{240}{100}\right)^{\frac{1.33-1}{1.33}} - 1\right] \quad \text{(kJ/kg)}$$

$$= 204\ \text{kJ/kg}$$

$$= 204\ \text{kJ/kg}$$

$\dot{W} = \dot{m}_{vapor}\ \text{x}\ W_{compressor} = 31\ \text{kg/hr} * 204\ \text{kJ/kg} = 6324\ \text{kJ/hr} = 1.76\ \text{kW}$

Turbine power needed to provide this: ~ 1.80 kW

Additional power requirements of the project set at 10% of the power for MVC; total power needed is $1.80 + (1.80 * 0.1) \approx 2$ kW

ChemCad Modelling

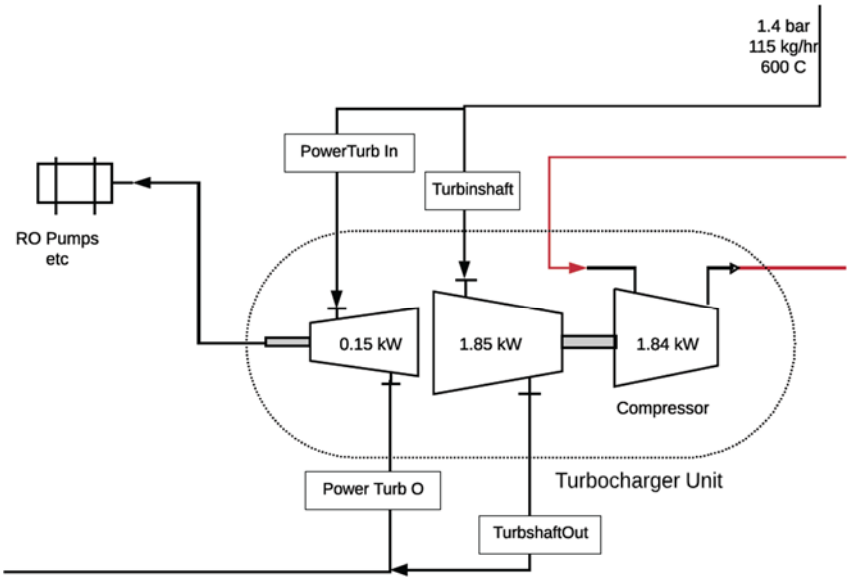

Figure 25: Turbocharger ChemCad Process Diagram

The essential requirement in this aspect of the ChemCad model was to provide the power required to the compressor. This was achieved by specifying the turbine efficiency at 0.75 and the actual power rating at 1.85 kW to allow for a small amount of loss in the transfer of energy to the compressor. The flow rate of air was then adjusted to exhaust out of the turbines at atmospheric pressure. Higher than this pressure would create an energy loss, lower than atmospheric pressure would create a suction as the turbines are non-condensing.

The power output of the smaller turbine (connected to an alternator, marked as 0.15kW in Figure 25) was based on pump power requirements of a reverse osmosis system with a feed rate of 0.1 m^3/hr at 13,000 mg/L achieving 55% recovery. An additional 20% of this was added to power other pumps (e.g. well & irrigation pumps), as well as process control power requirements. The turbocharger unit refers to the fact that these two turbines would be physically attached to each other, and as such the output pressures would be identical. This calibration was achieved using a splitter on the incoming **Amb Turbine** stream.

Results

Similar results between the two modelling scenarios, and both turbines combined were averaged to 2kW in both scenarios. This stage was to specify the compressor power required so that turbine power ratings could be proposed. This was then used to specify outlet temperatures & flowrates in later parts of this section.

Stage 5 Combustion, Compression & Air Heat Exchanger Process

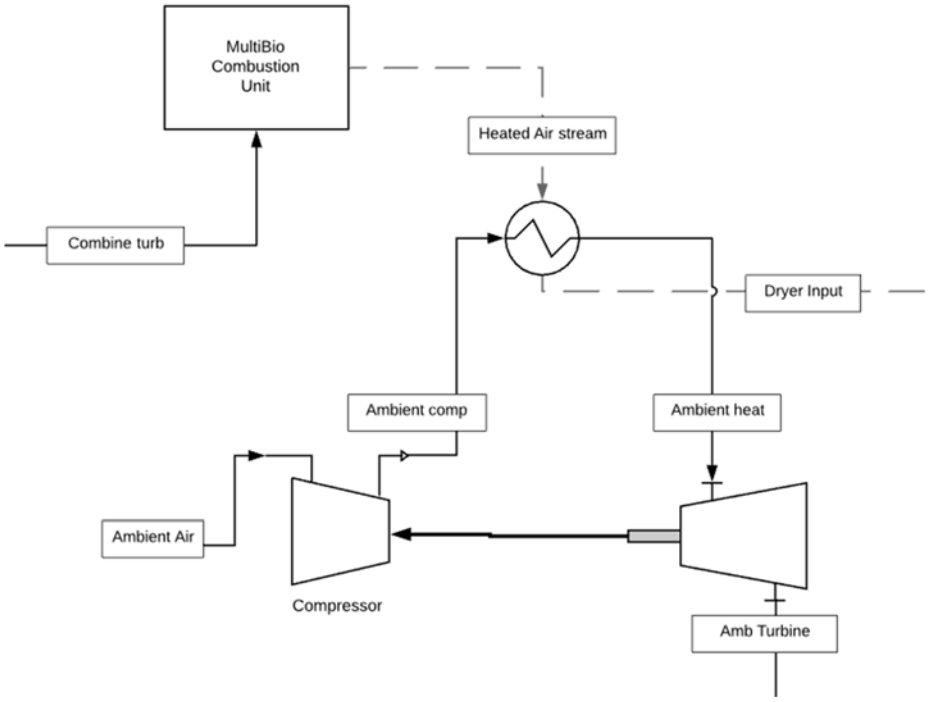

Figure 26: Combustion, Compression & Air Heat Exchanger Process Flow Diagram

The source of heat that drives the whole process is combustion. However, combustion flue gases are not suitable for turbines so a heat exchanger process is used to heat clean air which powers the turbines. The reasons to avoid using flue gas include the fact that hot air is generally not good for compression and its low density reduces mass flow and thereby power generation. Also unburnt fuel in the compressor could potentially catch fire.

The design of the system is to use the waste heat out of the turbines and as exhaust gas is heavily depleted of oxygen, and even with excess air added to the mix, carbon dioxide (and monoxide) build up would become a deterrent to combustion.

To model the heat exchanger, the cold inlet temperature is needed. As this is ambient air that gets compressed, it is already hot as it reaches the heat exchanger. The reason for this is that two outlet streams require sufficient heat whereby one goes to the turbines to run the compressor whilst the other hot outlet stream needs sufficient residual heat to dry the brine from the MVC process, as shown in the previous stage.

Air Compressor

Ambient Air inlet temperature was set at 25℃, pressure set at 1 bar. Pressure increase for a turbocharger compressor is 2.5 bar as per Figure 20.

Specific Volume of Air @ 25℃ $= 0.8447\ \mathrm{m}^3/\mathrm{kg}$

γ (specific heat ratio of air) $= 1.4$

Compressor efficiency $\eta = 0.8$

$$W_{compressor} = \left[\frac{\gamma}{\eta(\gamma-1)}\right] P_{ambient\ air} v_{ambient\ air} \left[\left(\frac{P_{ambient\ comp}}{P_{ambient\ air}}\right)^{\frac{\gamma-1}{\gamma}} - 1\right] \text{(kJ/kg)}$$

$$= \left[\frac{1.4}{0.8(1.4-1)}\right] 100\ \text{kPa} * 0.8447 \left[\left(\frac{250\ \text{kPa}}{100\ \text{kPa}}\right)^{\frac{1.4-1}{1.4}} - 1\right] \text{(kJ/kg)}$$

$$= 110.59\text{kJ/kg}$$

Optimised air intake rate set at 115 kg/hr (using What-If Analysis in excel)

$\dot{W} = \dot{m}_{ambient\ air}$ x $W_{compressor} = 115\ \text{kg/hr} * 110.59\ \text{kJ/kg} = 3.54\ \text{kW}$

Turbine power needed to provide this: $3.54 + 0.05 = 3.59\ \text{kW}$

Ambient Comp Outlet Temperature:

$$T_{Ambient\ Comp,ideal} = T_{ambient\ air} \left(\frac{P_{Ambient\ Comp}}{P_{ambient\ air}}\right)^{1-\frac{1}{\gamma}} = 298 \left(\frac{2.5}{1}\right)^{1-\frac{1}{1.4}} = 387.2\text{K}$$

$$\eta = 0.8 = \frac{\Delta T\ Ideal}{\Delta T\ Actual} = \frac{(T_2 - T_1)}{(T_{2'} - T_{1'})} = \frac{(387.2 - 298)}{(T_{2'} - 298)}$$

$$T_{Ambient\ Comp,actual} = 409.5\text{K} = 136.5℃$$

Spray Dryer

The heat required by the dryer was 7.54 kW (27141 kJ/hr), outlet temperature set at 115℃, flow rate at 115 kg/hr:

$Q = c_p m\Delta T = c_p * 115 * (T_{Dryer\ Input} - 115)$

$27141 = c_p * 115 * (T_{Dryer\ Input} - 115)$

Using Heat capacity tables $T_{Dryer\ Input} = 338.3$℃ (derived from Excel, see Appendix A, Table A.2)

Temperature required coming out of the heat exchanger hot stream outlet = 338.3℃

Combustion heat exchanger

The outlet for the combustion exhaust was set at 900℃ pressure set at 1 bar.

Assumption: no pressure reduction in the heat exchanger.

The streams are:

Cold: **Ambient Comp** – 136.5℃; **Ambient Heat** - TBD

Hot: **Heated Air Stream** – 900℃; **Dryer Input** - 338.3℃

$$\dot{m}_{Heated\ Air\ Stream}\ C_{P,hot}(T_{Heated\ Air\ Stream} - T_{Dryer\ Input}) = \dot{m}_{Ambient\ Comp}\ C_{P,cold}(T_{Ambient\ Heat} - T_{Ambient\ Comp})$$

$$115\ \text{kg/hr} * 1.121\ \text{kJ/kg℃} * (900 - 338.3) = 115\ \text{kg/hr} * 1.013 * (T_{Ambient\ Heat} - 136.5)$$

$$(T_{Ambient\ Heat}) = \left(\frac{1.121 * (900 - 338.3)}{1.013}\right) + 136.5$$

$T_{Ambient\ Heat} = 758.1$ ℃

Heat Exchanger Heat Transfer Area

$$A_{heat-ex} = \frac{\dot{m}_{Heated\ Air\ Stream}\ C_{P,h}(T_{Heated\ Air\ Stream} - T_{Dryer\ Input})}{U_{air\ heat-ex}(LMTD)_{air\ heat-ex}} = \frac{\dot{m}_{Ambient\ Comp}\ C_{P,c}\ (T_{Ambient\ Comp} - T_{Ambient\ Heat})}{U_{air\ heat-ex}(LMTD)_{air\ heat-ex}}$$

Where $U_{heat-ex}$ is the overall heat transfer coefficient in the heat exchanger

And $(LMTD)_{heat-ex} = \dfrac{(T_{Heated\ Air\ Stream} - T_{Dryer\ Input}) - (T_{Ambient\ Heat} - T_{Ambient\ Comp})}{\ln \dfrac{(T_{Heated\ Air\ Stream} - T_{Dryer\ Input})}{(T_{Ambient\ Heat} - T_{Ambient\ Comp}}}$

Assumption: Heat exchanger heat transfer coefficient $U_{heat-ex} = 1.2$ kW/m^2°C

Calculations from Appendix A, Table A.4:

$(LMTD)_{heat-ex} = 591.2$

Area of heat exchanger = 0.03.m^2

$\dot{Q}_{heat} = U$ x A x $(LMTD)_{heat-ex} = 1.2 * 0.03 * 591.2 = 21.28$ kW

Air Turbine

Turbine power needed: 3.59 kW at 75% efficiency.

$T_{Ambient\ Heat} = 758.1$°C

Flow rate: 115 kg/hr at 2.5 bar.

$Q = mc_p\Delta T = 115 * 1.147 * (758.1 - T_{Amb\ Turb})$

$12908.6 = 115 * 1.147 * (758.1 - T_{Amb\ Turb})$

$T_{Amb\ Turb} = 758.1 - \dfrac{12908.6}{115 * 1.147} = 660.2$°C

$T_{Amb\ Turb} = T_{Ambient\ Heat}\left(\dfrac{P_{Amb\ Turb}}{P_{Ambient\ Heat}}\right)^{1-\frac{1}{1.33}}$

$660.2 = 758.1\left(\dfrac{P_{Amb\ Turb}}{2.5}\right)^{\frac{1.33-1}{1.33}}$

$P_{Amb\ Turb} = 1.43$ bar

ChemCad Modelling

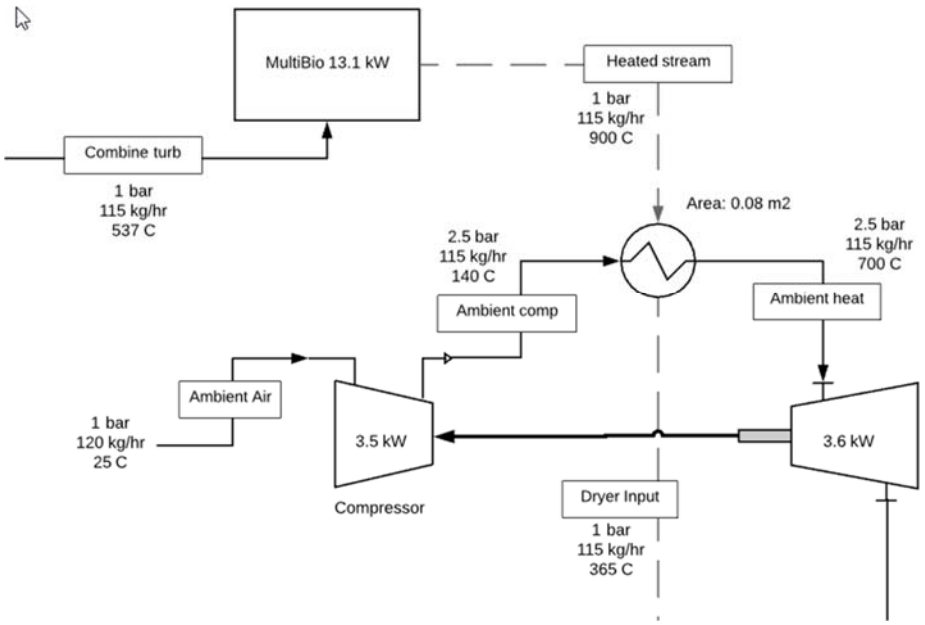

Figure 27: Combustion, Compression & Air Heat Exchanger ChemCad Process Flow Diagram

A Fired Heater (FIRE) module was used to model the combustion component; combustion exhaust temperature of 900C was specified. The **Combine turb** stream had a volumetric flow rate set at 115 kg/hr and the waste heat from the vapour compression was 537C. The Heat duty on this unit was 13.1 kW as shown in Figure 27.

The Air Heat Exchanger was configured to have a 700C heat output in the hot outlet stream (**Ambient heat**); this was adjusted to allow for 100% vapour in the exhaust of the dryer (and thus achieving zero liquid discharge). The feed rate into the heat exchanger was 115 kg/hr, the pressure was 2.5 bar and the temperature 140°C; the outlet, thus the **Dryer Input** exhaust stream had a temperature 365°C.

Results

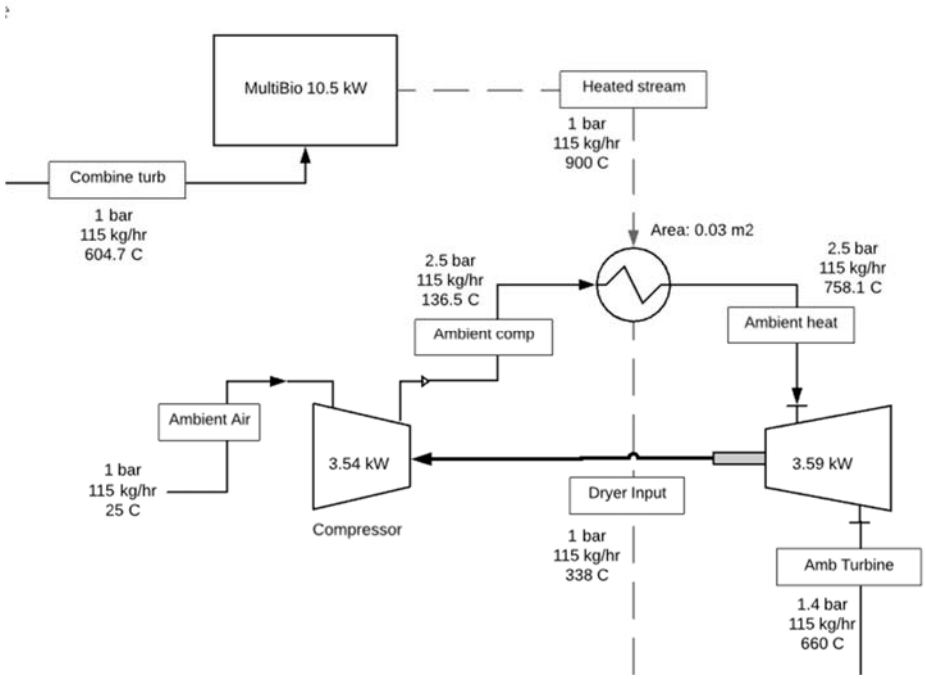

Figure 28: Combustion, Compression & Air Heat Exchanger Excel Process Flow Diagram

Excel modelling provided better capacity to minimize inputs and heat losses as shown in Figure 28. The heat sent to the dryer was minimized whilst still maintaining requisite heat exhaust. This allowed for larger amounts of heat recycling, which reduced the energy requirements of the combustor. This consequently reduced the surface area of the heat exchanger from 0.08 to 0.03m^2

Vapour Compression & power generation turbines

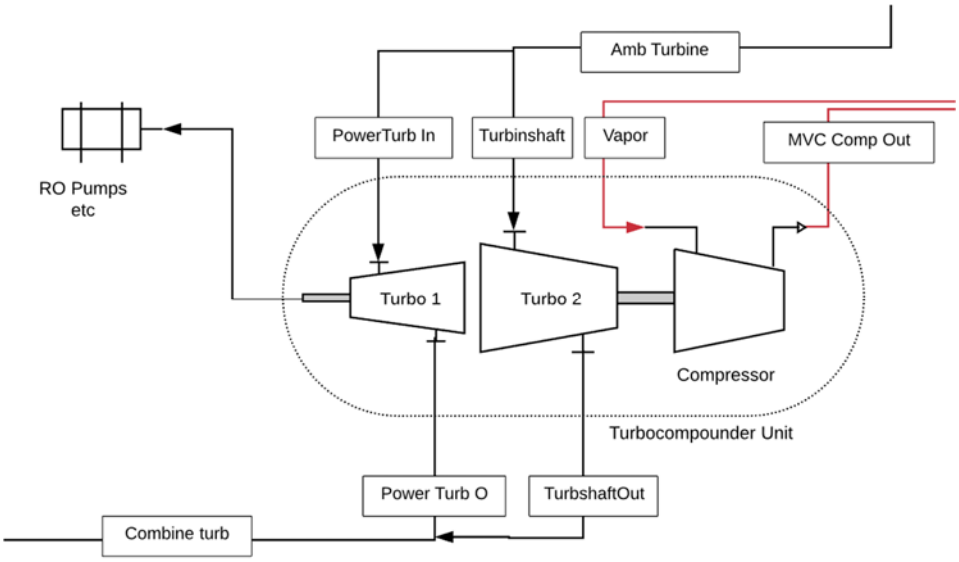

Figure 29: Vapour Compression & power generation turbines

The heat required by the vapour compression & power turbines was 2kw, and the final outlet pressure needs to be sitting on 1 bar to avoid vacuums being formed. The final outlet pressures and temperatures in the excel model can now be determined:

Turbine power needed: 2 kW (7200 kJ/hr) at 75% efficiency.

$T_{Amb\ Turbine} = 660.2°C$

Flow rate: 115 kg/s at 1.43 bar.

$Q = mc_p\Delta T = 115 * 1.127 * (660.2 - T_{Combine\ Turb})$

$7200 = 115 * 1.127 * (660.2 - T_{Combine\ Turb})$

$T_{Combine\ Turb} = 604.7°C$

$$T_{Combine\ Turb} = T_{Amb\ Turb}\left(\frac{P_{Combine\ Turb}}{P_{Amb\ Turb}}\right)^{1-\frac{1}{1.33}}$$

$$604.7 = 660.2\left(\frac{P_{Combine\ Turb}}{1.43}\right)^{\frac{1.33-1}{1.33}}$$

$P_{Combine\ Turb} = 1.005$ bar

Combustion & Biomass Modelling

Combustor Inlet:

$T_{Combine\ Turb} = 604.7°C$

$\dot{m}_{Combine\ Turb} = 115$ kg/hr

Combustor Outlet:

$T_{Heated\ Air\ Stream} = 900°C$

$\dot{m}_{Heated\ Air\ Stream} = 115$ kg/hr

Combustor capacity required:

$Q = \dot{m}c_p\Delta T = 115 * 1.115 * 900 - 604.7 = 37864.8$ kJ/hr $= 10.5$ kW

The combustion energy balance is derived from the "Btu Method" from Babcock & Wilcox Co. (2017). They specify efficiency losses in combustion including dry flue gas losses, moisture in fuel, latent heat, unburned fuel, radiation and miscellaneous. The manufacturers of the MultiBio combustion unit specify up to 96% efficiency (Petrojet Trade s.r.o. 2017) which will cover combustion unit efficiency losses.

$$\dot{Q} = \dot{b}\ x\ NCV\ x\ \left(\frac{96}{100}\right)$$

Where $\dot{b} =$ biomass flow rate (kg/hr)

Plantation waste -Eucalyptus Globulus (Bluegum) and Pinus Radiata (Pine)

$NCV = 15.84$ MJ/kg (Connell Wagner Pty Ltd 2008)

$$\dot{b} = \frac{\dot{Q}}{NCV\ x\ \left(\frac{96}{100}\right)} = \frac{37864.8\ \text{kJ/hr}}{15840\ \text{x}\ \left(\frac{96}{100}\right)} = 2.5\ \text{kg/hr}$$

Volume of Biomass required 2. 5 kg/hr

Specific Energy Consumption

RO used 0.19kW in Excel and 0.15kW in ChemCad because the total output from the Vapour Turbocharger was set at 2kW. The difference was the MVC energy consumption due to initial temperature differences. RO energy consumption was averaged to 0.17kW.

Dryer energy consumption was calculated as 7.54kW in Excel and 8.05kW in ChemCad; dryer energy consumption was averaged to 8kWh.

MVC power draw was calculated as all the energy generated for the system by the combustor minus the energy required for RO and drying; both heat exchangers & both turbines are assumed as necessary MVC componentry and are thus included in the MVC energy requirements.

Combustion energy output was determined to be 10.5kW in Excel and 13.1kW in ChemCad; averaged this was 11.8kW.

$$Total\ Power\ Output - RO\ Power\ - Dryer\ Power\ = MVC\ Power$$

$$11.8 - 0.17 - 8\ = 3.63$$

Calculated Specific Energy Consumption is thus shown in Table 5:

Component	Power Draw	Volume H_2O treated	TDS	SEC (kWh/m³)
RO	0.17 kWh	0.1 m^3/hr	11,000 mg/L	1.7 kWh_e/m^3
MVC	3.63 kWh	0.045 m^3/hr	24,440 mg/L	80.7 kWh_t/m^3
Dryer	8 kWh	0.014 m^3/hr	78,570 mg/L	570 kWh_t/m^3

Table 5: Enerbi BZLD component SEC

Chapter 4: 60ML Case Study

The Pilot Plant modelled in the previous section was scaled up for a higher volume flow. The scenario of interest from a commercial venture standpoint is treating 60ML per year. The process model flow sheet for the scenario is attached as Appendix C.

Biomass Consumption

There are two scenarios for Biomass quality and cost. The 'low' case representing waste biomass with examples being agricultural residue or green waste. The example used in this report is plantation waste, with a delivered cost of $10/green tonne. The high case represents farmed biomass (e.g.: Oil Mallee) with a delivered cost of $60/green tonne (Enerbi Pty Ltd 2017).

The air flow rate was set at 7700 kg/hr coming into the combustor at a temperature of ~520°C, as a result, the energy requirement of the combustor was ~920 kW. Masses of both types of biomass required was determined, assuming a 96% combustor efficiency according to the combustion unit manufacturer (PetroJet Trade SRO 2018).

Low Case

The fuel criteria used for plantation waste is shown in Table 6:

Fuel Criteria	ultimate analysis wt%, dry and ash-free basis)
Moisture Content	7.3 %
Hydrogen	5.63 %
Gross Calorific Value (GCV)	18.51 MJ/kg

Table 6: Plantation Waste Fuel Properties (Connell Wagner Pty Ltd 2008)

Net Calorific Value (NCV)

$$= GCV\left(1-\frac{w}{100}\right)-\left(2.444*\frac{w}{100}\right)-\left(2.444*\frac{h}{100}*8.936\left(1-\frac{w}{100}\right)\right)$$

$$NCV = 18.51\left(1-\frac{7.3}{100}\right)-\left(2.444*\frac{7.3}{100}\right)-\left(2.444*\frac{5.63}{100}*8.936\left(1-\frac{7.3}{100}\right)\right)=15.84\ \text{MJ/kg}$$

$$\text{Biomass (kg/hr)} = \frac{\dot{Q}}{\text{NCV x } \left(\frac{96}{100}\right)} = \frac{3304800 \text{ kJ/hr}}{15840 \text{ x } \left(\frac{96}{100}\right)} = 217 \text{ kg/hr}$$

The volume of Biomass required 0.217 tonne/hr

This quantity of Biomass (assuming that the process runs every day of the year) is equivalent to 1903 tonne/pa. The delivered cost of $10/green tonne is $19,035/pa.

High Case

Fuel criteria used for Oil Mallee raw biomass (Yani 2015) is outlined in Table 7:

Fuel Criteria	ultimate analysis wt%, dry and ash-free basis)
Moisture Content	5.0 %
Hydrogen	7.1 %
Gross Calorific Value	19.6 MJ/kg

Table 7: Oil Mallee Fuel Properties (Yani 2015)

Net Calorific Value (NCV)

$$= GCV\ \left(1 - \frac{w}{100}\right) - \left(2.444 * \frac{w}{100}\right) - \left(2.444 * \frac{h}{100} * 8.936\left(1 - \frac{w}{100}\right)\right)$$

$$NCV\ = 19.6\ \left(1 - \frac{5}{100}\right) - \left(2.444 * \frac{5}{100}\right) - \left(2.444 * \frac{7.1}{100} * 8.936\left(1 - \frac{5}{100}\right)\right) = 17.025 \text{ MJ/kg}$$

$$\text{Biomass (kg/hr)} = \frac{\dot{Q}}{\text{NCV x } \left(\frac{96}{100}\right)} = \frac{3304800 \text{ kJ/hr}}{17025 \text{ x } \left(\frac{96}{100}\right)} = 202 \text{ kg/hr}$$

The volume of Biomass required 0.202 tonne/hr

This quantity of Biomass (assuming that the process runs every day of the year) is equivalent to 1769.5 tonne/pa. The delivered cost of $60/green tonne is $106,171/pa.

The volume of fresh water produced per annum is 51 ML and thus the cost of water production is presented in Table 8:

Production cost	Biomass Low	Biomass high	
Operation and maintenance*	$1.08	$1.08	$/kL
Biomass	$0.37	$2.08	$/kL
Total	**$1.45**	**$3.16**	**$/kL**
*Figure provided by Enerbi Pty Ltd.			

Table 8: Cost of Water Production

Irrigation

Soil salinity treatment is one of the primary uses for the water produced by this project. Areas suffering from salinity issues are most likely ones with inundation or drainage issues, compounded by reduced vegetation. So irrigation alone will unlikely solve many issues, and often will compound them by mobilizing salts. The accepted approach is to use vegetation, preferably perennial and preferably deep-rooted trees to intercept mobile water in winter through root absorption. Much research has looked into combining agroforestry with pastures (Dunin 2002; Hatton et al. 2002; Silberstein et al. 1999; R.A Sudmeyer and Flugge 2005; Robert A Sudmeyer and Hall 2015; Turner and Ward 2002; Ward, Dunin, and Micin 2002).

Alley farming & Cropping

This is the most popular approach, as it provides shelter belts for existing pastures (and animals), allowing the farm to maintain its annual income whilst the trees mature. On flatter pasture-crop type land irrigation will increase the height of the water table so that water moves laterally, taking salt with it. Tree selection is often mallee-root in form meaning that the trees have a large subterranean root ball that ensures the survival of the tree, especially during fires (J. R. Bartle and Abadi 2010). Many of them are salt-tolerant (Wildy 2003) which increases their chances of survival. They extend their lateral roots extensively so that in Alley formation and will assist in draining the non-irrigated surrounding soil (Robinson, Harper, and Smettem 2006; Robert A Sudmeyer and Hall 2015).

Once the trees are old enough the wood is harvested via coppicing, leaving the mallee root intact. As this approach shows the most promise it is the area that has received the most R&D.

Oil-Mallee trees are pertinent for several specific reasons listed below.

- As illustrated in Figure 30, growth is linked to soil conditions and available water, with similar production across a wide range of rainfalls:

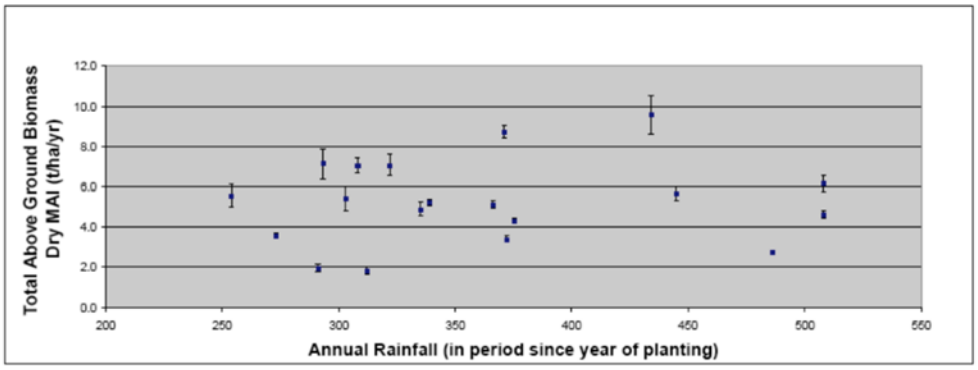

Figure 30: Relationship between mallee yield and rainfall in the wheat/sheep zone in WA (J Bartle et al. 2008)

- Mallee trees have exceptional transpiration capacity, with the biomass response to match. This is often detrimental to cropping, and recent research advocates for separate plantations over traditional alley cropping due to the economic impact of Mallee stands next to pastures (Robert A Sudmeyer and Hall 2015). Mallee roots have been found to extend 20 m laterally and to a depth of 28 m (Robinson, Harper, and Smettem 2006).
- Mallee is able to reduce water use to cope with drought and respond rapidly when the rain comes. This plasticity bodes well for decommissioning the desalination plant when there is a need.
- A yield of 9-10 tonnes/ha/yr is entirely feasible given proper site selection with the guarantee of water supply all year round (J Bartle et al. 2008).

The design has two salinity treatment processes as listed below:

1. The principal cause of salinity is rain in excess of demand by annual crops and pastures, which then percolates through the soil, recharges groundwater and mobilizes salt stored in

subsoils (J Bartle et al. 2008). By promoting mature stands of trees via irrigation through summer the trees then function as pumps to remove excess water throughout winter.

2. The desalination plant literally works as a pump through dry periods. Excess site water not intercepted is harvested and used as desalinated feedwater.

The ultimate aim to this project when applying this technology to agroforestry is to produce sufficient biomass on-site to power the desalination so that the only OPEX is the disposal of the dry salt waste product. To achieve this the plant running 8 months of the year produces 34ML and requires ~1180 tonne oil-mallee biomass. Assuming a yield of 10 tonnes/ha/yr would require 118 ha. The BZLD system would therefore irrigate this the equivalent of 28.8mm per year.

On sites where salinity is a bigger problem (e.g. more saline groundwater or more waterlogged) it would better to run the desalination plant all year. This would remove the excess winter water so that it doesn't end up recharging the groundwater and mobilizing salt, and that surplus water (some 17ML year for a 60ML capacity system) can go into a series of tanks or a small dam and be used for irrigation in Summer. The water is more diluted during winter, so it would mean less energy would be required to extract the water (the RO system could be run at higher recovery volumes for example).

A financially superior scenario would be mixed pasture & agroforestry where the desalination system is run on agricultural waste at $10/tonne delivered, and the oil-mallee is sold as an income. This approach using the 60ML production as a reference would mean 51ML produced at a cost of $19,000. To recoup this would mean producing 317 tonnes of oil-mallee and selling at $60 tonne, which would require 31.7 hectares of Mallee. This approach provides ~160mm per year. Many towns don't have a use for their green waste (or sewage sludge) and thus it could actually be available as a free source, or the cost of handling and haulage.

Another way of viewing this is that 60ML per year is prevented from going to deep drainage, mobilizing salts which in turn will make the farm a little less productive when it rises to the surface the following winter. If the alternative is slowly losing (for example) vineyards that provide an income of $2 million pa (South Australian Wine Industry Association Incorporated 2017), then $19,000/pa is a bargain.

It is actually difficult to quantify how much land gets desalinated by revegetation or agroforestry. One of the only examples is the 'Ucarro' farm in the upper reaches of the Blackwood River catchment, which to prevent further low-lying areas becoming more saline, was contoured with swales that had belts of Eucalypt species in 8m wide belts adjacent below the swale. The trees removed about 150mm of water over the rainfall amount. However to reduce annual deep drainage to 5mm, the amount that would have been the case prior to clearing, some 16-22% of the catchment would need to be tree belts (Turner and Ward 2002).

Chapter 5: Pilot Plant Design

Components

The following components are selected for the 'Low case' scenario where plantation waste is the biomass material. The entire flow diagram with all of the components specified in the following chapter is attached as Appendix D, Figure D.1.

Due to the compressor volumetric capacity of the available turbochargers on the market the volume of water treated was raised from 100 L/h to 120 L/h; to fuel this plus extra power requirements the rate of airflow was increased to 190 kg/h, combustor output was increased to 18.6 kW and the volume of biomass needed to be increased to 4.4 kg/h:

$$\text{Biomass (kg/hr)} = \frac{\dot{Q}}{\text{NCV x } \left(\frac{96}{100}\right)} = \frac{66960 \text{ kJ/hr}}{15840 \text{ x } \left(\frac{96}{100}\right)} = 4.4 \text{ kg/hr}$$

The updated flow chart showing these changes is attached as Appendix 4, Figure D.2.

Hammer mill

The W-6-H Laboratory Scale Hammer Mill (Schutte-Buffalo Hammermill 2018) is a gravity discharge hammer mill with a 9" (230mm) diameter rotor with swinging or fixed mounted hammers. It has a 0.25 - 2 kW power range, and a 390 cm^2 screen size weighing 100kg. This would be programmed to turn on once a day via the central process control unit to fill particle bin. Accessories include a galvanized pipe feed shute (with a round to square adaptor) from the modified front outlet into the Particle Bin.

Particle Bin

This is the storage for the daily amount of wood particles (122kg) fed to the combustion unit. Bin to be a 140L HDPE Wheelie/Sulo Bin with dimensions 535mm(L) x 615mm(B) x 925mm(H), weighs 10.4kg (peopleinplastic 2018).

Woodchip Hopper

An appropriate storage volume would be sufficient to be loaded once a week; $5.1\ kg/hr * 168 = 860\ kg$ consumed per week. Assuming the bulk density of plantation waste is 400 kg/m^3 (Connell Wagner Pty Ltd 2008) a minimum storage capacity of 2.05m^3 would be required.

A suitable set up for this would be 2x 1.2m^3 rectangular side-discharge Bulka Hopper Bins (Polymaster 2018) sited back-to-back with the side discharge facing inwards. A custom–made galvanized metal tee would be fitted to gravity feed both bins into the Feed Shute of the Hammer Mill. Extension legs would be required to site the Hammer Mill under the Hoppers, the height would need to be kept low enough so that the Hoppers can be filled via bobcat or front end loader.

Combustor

It is calculated that 21.5 kW of power is required to run the proposed Pilot Plant. A suitable model would be the MultiBio 30 Pellet Furnace which is rated to 10 - 30 kW (PetroJet Trade SRO 2018). Its Length is 1649mm (including burner); Width 697mm; Height 1550mm and Weight ~419kg. The combustor comes supplied with a fuel conveyor that automatically feeds the combustor at the required amount.

Air Turbocharger

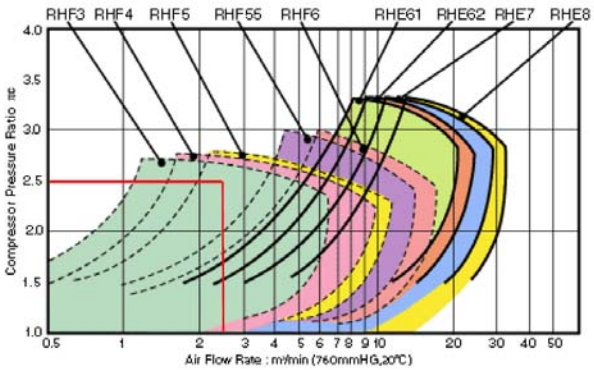

Figure 31: IHI RHF-Series Turbo Compression Map (Vespa Labs 2017)

A IHI Model RHF3 turbocharger is the best compressor to provide the necessary 2.5 pressure ratio at the adjusted flow rate of 190 kg/hr (2.35 m^3/min) as shown with the red line on Figure 29 (Vespa Labs 2017).

Accessories required include a hose able to tolerate the heat of the airflow at ~760°C, suitable would be a braided stainless steel metal hose with a screw-on fitting (Flexicraft Industries 2017) which is tolerant to temperatures up to ~1227°C. This hose needs to attach the cool outlet of the Air heat exchanger to the inlet of the turbocharger which is designed to be attached directly to the exhaust manifold of a car engine (see Figure 32) so a high-temperature tailor-made fitting would need to be made to achieve this (one of these would also need to be made for the Vapour Turbocharger).

Figure 32:IHI RHF3 TurboCharger Turbine Inlet (Vespa Labs 2017)

Figure 33: IHI RHF3 Turbocharger Compressor Outlet (Vespa Labs 2017)

The turbine outlet as well as the compressor inlet & outlet fittings all have the flange shown in the bottom right corner of Figure 33. The turbine outlet needs to be connected to braided metal pipe with screw fittings which connects to the turbine inlet of the Vapour Turbocharger.

The compressor inlet needs to have an electric actuated butterfly valve attached, most likely one with a flange fitting specified to fit directly to the turbocharger. This valve is electrically controlled, and controls the air flow throughout the system as required with feedback from the

flow meter. The compressor outlet is connected to the Cool Inlet of the Air Heat Exchanger via metal braided pipe.

Air Heat Exchanger

The Heat Exchanger selected was a Kaori H205. It was selected because it is made of heat-resistant stainless steel and able to sustain temperatures up to 900C. They are often used in fuel cells, combustion exhaust heat recovery and the chemical industry. 2x plates 0.11m^2 area each make up the 0.12m^2 required and achieve the 31.5kW heat duty (Kaori Heat Treatment Co. 2018).

Reverse Osmosis System

The model chosen was a Novatron BWE 3000. It is capable of producing up to 3,000 Litres every 24 Hours. This model was chosen because it was produced local to the potential Pilot Plant. It is designed specifically for Brackish Water and it was the model closest in treatment volume to the Pilot plant (120L/hr equivalent to 2,880L/Day).

Components/Features as detailed by the supplier include:

Cartridge filtration (5 & 1 Micron) prior to going into the High Pressure Pump

RO HP Pump: Brass or 316 Stainless Steel, Positive Displacement with a power rating of up to 1.1 kW. A pressure relief valve (rated to 600 PSI) is provided to avoid excess pressure overloading the RO system and damaging the membranes. Additional protective devices include Low Feed Pressure Switches, Motor Overloads and a Differential Pressure Gauge rated to 4,000 kPa.

The Reverse Osmosis component comprises 2x 25E40 pressure vessels each containing 2540 thin-film composite polyamide membranes. Flow Meters are provided for product and reject streams. Fittings are Brass, 316 Stainless Steel & Engineering Grade Plastics

The frame is constructed from epoxy-coated aluminium and measures 1250mm x 525mm x 920mm (Novatron 2017)

Water tank & Pump with Irrigation controller

Tank

Approximately 2450L of irrigation water is recovered daily. Assuming that the water is used for irrigation an appropriate irrigation interval set at every 48 hours would require 5000L minimum storage capacity (Tank Master 2018).

Irrigation pump

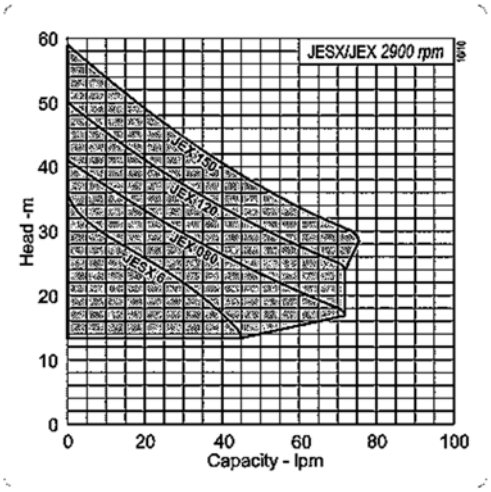

Figure 34: JEX Pump Flow Chart (Pumps Australia Pty Ltd 2018)

Model selected was a JEX M6-PC15 Stainless Steel pump. It's power rating is 0.44kW and it is fitted with an Automatic Controller as well as automatic float switch (inside water tank) (Pumps Australia Pty Ltd 2018). The same model (without the float switch) is to be used as the ground-water pump to feed the Reverse Osmosis system.

This pump was selected due to its low capacity requirements as a ground water pump (2 LPM) and being able to pump water from depths up to 8m. Assuming the water is utilised in an agroforestry or Alley Crop (e.g. Vineyards) then the irrigation type used would be drip irrigation. Commercial Netafim Techline drip irrigation has a pressure operating range up to 300 kPa (Netafim 2018). The maximum pump head available at 2 LPM according to Figure 34 is 34m.

$$h_a = \frac{p_2 - p_1}{\rho g} + \frac{h_2 - h_1}{2g}$$

Where h_a is actual head rise; h_1 is the initial height of the water (set to zero) and h_2 is the actual change in elevation available to the pump.

$$34m = \frac{300000\ N/m^2 - 100000 N/m^2}{(1000\ kg/m^3)\ (9.81\ m/s^2)} + \frac{h_2}{2 * (9.81\ m/s^2)}$$

$$\frac{h_2}{19.62} = 34 - \frac{200000}{9810}$$

$$h_2 = 267m$$

There are no issues with flow rate and height of irrigation elevation is 267m before the pump performance will begin to be compromised.

Brine Heat Exchanger

The duty calculated using ChemCad was 3.1 kW and the Shell area calculated was 0.32m^2

Heat exchanger model was determined using Exergy Online Heat Exchanger calculator (Exergy LLC 2018). Model chosen was Exergy Shell & Tube Heat Exchanger 54 Series, Model No. 00486-02.

All Components are 316L Stainless Steel. The shell has an outside diameter of 57mm and length of 457mm. The tube count is 127 with a tube length 381mm. This provides a total transfer area of 0.46m^2 (Exergy LLC 2018).

Evaporator Vessel with Condenser Pipes

The upsizing of the Pilot Plant increased the thermal load of the evaporator from 20.1kW to 24.4kW. A vertical falling-film profile was chosen due to the very small minimum heat transfer area required (0.11m^2). This is due to the relatively low feed rate as well as the ~100°C temperature difference between the vapour and the brine feed. The vertical falling film option is preferable as it limits the opportunities for scaling and fouling as the evaporation occurs on top of the film rather than on the metal surface (Thermopedia 2011).

Evaporator Design

The evaporator was designed following the guidelines of Edwards (2008).

Tube internal and external dimensions and length

Heat transfer is increased by reducing tube diameter and increasing tube number. There is a small flow so the smallest practical diameter pipe was chosen to assist in cost and cleaning. Tubes of an external diameter of 16 mm and an internal diameter 12mm were chosen for the design. The temperature difference creates a high heat transfer capacity combined with low flow meant that only short tube lengths were necessary; the chosen tube length was 0.35m.

Number of tubes required

External Tube Diameter $d_o = 16$mm; Tube Length: 0.3mm

Heat transfer area single tube: $\pi * 0.016 * 0.3 = 0.015\text{m}^2$

The surface area of pipes required to operate evaporator successfully: 0.11m^2

Number of tubes $N_t = \frac{0.11}{0.015} \approx 7$

Scaling up x3 – total number of pipes $= 21$

Suitable tube arrangement

Tube arrangement will be a triangular pitch.

Bundle diameter

$$D_{bundle} = d_o \left(\frac{N_t}{K_1}\right)^{\frac{1}{n_1}}$$

Triangular Pitch $p_t = 1.25\ d_o$					
Number Passes	1	2	4	6	8
K_1	0.319	0.249	0.175	0.0743	0.0365
n	2.142	2.207	2.285	2.499	2.675

Square Pitch $p_t = 1.25\ d_o$					
Number Passes	1	2	4	6	8
K_1	0.215	0.156	0.158	0.0402	0.0331
n	2.207	2.291	2.263	2.617	2.643

Table 9: Bundle Diameter Constants (Edwards 2008)

$K_1 = 0.319$

$n_1 = 2.142$

$$D_{bundle} = d_o \left(\frac{N_t}{K_1}\right)^{\frac{1}{n_1}} = 16\left(\frac{21}{0.319}\right)^{\frac{1}{2.142}} \approx 115\text{mm}$$

Evaporator shell internal diameter

Minimum bundle clearance for fixed-type tubes $= 10$mm,

so shell internal diameter is $115 + 10 = 125$mm

Vapour can collect moisture droplets (entrainment) as it rises so typically a barrier is provided to prevent this. The height of the vessel is usually 2-5 times the internal diameter of the shell, 500mm height chosen. Plate thickness is designed to withstand 2 bar pressure (recommended minimum 10mm thickness) (Edwards 2008).

Final design: Top fed Vertical Falling Film (Calandria or Roberts design) cylinder 500mm high & 135mm diameter

Dryer

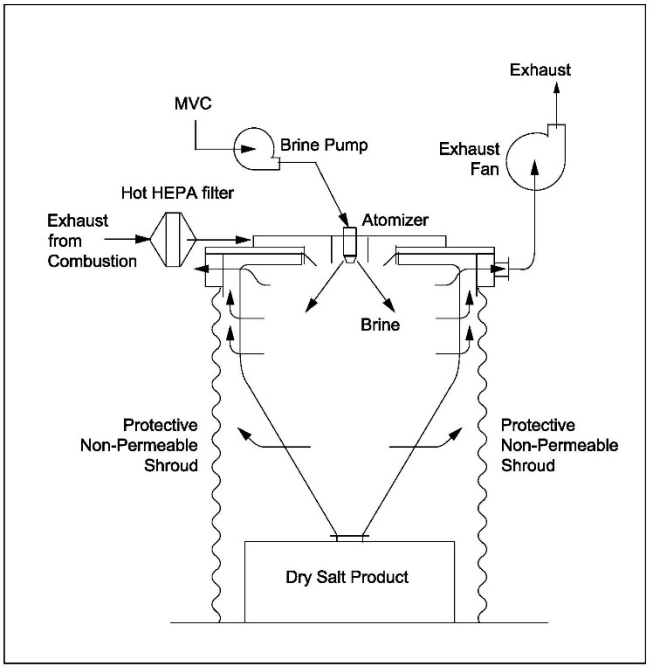

Figure 35: Process Flow BDP-Series Spray Bag Dryer (derived from Ohkawara Kakohki Co. Ltd. 2017)

The dryer model chosen is a BDP-30 Spray Bag Dryer. It has a removable and washable cloth-made filter chamber that operates as the drying vessel. Normally it operates at 150-200°C, however this system can be modified to accommodate 350°C as per the temperatures required for brine evaporation. As shown in Figure 35 a protective non-permeable heavy fabric shroud collects the air as it moves through the fabric and expels it via an exhaust fan as a safety measure.

The bag diameter is 2.23m and the external shroud dimensions are 2.46 x 3.95 x 4.78 (L x W x H). The entire unit (including frame) weighs 1600 kg. The system will evaporate up to 40 kg/h brine and is fitted with an OCA-023 model atomizer with an MC-84 rotary disc (Ohkawara Kakohki Co. Ltd. 2017). Accessories required include a Hot High-Efficiency Particulate Air (HEPA) filter which is suitable up to 350°C. This is used to filter incoming hot combustion

exhaust, as shown in Figure 35. Additionally, a 55-watt exhaust fan rated to extract 260m³/hr is also required.

Brine Pump

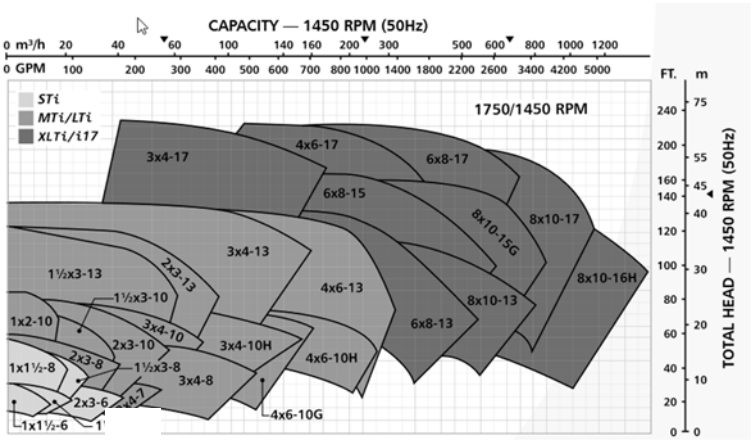

Figure 36: Goulds Process Pump Capacity vs Total Head (Goulds Pumps 2018)

A pump is required to provide sufficient pressure create a rotational spray to atomize the brine from the MVC inside the dryer. To do this the pump chosen is a Goulds STi Low-Flow 3196 i-*Frame* ANSI Process Pump with i-ALERT equipment health monitor. It has a power rating of 0.82 kW per 100RPM and the maximum liquid temperature it can tolerate without cooling is 177°C. The pump size selected is $1 \times 1\,{}^{1}/_{2} - 6$ as indicated in the bottom left corner of Figure 36. The total head operating at 1450 RPM is 5-10m and the flow rate is 0-10m³/hr. (Goulds Pumps 2018).

Salt Bin

The volume of salt produced per day is 31.7kg. If the system is emptied once a fortnight, then a receptacle with ~450L capacity is required. The product selected was a E363 500L Pallet Bin with Lid (Silverlock Packaging 2018).

Vapour Turbocharger with Power Generator

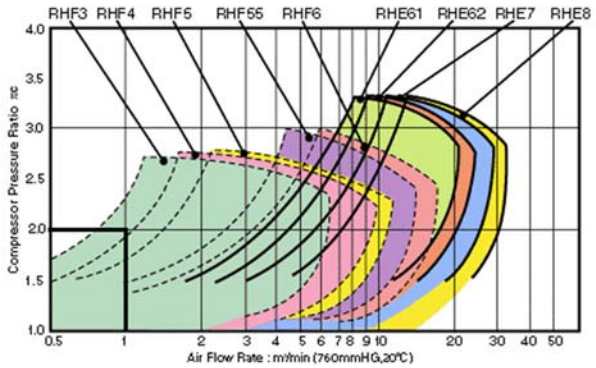

Figure 37: IHI RHF series Turbochargers Compression Map (Vespa Labs 2017)

The IHI RHF3 turbocharger provides the vapour compression and would be modified to generate power to run various electrical devices including RO & Irrigation pumps. To do this the Pressure ratio was dropped from 2.3 to 2 and the quantity of total water treated raised from 100 to 120 kg/hr) to allow sufficient vapour compression to occur (Vespa Labs 2017).

This increase was to produce 36 kg/hr of vapour, equivalent to 1 m^3/min as shown marked as red lines in Figure 37 with the pressure ratio of 2 as required. Within this area of the compressor map the efficiency will be lower than optimum, ~65%, however this is covered by the increased airflow through the connected turbine when modelled in ChemCad.

Power Turbine Calculations

The volume of flow going through the vapour turbine is 190kg/hr at 660°C, producing 3.82 kW at 75% efficiency; 1.65 kW is needed for vapour compression, the other 2.17 kW is to power the rest of the system by adapting an alternator so that it's shaft power is provided by the same vapour turbocharger. The power supply is needed for various pumps: The Reverse Osmosis high pressure pump (1.1 kW for 2.3 hr/day); the Reverse Osmosis groundwater pump (0.44 kW for 2.3 hr/day); the Irrigation Pump (0.44 kW operating 1 hr/day); Brine Pump (0.82 kW for 30mins every hour) as demonstrated in the Excel Table in Appendix B.

The Hammer Mill has a maximum capacity of 2 kW (Schutte-Buffalo Hammermill 2018). The power consumption of Hammer Mills for Eucalypt grinding was estimated at 500 MJ/tonne (Goble and Peck 2012). Biomass consumption was calculated as 0.86 tonne/week, which means

a power consumption of 120 kWh. Operating at maximum capacity the hammer mill would require 60 hours to process 900kg wood chips, the equivalent of running 8.5 hours/day.
Other power demands include the feed conveyor that is supplied with the combustion unit. This runs constantly with a power draw of ~0.25kWh, derived using an online bulk handling calculator (bulksolidsflow 2018). Power is required for the dryer exhaust fan (0.055 kW for 2.3 hours/day). In addition, Instrumentation and Process Control (including sensors & valves) require ~0.1 kWh for 24 hours/day.
When adjusted so that the power draw is evened out over 24 hours an extra 2.1kW of power per hour is required (see Appendix B). A 2.625 kVA alternator could be rigged to meet these requirements, a suitable model would be a Mecc Alte S15W-102/2 (Macfarlane Generators Pty Ltd 2018). Power drawn unevenly throughout the day means that in addition a 3 kVA Regulator, a Victron 2.5kW Inverter Charger system; 8x Delkor GC2 Deep cycle flooded cell batteries; a Victron BMV-700 Battery monitor and MPPT Control Screen with cabling and circuit breakers.

Sensors

Sensors required for process control include:
Magnetic Flow Meter to be sited between evaporator and brine pump. The sensor is to be specified to be attached to inlet flange of the brine pump, flange matching.
Temperature Sensor is required to monitoring exhaust heat from the combustion process. This sensor is integral to the system as it is an indication of the capacity of the system to do work, and it would be calibrated to the high pressure pump which would control the amount of brine produced and thus the volume of feedwater going into the brine heat exchanger.
Flow meters are to be sited between the RO unit and the brine heat exchanger to allow for monitoring the volume of feedwater going into the and between the air turbine and vapour turbine.

Pressure transmitters are to be sited

- between the High pressure pump and the RO unit to monitor RO production.
- inline between the air heat exchanger and the air turbine to monitor adequate pressure to ensure adequate vapour compressor performance and to prevent suction occurring at the outlet of the vapour turbine.
- inline between the vapour compressor and evaporator to ensure sufficient pressure to maintain the high boiling point required to ensure the evaporator operates adequately.

Pressure gauges where required.

Float level switch is required inside the water tank turns on irrigation pump automatically.

Valves

Valves required include AVCO ball valves; Spring return actuators; Analog control valves; low point and isolation valves; Check valves and Air solenoid valves with Ethernet/IP control.

Piping

The design requires minimal piping to maintain as much heat in the system as possible. Pipes need to be high-temperature tolerant stainless steel with thermal insulation e.g. Stenca HT Pipe (Stenca Solutions 2018). Accessories required include EPDM Expansion joints where necessary as well as industrial pipe supports.

Salinity Modelling

ChemCad (Chemstations 2018) was used to run various scenarios of the Pilot Plant configuration with salinity up to 85,000 mg/L. Reverse Osmosis power demand was adjusted as the salinity of the water increased. To achieve this the combined Groundwater and High Pressure pump power demand was set as the baseline, this being 0.147 kWh as per Appendix B, and the incremental increase was derived from the trend line derived from Poovanaesvaran et al. (2011), shown as Figure 38.

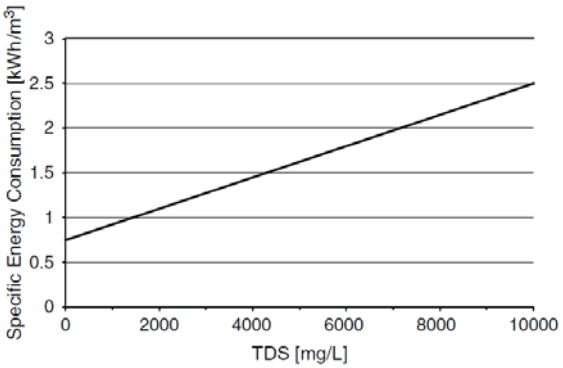

Figure 38: Energy consumption of the RO desalination sub-unit as a function of TDS

The cost of water production (based on plantation waste) was $1.51 up to 65,000 mg/L, and it rose slightly to a maximum of $1.54 at 85,000 mg/L. Specific Energy Consumption rose consistently as shown in Figure 39, with water reclamation volume dropping slowly as would be expected. Due to the consistent trend between 11000 – 40000 mg/L the trend was then recalculated from 65,000 mg/L strictly to ascertain the upper limit capacity of the system in salinity. The two sets of data were plotted together on Figure 39 to indicate the overall trend.

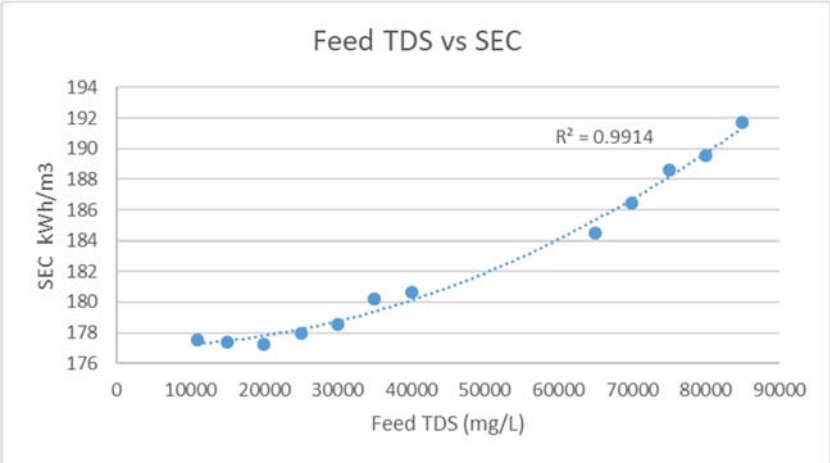

Figure 39 Feed TDS vs SEC:

The boiling point of the MVC brine gradually increased as the salinity of the feed increased. This temperature increase raises the vapour compression ratio required so the temperature drop in the evaporator required as well as the amount of heat directed to the dryer, making feedwater TDS of 85,000 mg/L the upper limit of this design.

3D Concept

The 3D model was based on the 60ML plant as the model was drawn for illustrative purposes and the size of the Pilot Plant was too small to identify particular components/parts. The models were selected from online collections in Sketchup 2017 (Trimble Inc. 2019) and GrabCad (STRATASYS 2019). Solidworks (Dassault Systèmes 2019) models were stripped to shells in Sketchup if necessary. The pipes & associated fittings were constructed in AutoCAD Plant 3D 2018 (Autodesk Inc. 2018b). The model was amalgamated in AutoCAD 2017 (Autodesk Inc. 2018a) and final renderings were created in Lumion Pro (Act-3D B.V. 2018).

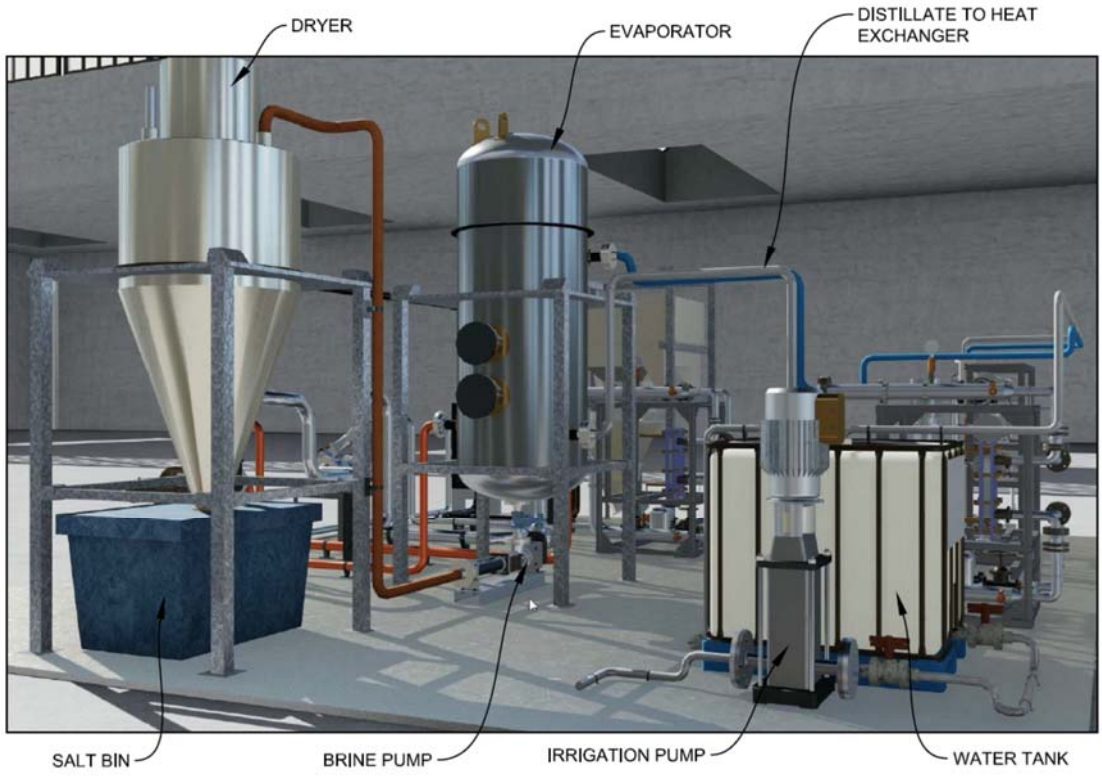

Figure 40: Northeast Corner 3D Concept

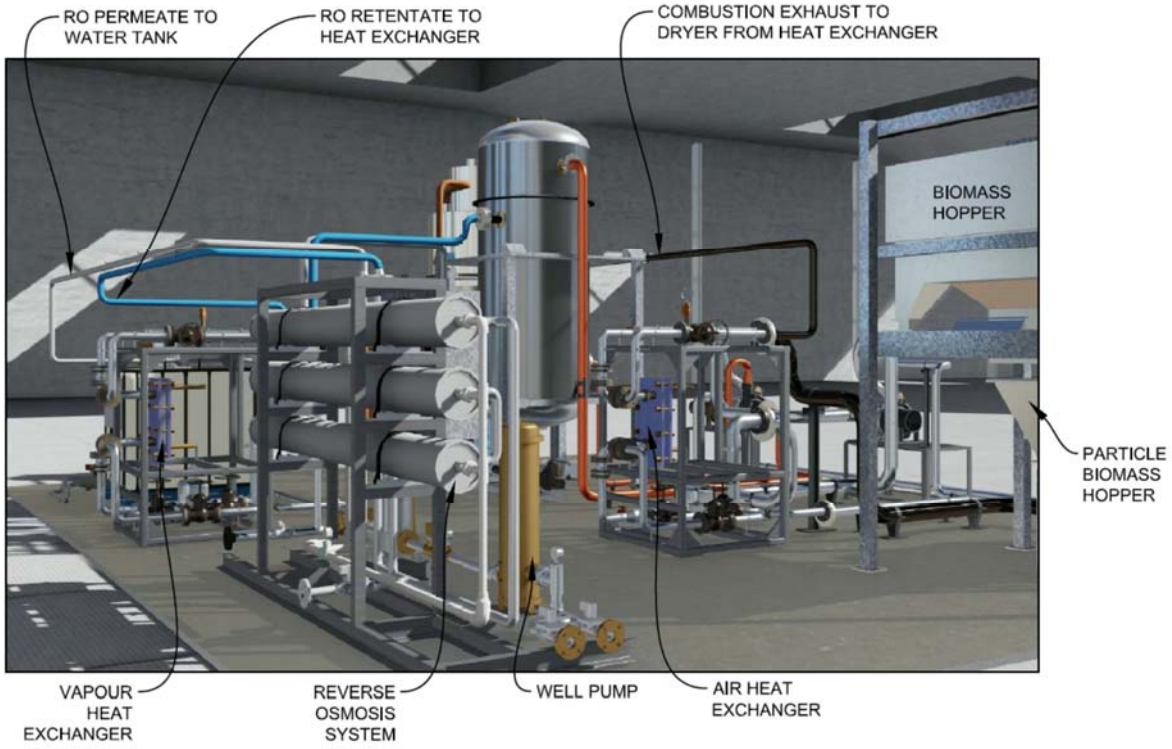

Figure 41: Northwest Corner 3D Concept

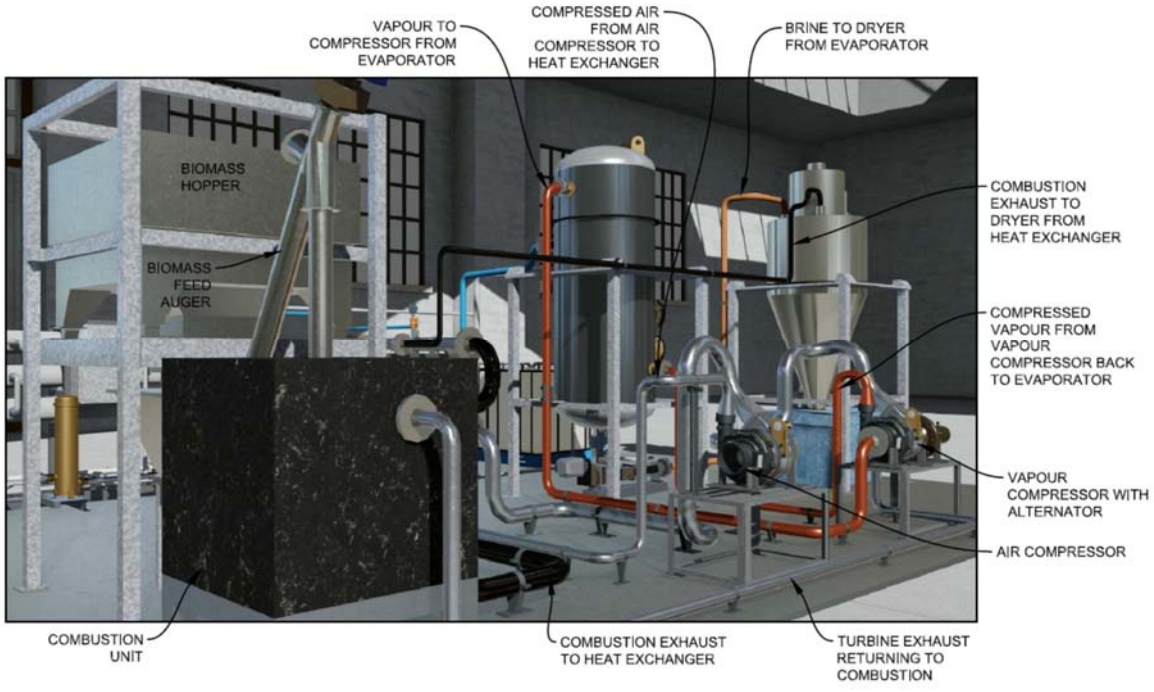

Figure 42: Southwest Corner 3D Concept

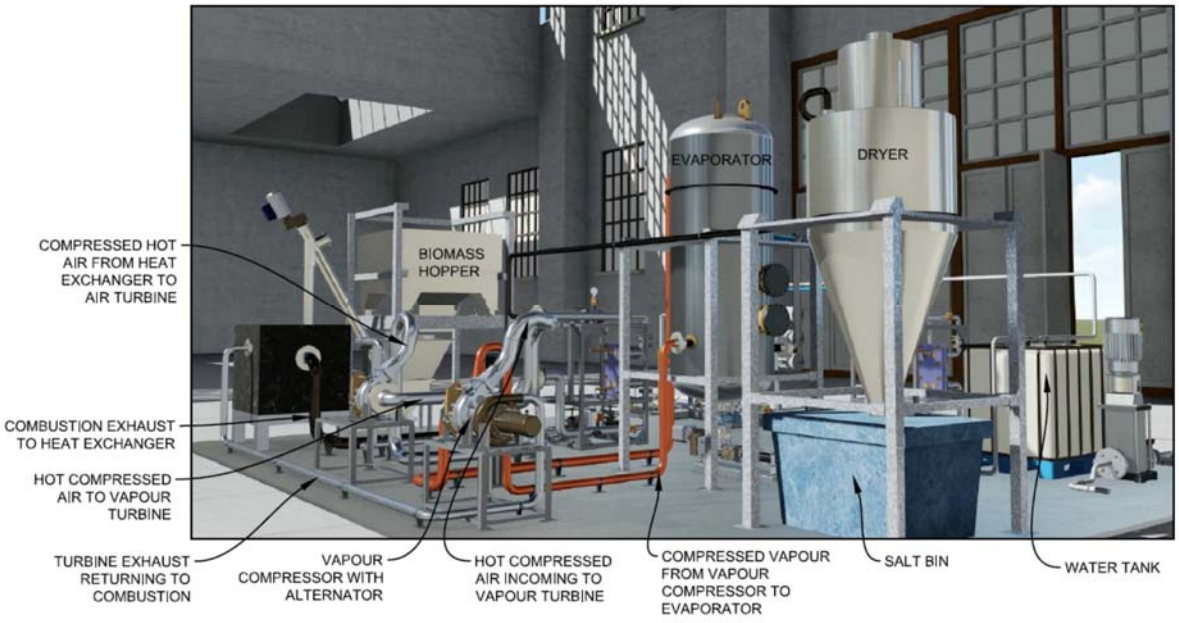

Figure 43: Southeast Corner 3D Concept

Chapter 6: Conclusion

The Objectives as outlined were achieved. The existing available technology was found to be either not up to the task of upgrading to a larger scale or if so required expensive technology and large evaporation ponds. The zero liquid discharge concept provided by Enerbi Pty Ltd was modelled in Excel and ChemCad and there were no technical issues with the concept that prevented it being scaled up to 'real world' scenarios at 60ML production levels. Scenarios where the Pilot Plant generates power solely from biomass input were discussed in some detail, looking at Agroforestry and Viticulture options.

Optimization

At the introduction to Chapter 3 the four 'corners' of the optimization process were mentioned. These are

- minimizing the volume of biomass required to treat the volume of water;
- minimizing the amount of heat lost to the environment through the dryer exhaust;
- minimizing the area of the heat exchangers
- minimizing the area of the evaporator.

This approach will be used to analyse the Enerbi model and examine future directions. The initial design as it was described by Enerbi Pty Ltd at 100L/hr did not ultimately change in design when upgraded to 60ML and to the final Pilot Plant design, apart from adjustments to provide sufficient vapour flow into the compressor to match the specific requirements of the turbocharger design. This section will emphasize possible problems that may occur with the design and how they may be addressed.

Biomass Feedstock

The factor that impacts the design the most is the quality and cost of the biomass feedstock. Given its variability the design of the system would most suit being custom-made to a site with

biomass locally sourced (preferably on-site) with local salinity issues that can be met sustainably with the use of the desalination system proposed. Examples include:

- Within a shipping container on a trailer, parked at a farm (or anywhere with a stockpile of biomass) for a short interval and producing drinking water for storage in the house tank, using the annual stockpile of waste biomass;
- Adjacent to a sewage farm to utilise the dry treated sewage biomass; onsite saline water treatment and desalinated water returned to mains water system;
- Allied to a green waste facility to augment municipal drinking water supply for country towns;
- On-site water for remote forestry operations.

Biomass feedstock becomes an issue particularly when it is highly variable in quality and HHV (e.g. municipal green waste) as this reduces the available heat and the system will operate at lower compression values leading to reduced MVC evaporation performance. If combustion exhaust temperatures drop low enough the ZLD product could be compromised as there is insufficient heat in the system to run compressors and fully evaporate the brine waste product. Heat exchangers designed for the specified heat input and as such will have an operating range within specific temperature differences will also be compromised and be reduced in efficiency.

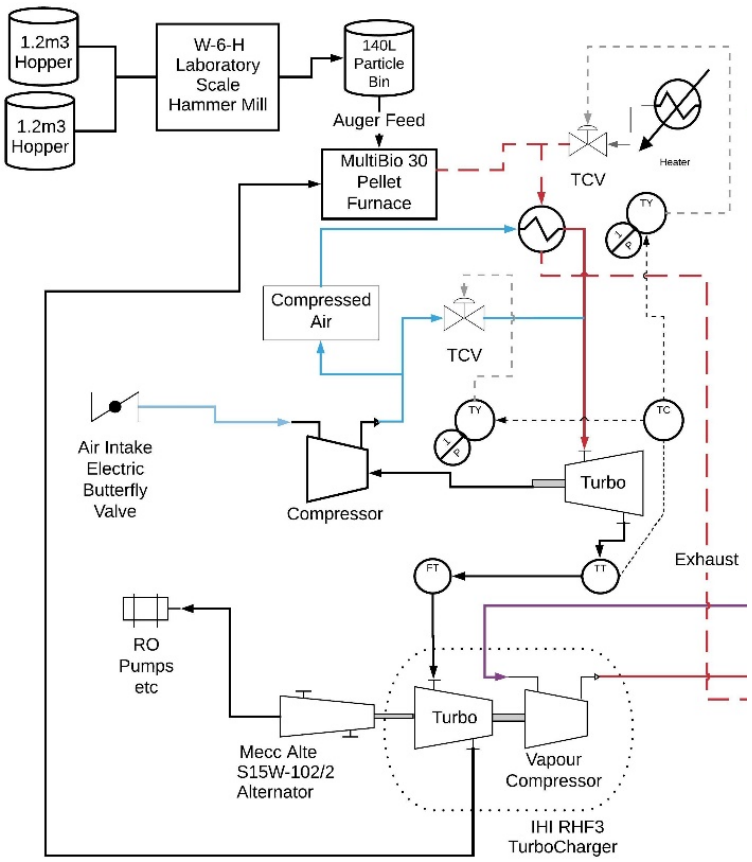

Figure 44: Flow Diagram with TCVs

A potential work-around would be to have back-up heat available to add to the system. This would be via a Temperature Control Valve (TCV in Figure 44) which would be controlled with a temperature controller (TC) with an established set-point with feedback from a temperature transmitter (TT) so that the temperature stays as close to 900°C. This could well be a syngas burner to tie in with the biomass utilization ethos.

This same set-up could also add cooler air in the situation that the temperature gets too high. This would be the case with the temperature going above 950°C which is the maximum temperature that the turbochargers selected can tolerate. The cooler air could be sourced from the Compressed Air line prior to it going through the heat exchanger, as shown with the TCV in the middle of Figure 44. Adding extra air to the line is likely to affect the volumetric flow rate so the same process can occur to maintain the amount of air in the lines at a set-point using a Flow Transmitter (FT) to provide the feedback to adjust the Air Intake Electric Butterfly Valve. (The Control system for this is not shown).

Further research would model the control system that monitors the heat parameters and if necessary adjusts the vapour flow into the vapour compressor. To do this it would probably be a case of optimizing the design of the evaporator to have extra vapour storage capacity

sufficient to allow for possible drops in compressor rpm due to changes in turbine rpm. Once the control system is fully modelled then the upper and lower temperatures of the system can be established which would allow for the surface areas of the heat exchangers & the evaporator to be optimized.

The dryer needs to be optimized so that the brine flowing into the dryer is always evaporated. This could be achieved with another Temperature Transmitter at the dryer hot air inlet which would provide feedback to a temperature controller, which could be connected to a TVC with the extra heat coming from the same heater that feeds in adjacent to the combustion unit.

The system would need to be optimized so that there is always enough power. Any extra power draw would need to be met in the battery storage & alternator configuration. The system is thus optimized so that the CHP side of the system has checks and balances via Process Control to maintain the heat level required. This means that the RO and MVC side of the system can be set to run automatically with very little Process Control required apart from flow and pressure meters that create an alert if something stops working.

Bibliography

Act-3D B.V. 2018. “Lumion 9.” 2018. https://lumion.com/product.html.

Al-Juwayhel, Faisal, Hisham El-Dessouky, and Hisham Ettouney. 1997. “Analysis of Single-Effect Evaporator Desalination Systems Combined with Vapor Compression Heat Pumps.” *Desalination* 114 (3): 253–75. https://doi.org/10.1016/S0011-9164(98)00017-4.

Al-Karaghouli, Ali, and Lawrence L. Kazmerski. 2013. “Energy Consumption and Water Production Cost of Conventional and Renewable-Energy-Powered Desalination Processes.” *Renewable and Sustainable Energy Reviews* 24: 343–56.

Aly, Narmine H., and Adel K. El-Fiqi. 2003. “Mechanical Vapor Compression Desalination Systems - A Case Study.” *Desalination* 158 (1–3): 143–50.

Amy, Gary, Noreddine Ghaffour, Zhenyu Li, Lijo Francis, Rodrigo Valladares Linares, Thomas Missimer, and Sabine Lattemann. 2017. “Membrane-Based Seawater Desalination: Present and Future Prospects.” *Desalination* 401. Elsevier B.V.: 16–21.

Aquaback Pty Ltd. 2018. “How Vapor Compression Distillation Works.” 2018. http://aquaback.com/technology/how-it-works.

Arakel, Aharon, and Mike Mickley. 2011. “Inland Desalination Brine Management.” In *National Desalination Research Roadmapping Workshop*, edited by Mike Mickley and Jim Jordahl. Alexandria, VA.

Autodesk Inc. 2018a. “AutoCAD.” 2018. https://www.autodesk.com.au/campaigns/original-autocad.

———. 2018b. “AutoCAD Plant 3D.” 2018. https://www.autodesk.com/campaigns/bim-for-plant.

Babcock & Wilcox Co. 2017. *Steam, Its Generation and Use: With Catalogue of the Manufactures of the Babcock & Wilcox Co., New York, and Babcock & Wilcox, Limited, London*. CHIZINE PUBN. https://books.google.com.au/books?id=xVzatAEACAAJ.

Bartle, J, M Bennell, T J Hobbs, and D Huxtable. 2008. "New Woody Crops and Industries for the Wheat Belt of Southern Australia." In *2nd International Salinity Forum*. Adelaide, SA: International Salinity Forum.

Bartle, John, Don Cooper, Graeme Olsen, and Jerome Carslake. 2002. "Acacia Species as Large-Scale Crop Plants in the Western Australian Wheatbelt." *Conservation Science Western Australia* 4 (3): 96–108.

Bartle, John R., and Amir Abadi. 2010. "Toward Sustainable Production of Second Generation Bioenergy Feedstocks." *Energy and Fuels* 24 (1): 2–9. https://doi.org/10.1021/ef9006438.

Brandhuber, Philip J., Adriano Vieira, Karla Kinser, and Jennifer Gelmini. 2014. "Pilot Testing of Membrane Zero Liquid Discharge for Drinking Water Systems." *WERF Project WERF5T10a*. http://www.werf.org/a/ka/Search/ResearchProfile.aspx?ReportId=WERF5T10.

Briggs, Ian. 2012. "Modelling a Turbogenerator for Waste Heat Recovery on a Diesel-Electric Hybrid Bus." *15th Annual Sir Bernard Crossland Symposium*. http://www4.dcu.ie/sites/default/files/conference_sbc/Ian Briggs_Queens.pdf.

Brooksbank, Kim, Mitchell Lever, Harriet Paterson, and Melissa Weybury. 2014. "Biomass Scoping Study Opportunities for Agriculture in Western Australia." Perth.

bulksolidsflow. 2018. "Bulk Handling Global." 2018. http://bulksolidsflow.com.au/free_programs/screw_conveyor_design/screw_conveyor_design.html.

Bureau of Meteorology. 2018. “BOM.” 2018. http://www.bom.gov.au/.

Chemstations. 2018. “CHEMCAD 7.” 2018. https://www.chemstations.com/.

Clark, Graeme F., Nathan A. Knott, Brett M. Miller, Brendan P. Kelaher, Melinda A. Coleman, Shinjiro Ushiama, and Emma L. Johnston. 2018. “First Large-Scale Ecological Impact Study of Desalination Outfall Reveals Trade-Offs in Effects of Hypersalinity and Hydrodynamics.” *Water Research* 145. Elsevier Ltd: 757–68. https://doi.org/10.1016/j.watres.2018.08.071.

Cohen, Yoram, Raphael Semiat, and Anditya Rahardianto. 2017. “A Perspective on Reverse Osmosis Water Desalination.” *AIChE Journal* 63 (6): 1771–84.

Connell, Michael J O, Nicholas F Wakim, and Nicholas F Wakim. 2011. “Low Temperature Thermal Distillation With Zld and Selective Solids Harvesting.” In *IDAWC/PER11-228*. Perth WA: IDA.

Connell Wagner Pty Ltd. 2008. “Proposed Biomass Power Plant , Palings Road , Diamond Tree , Manjimup - EPA Assessment.” Perth WA.

Dassault Systèmes. 2019. “SOLIDWORKS 2019.” 2019. https://www.solidworks.com/.

desaln8. 2018. “Victorian Winery Installs Fi Rst In Situ Desalination System.” Notting Hill, Victoria.

Dunin, Frank X. 2002. “Integrating Agroforestry and Perennial Pastures to Mitigate Water Logging and Secondary Salinity.” *Agricultural Water Management* 53 (1–3): 259–70.

Duong, Hung C., Paul Cooper, Bart Nelemans, Tzahi Y. Cath, and Long D. Nghiem. 2015. “Optimising Thermal Efficiency of Direct Contact Membrane Distillation by Brine Recycling for Small-Scale Seawater Desalination.” *Desalination* 374: 1–9.

Edwards, John E. 2008. “Design and Rating Shell and Tube Heat Exchangers.” *Chemical Engineering*, 30.

El-Feky, A K. 2016. “Mechanical Vapor Compression (MVC) Desalination System Optimal Design.” *Arab Journal of Nuclear Science and Applications* 94 (3): 1–13. http://www.esnsa-eg.com/download/researchFiles/(1) 54 -2015.pdf.

El-Manharawy, Samir, and Azza Hafez. 2001. “Water Type and Guidelines for RO System Design.” *Desalination* 139 (1–3): 97–113.

Enerbi Pty Ltd. 2017. “Zero Liquid Discharge Desalination Using Biomass.”

Ettouney, Hisham. 2006. “Design of Single-Effect Mechanical Vapor Compression.” *Desalination* 190 (1–3): 1–15.

Exergy LLC. 2018. “Model # 00486-02, Shell & Tube Heat Exchanger.” 2018. http://heat-exchangers.exergyllc.com/item/shell-tube-heat-exchangers/54-series-shell-tube-heat-exchangers/00486-02.

Flexicraft Industries. 2017. “SB1 BRAIDED STAINLESS.” 2017. http://www.flexicraft.com/Industrial_Hose/SB1/.

Foster, P. J., A. Burgoyne, and M. M. Vahdati. 2001. “Improved Process Topology for Membrane Distillation.” *Separation and Purification Technology* 21 (3): 205–17. https://doi.org/10.1016/S1383-5866(00)00201-X.

Foundation, Water Research. 2010. “Guidelines for Implementing Seawater and Brackish Water Desalination Facilities.” USA: Water Research Foundation and Arsenic Water Technology Partnership. http://www.waterrf.org/PublicReportLibrary/4078.pdf.

Franca, Nelson Da, and Ribeiro Dos Anjos. 1998. “Source Book of Alternative Technologies for Freshwater Augmentation in Latin America and the Caribbean.” *International Journal of Water Resources Development* 14 (3): 365–98.

Fritzmann, C., J. Löwenberg, T. Wintgens, and T. Melin. 2007. “State-of-the-Art of Reverse

Osmosis Desalination." *Desalination* 216 (1–3): 1–76.

García-Rodríguez, Lourdes. 2003. "Renewable Energy Applications in Desalination: State of the Art." *Solar Energy* 75 (5): 381–93.

Geo-Processors Pty Ltd. 2008. Process and apparatus for the treatment of saline water. 2003254392, issued 2008.

Ghalavand, Younes, Mohammad Sadegh Hatamipour, and Amir Rahimi. 2015. "A Review on Energy Consumption of Desalination Processes." *Desalination and Water Treatment* 54 (6): 1526–41.

Goble, Dean, and Malcolm Peck. 2012. "Opportunities for Using Sawmill Residues in Australia." Melbourne, Victoria.

Goulds Pumps. 2018. "3196 I-FRAME Process Pump." 2018. https://www.gouldspumps.com/ittgp/medialibrary/goulds/website/Products/3196-i-FRAME/3196_i_FRAME_bulletin.pdf?ext=.pdf.

Gray, S, Raphael Semiat, Mikel Duke, Anditya Rahardianto, and Yoram Cohen. 2011. "Seawater Use and Desalination Technology, Treatise on Water Science." *Water Quality Engineering* 4: 73–109.

Hatton, T. J., G. A. Bartle, R. P. Silberstein, R. B. Salama, G. Hodgson, P. R. Ward, P. Lambert, and D. R. Williamson. 2002. "Predicting and Controlling Water Logging and Groundwater Flow in Sloping Duplex Soils in Western Australia." *Agricultural Water Management* 53 (1–3): 57–81. https://doi.org/10.1016/S0378-3774(01)00156-1.

Igunnu, Ebenezer T., and George Z. Chen. 2014. "Produced Water Treatment Technologies." *International Journal of Low-Carbon Technologies* 9 (3): 157–77.

Joo, Sung Hee, and Berrin Tansel. 2015. "Novel Technologies for Reverse Osmosis Concentrate

Treatment: A Review." *Journal of Environmental Management* 150. Elsevier Ltd: 322–35.

Kaori Heat Treatment Co., Ltd. 2018. "H205." 2018. https://www.kaori-bphe.com/en/Products/p/H205.

Khan, Stuart J., David Murchland, Michelle Rhodes, and T. David Waite. 2009. "Management of Concentrated Waste Streams from High-Pressure Membrane Water Treatment Systems." *Critical Reviews in Environmental Science and Technology* 39 (5): 367–415.

Landshark. 2018. "Landshark Wastewater Evaporator." 2018. https://www.resourcewest.net/landshark-wastewater-evaporator/.

Li, Mingheng. 2012. "Optimal Plant Operation of Brackish Water Reverse Osmosis (BWRO) Desalination." *Desalination* 293. Elsevier B.V.: 61–68.

Macfarlane Generators Pty Ltd. 2018. "Macfarlane Generators." 2018. https://www.macfarlanegenerators.com.au/products/710/Mecc-Alte-S-Series-Alternator-2-Pole.

Martin, Jeremy, and Douglas Eisberg. 2007. "Brackish Water Desalination – Energy and Cost Considerations." In *International Desalination Association World Congress Desalination and Water Reuse 2007*, 22:99–131. https://doi.org/10.1016/S0733-8619(03)00096-3.

Martinetti, C. Riziero, Amy E. Childress, and Tzahi Y. Cath. 2009. "High Recovery of Concentrated RO Brines Using Forward Osmosis and Membrane Distillation." *Journal of Membrane Science* 331 (1–2): 31–39.

McCool, Brian C., Anditya Rahardianto, Jose I. Faria, and Yoram Cohen. 2013. "Evaluation of Chemically-Enhanced Seeded Precipitation of RO Concentrate for High Recovery Desalting of High Salinity Brackish Water." *Desalination* 317: 116–26.

Mickley, Michael. 2008. *Survey of High-Recovery and Zero Liquid Discharge Technologies for*

Water Utilities. *Membrane Technology*. Vol. 2008. Alexandria, VA: WateReuse Foundation.

Mickley, Mike. 2001. “Membrane Concentrate Disposal.” Washington D.C.

———. 2007. “Survey of High-Recovery and Zero Liquid Discharge Technologies for Water Utilities.” Alexandria, VA: WateReuse Foundation.

———. 2010. “BRACKISH GROUNDWATER CONCENTRATE MANAGEMENT.” Boulder, Colorado.

Miller, Sydney, Hilla Shemer, and Raphael Semiat. 2014. “Energy and Environmental Issues in Desalination.” *Desalination* 366. Elsevier B.V.: 2–8.

Murray, Brendan, David Mcminn, and Jack Gilron. 2015. “Waiv Technology : An Alternative Solution for Brine Management.” *Water - Journal of the Australian Water Association* 42 (August): 77.

Netafim. 2018. “SMART SOLUTIONS FOR SUB-SURFACE LANDSCAPE APPLICATIONS.” 2018. https://cdn.shopify.com/s/files/1/1845/4805/files/Netafim_Techline_AS_XR_brochure_web_1.pdf?4838826560808569814.

Nguyen-Schäfer, Hung, ed. 2015. “Thermodynamics of Turbochargers.” In *Rotordynamics of Automotive Turbochargers*. Switzerland: Springer International Publishing.

Ning, Robert Y., and Thomas L. Troyer. 2009. “Tandom Reverse Osmosis Process for Zero-Liquid Discharge.” *Desalination* 237 (1–3): 238–42.

Novatron. 2017. “Novatron BWE 3000.” 2017. http://www.novatron.net.au/equip_bwe3k.php.

NSW Public Works. 2011. “Brackish Groundwater: A Viable Community Water Supply Option?” *Waterlines Report Series*. Canberra.

peopleinplastic. 2018. “140L Wheelie Bin [WB140].” 2018.

https://peopleinplastic.com.au/product/wb140r_-_140l_wheelie_bin_red/.

Petrojet Trade s.r.o. 2017. “Model 30kW - Pellet Furnaces.” 2017. https://www.environmental-expert.com/products/model-30kw-pellet-furnaces-411565.

PetroJet Trade SRO. 2018. “Model 30kW - Pellet Furnaces.” 2018. https://www.environmental-expert.com/products/model-30kw-pellet-furnaces-411565.

Polymaster. 2018. “Bulka Bin 1.2 Cubic Metre.” 2018. https://www.polymaster.com.au/catalogue/agriculture/storage--farm-equipment/bulk-storage/bulka-bin-12-cubic-metre.

Poovanaesvaran, P., M.A. Alghoul, K. Sopian, N. Amin, M.I. Fadhel, and M. Yahya. 2011. “Design Aspects of Small-Scale Photovoltaic Brackish Water Reverse Osmosis (PV-BWRO) System.” *Desalination and Water Treatment* 27 (1–3): 210–23. http://www.tandfonline.com/doi/abs/10.5004/dwt.2011.1824.

Pumps Australia Pty Ltd. 2018. “JEX M6-PC15.” 2018. http://www.pumpsaustralia.com.au/en/jex-m6-pc15.

Rao, Prakash, Arian Aghajanzadeh, Paul Sheaffer, William R Morrow, Sabine Brueske, Caroline Dollinger, Kevin Price, Prateeti Sarker, and Joe Cresko. 2016. “Volume 1: Survey of Available Information in Support of the Energy-Water Bandwidth Study of Desalination Systems.” Vol. 1.

Rioyo, J., V. Aravinthan, J. Bundschuh, and M. Lynch. 2017. “A Review of Strategies for RO Brine Minimization in Inland Desalination Plants.” *Desalination and Water Treatment* 90: 110–23.

Robinson, N., R. J. Harper, and K. R.J. Smettem. 2006. “Soil Water Depletion by Eucalyptus Spp. Integrated into Dryland Agricultural Systems.” *Plant and Soil* 286 (1–2): 141–51.

https://doi.org/10.1007/s11104-006-9032-4.

RPS Environment and Planning. 2009. “Effects of Saline Discharges on the Marine Environment of Barrow Island.” Perth WA.

Sanciolo, P., N. Milne, K. Taylor, M. Mullet, and S. Gray. 2014. “Silica Scale Mitigation for High Recovery Reverse Osmosis of Groundwater for a Mining Process.” *Desalination* 340 (1): 49–58.

Schutte-Buffalo Hammermill. 2018. “W Series Laboratory Scale Hammer Mills.” 2018. https://www.hammermills.com/wp-content/uploads/2017/05/Laboratory-Scale-Hammer-Mill.Brochure.pdf.

Semiat, Raphael. 2000. “Desalination : Present and Future.” *Water* 25: 54–65.

———. 2008. “Energy Issues in Desalination Processes.” *Environmental Science and Technology* 42: 8193–8201.

Semiat, Raphael, and David Hasson. 2010. “Seawater and Brackish-Water Desalination with Membrane Operations.” In *Membrane Technology*, edited by K-V Peinemann and SP Nunez. Wiley -VCH Verlag GmbH & Co.

Semiat, Raphael, Jacob Sapoznik, and David Hasson. 2010. “Energy Aspects in Osmotic Processes.” *Desalination and Water Treatment* 15 (1–3): 228–35.

Silberstein, R. P., R. A. Vertessy, J. Morris, and P. M. Feikema. 1999. “Modelling the Effects of Soil Moisture and Solute Conditions on Long-Term Tree Growth and Water Use: A Case Study from the Shepparton Irrigation Area, Australia.” *Agricultural Water Management* 39 (2–3): 283–315. https://doi.org/10.1016/S0378-3774(98)00083-3.

Silverlock Packaging. 2018. “E363 500L Pallet Bin Various Colours.” 2018. http://www.silverlock.com.au/e363-500l-pallet-bin-various-colours.

Silverstein, Jeffrey L. 2016. “Using CHEMCAD to Solve EPA Air Emission Problems: Estimating Emissions While Charging Solvents to an Empty Vessel.”

Song, Lianfa, J Y Hu, S L Ong, W J Ng, Menachem Elimelech, and Mark Wilt. 2003. “Emergence of Thermodynamic Restriction and Its Implications for Full-Scale Reverse Osmosis Processes” 155: 213–28.

South Australian Wine Industry Association Incorporated. 2017. “South Australian Wine Industry – July 2017 Snapshot.” Adelaide, SA.

Stenca Solutions. 2018. “Thermal Insulation for High Temperature Pipes.” 2018. http://stenca.com/Stenca_HT_Pipe.

STRATASYS. 2019. “Grabcad.” 2019. https://grabcad.com/.

Sudmeyer, R.A, and F. Flugge. 2005. “The Economics of Managing Tree-Crop Competition in Windbreak and Alley Systems.” *Australian Journal of Experimental Agriculture* 45 (11): 1403–14. https://doi.org/10.1071/EA04155.

Sudmeyer, Robert A, and David J.M. Hall. 2015. “Competition for Water between Annual Crops and Short Rotation Mallee in Dry Climate Agroforestry: The Case for Crop Segregation Rather than Integration.” *Biomass and Bioenergy* 73. Elsevier Ltd: 195–208.

Swaminathan, Jaichander, Kishor G. Nayar, and John H. Lienhard V. 2016. “Mechanical Vapor Compression—Membrane Distillation Hybrids for Reduced Specific Energy Consumption.” *Desalination and Water Treatment* 57 (55): 26507–17.

Tank Master. 2018. “Poly Round Tanks.” 2018. https://tankmaster.com.au/water-tanks/poly-round-tanks/.

Thermopedia. 2011. “EVAPORATORS.” 2011. http://www.thermopedia.com/content/744/.

Trimble Inc. 2019. “Sketchup.” 2019. https://www.sketchup.com/.

Turner, Neil C., and Philip R. Ward. 2002. “The Role of Agroforestry and Perennial Pasture in Mitigating Water Logging and Secondary Salinity: Summary.” *Agricultural Water Management* 53 (1–3): 271–75.

Veolia Water Technologies. 2017. “Desalination Plant.” 2017. http://www.veoliawatertechnologies.co.za/water-solutions/desalination/desalination-plant/.

Vespa Labs. 2017. “IHI RHB31 Turbo Charger.” 2017. http://www.vespalabs.org/lab-notebook/shelved-till-later/ihi-rhb31-turbo-charger.

Veza, JoséM. 1995. “Mechanical Vapour Compression Desalination Plants - A Case Study.” *Desalination* 101 (1): 1–10.

VirgiliPankratz, F, and TJ. Gasson. 2016. “IDA Desalination Yearbook - 2015-2016.” Oxford, UK.

Ward, P. R., F. X. Dunin, and S. F. Micin. 2002. “Water Use and Root Growth by Annual and Perennial Pastures and Subsequent Crops in a Phase Rotation.” *Agricultural Water Management* 53 (1–3): 83–97. https://doi.org/10.1016/S0378-3774(01)00157-3.

Warsinger, David M., Karan H. Mistry, Kishor G. Nayar, Hyung Won Chung, and John H.V. Lienhard. 2015. “Entropy Generation of Desalination Powered by Variable Temperature Waste Heat.” *Entropy* 17 (11): 7530–66. https://doi.org/10.3390/e17117530.

Watson, Ian C, O J Morin, and Lisa Henthorne. 2003. “Desalting Handbook for Planners.” *Desalination and Water Purification Research and Development Program Report*. Denver, Co.

Wildy, Daniel Thomas. 2003. “Growing Mallee Eucalypts as Short-Rotation Tree Crops in the Semi-Arid Wheatbelt of Western Australia.” *Water*, no. June.

Xu, Pei, Tzahi Y. Cath, Alexander P. Robertson, Martin Reinhard, James O. Leckie, and Jörg E.

Drewes. 2013. “Critical Review of Desalination Concentrate Management, Treatment and Beneficial Use.” *Environmental Engineering Science* 30 (8): 502–14.

Yani, Syamsuddin. 2015. “Distillation of Mallee Biomass for Eucalyptus Oil Extraction and Thermochemical Behaviour of the Spent Biomass.” Curtin University.

Zaragoza, G. 2018. “Commercial Scale Membrane Distillation for Solar Desalination.” *Clean Water* 20. https://doi.org/10.1038/s41545-018-0020-z.

Zhani, K., K. Zarzoum, H. Ben Bacha, J. Koschikowski, and D. Pfeifle. 2016. “Autonomous Solar Powered Membrane Distillation Systems: State of the Art.” *Desalination and Water Treatment* 57 (48–49): 23038–51.

Zhu, Aihua, Panagiotis D. Christofides, and Yoram Cohen. 2009. “Effect of Thermodynamic Restriction on Energy Cost Optimization of RO Membrane Water Desalination.” *Industrial and Engineering Chemistry Research* 48 (13): 6010–21.

Appendix

APPENDIX A

This appendix is the Excel Raw Data that was used to calculate the initial model of the Enerbi BWRO concept, and it was these inputs that were used to create the ChemCad model.

Table A.1 is the feedwater data used that provided the initial volume of water & salts in the system, including TDS levels.

FEEDWATER							
	Fresh product (L)	Salt mg Product	Salt g Product	Salt kg Product	Total	kg/h	mg/L
RO in	98.9	1100000	1100	1.1	100		11000
RO fresh out	55					55	
RO Brine out	43.9	1100000	1100	1.1	45	45	24444.4444
MVC Fresh out	31					31	
MVC Brine out	12.9	1100000	1100	1.1	14	14	78571.4286
Fresh Product	86						

Table A.1: Feedwater 100L/hr – Excel

Table A.2 is the Dryer calculations used to model the heat required to create a ZLD product.

Flowchart designation	Description	Units	Value	Q_evap	Total
$\dot{m}$_mvc brine	mass flow rate	kg/s	14	27142.245	27142.25
		kg/min	840		
			50400		
TS	%solids of brine feed	ratio	0.078571429		
TM	%moisture of brine feed		0.921428571		
	Moisture in		12.9		
Solids					
u_powder	% powder moisture content allowed	ratio	0		
C_powder	specific heat capacity of dry powder	kJ/kgK	1.26		
Water					
ΔH_water	Latent heat of water evap	kJ/kg	2076		
		BTU/pound	967		
C_v,dryer exh	specific heat capacity of water vapour @ outlet	kJ/kgK	1.87		
Heat Capacity					
C_(v,dryer exh)	specific heat capacity of air at dryer's outlet temperature	kJ/kgK	1.051		
Temperature			K	Celcius	
t_outlet	Exhaust air temperature at outlet	Degrees K	388	115	
t_brine	MVC brine temperature	Degrees K	373	100	

Table A.2: Spray Dryer 100L/hr – Excel

Distillate [°C]	C_P [kJ/(kg K)]	C_P* (T_"distillate" -35)
100	4.2157	274.0205
110	4.2283	317.1225
120	4.2435	360.6975
140	4.2826	449.673
160	4.3354	541.925
180	4.405	638.725
200	4.4958	741.807
220	4.6146	853.701
240	4.7719	978.2395

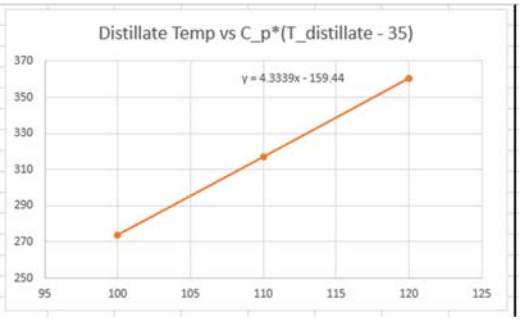

Table A.3 Distillate Temp vs Heat Capacity

Flowchart designation	Units	Value	Brine flow rate m_b (kg/h)	Distillate flow rate (kg/h)	Area of Evaporator	Area of Heat Exchanger	Evaporator thermal load kJ/hr
MVC feed flow rate	kg/h	45	14	31	0.0697885944	0.552752248	68136
MVC feed flow rate	m3/h	0.04					18.92666667
cPv	kJ/kgC	1.87	Brine flow rate m_b (m3/h)	Brine flow rate m_b (m3/h)			
cP kJ/kgC (heat exchanger)	kJ/kgC	4.1	0.01	0.03			
cP kJ/kgC (brine @ 8%)	kJ/kgC	3.8					
cP kJ/kgC (mvc feed @ 85°C)	kJ/kgC	4.2					
U_evaporat	kW/m^2°C	2.4					
U_(heat-ex)	kW/m^2°C	0.37					
T_RO retent (incoming temp)	°C	25					
T_distill (outgoing temp)	°C	116					
T_(mvc comp out)	°C	213					
T_brine & vapor	°C	100					
T_mvc Feed	°C	80.00					
T_(mvc-perm)	°C	35.00					
X_feed	g/L	0.00					
X_brine	g/L	78.57					
specific heat ratio		1.33					
Compressor efficiency		0.8					
LMTD heat exchanger		20.30					
latent heat of water evaporation 120°C	kJ/kg	2202.1					
latent heat of vaporization 100°C & 80g/kg	kJ/kg	2076					
Saturated Steam Pressure @ °C (kPa)	kJ/kg	25.04					
Saturated Steam Pressure Brine@ 100 °C	kPa	101.42					
mvc Brine density	kg/m3	1018.98					
ro retent density	kg/m3	1002.2					
MVC Feed Concentration	%	0.00%					
Brine Concentration	%	7.86%					

Latent heat of vaporization of seawater, kJ/kg — **P = P0 (1 atm for t <=100°C. Seawater vapor pressure for t > 100 °C)** — 9

Temp. °C	Salinity, g/kg												
	0	10	20	30	40	50	60	70	80	90	100	110	120
0	2500.9	2475.9	2450.9	2425.9	2400.9	2375.9	2350.8	2325.8	2300.8	2275.8	2250.8	2225.8	2200.8
10	2477.2	2452.5	2427.7	2402.9	2378.1	2353.4	2328.6	2303.8	2279.0	2254.3	2229.5	2204.7	2180.0
20	2453.6	2429.0	2404.5	2379.9	2355.4	2330.9	2306.3	2281.8	2257.3	2232.7	2208.2	2183.7	2159.1
30	2429.8	2405.5	2381.2	2356.9	2332.6	2308.3	2284.0	2259.7	2235.4	2211.1	2186.8	2162.5	2138.2
40	2406.0	2381.9	2357.9	2333.8	2309.7	2285.7	2261.6	2237.6	2213.5	2189.4	2165.4	2141.3	2117.3
50	2382.0	2358.1	2334.3	2310.5	2286.7	2262.9	2239.0	2215.2	2191.4	2167.6	2143.8	2120.0	2096.1
60	2357.7	2334.1	2310.5	2287.0	2263.4	2239.8	2216.2	2192.7	2169.1	2145.5	2121.9	2098.3	2074.8
70	2333.1	2309.8	2286.4	2263.1	2239.8	2216.4	2193.1	2169.8	2146.4	2123.1	2099.8	2076.5	2053.1
80	2308.1	2285.0	2261.9	2238.8	2215.8	2192.7	2169.6	2146.5	2123.4	2100.4	2077.3	2054.2	2031.1
90	2282.6	2259.7	2236.9	2214.1	2191.3	2168.4	2145.6	2122.8	2100.0	2077.1	2054.3	2031.5	2008.7
100	2256.5	2233.9	2211.3	2188.8	2166.2	2143.7	2121.1	2098.5	2076.0	2053.4	2030.8	2008.3	1985.7
110	2229.7	2207.4	2185.1	2162.8	2140.5	2118.2	2095.9	2073.6	2051.3	2029.0	2006.7	1984.4	1962.1
120	2202.1	2180.1	2158.1	2136.1	2114.1	2092.0	2070.0	2048.0	2026.0	2003.9	1981.9	1959.9	1937.9

Table A.4: Heat Exchanger & MVC Data – 100L/hr Excel

Flowchart designation	Description	Units	Value
Air Compressor			
m_Ambient Air	Air flow	kg/hr	115
γ	specific heat ratio of air		1.4
η	Compressor efficiency		0.8
P_(ambient air)	Inlet Air pressure	kPa	100
T_(ambient air)		K	298
v_(ambient air)	Specific Volume of Air @ 25C	m^3/kg	0.8447
P_(ambient comp)	Outlet Air pressure	kPa	250
Conversion factor	kJ/hr - kW		0.000278
T_Ambient comp	Temperature of Air out of Air compressor Ideal	K	387.18
	Temperature of Air out of Air compressor Actual	K	409.48
T_Ambient comp	Temperature of Air out of Air compressor Actual	C	136.48
r_p	pressure compression ratio		2.5
Spray Dryer			
Q_evap	Heat required from dryer	kJ/hr	27142.25
Conversion factor	kJ/hr - kW		0.000278
t_outlet	Temp required coming out	C	115
t_inlet	Temp required coming in (from graph 1)	C	338.2689565
Heat Exchanger			
Hot Stream			
T_Heater Air stream	Inlet Temp of Hot Stream (from combustor)	C	900
P_Heater Air stream	Pressure of Stream coming from combustion	kPa	100
C_P,hot	Heat capacity Hot Stream	kJ/kg°C	1.121
T_Dryer Input	Outlet Temp of Hot Stream to Dryer	C	338.2689565
Cold Stream			
T_Ambient comp	Inlet Temp of Cold Stream (from Compressor)	C	136.4755504
P_Ambient comp	Pressure of Stream coming from Compressor	kPa	250
C_P,cold	Heat capacity Cold Stream	kJ/kg°C	1.013
T_Ambient Heat	Outlet Temp of Cold Stream to Air Turbine	C	758.0949973
LMTD heat exchanger		kW/m^2°C	591.17
U_air heat-ex		kW/m^2°C	1.20
Air Turbine			
γ	specific heat ratio of air		1.33
T_Ambient Heat	turbine inlet temperature	C	758.09
m_Ambient Heat	Air flow into Air Turbine	kg/hr	115.00
P_Ambient Heat	turbine inlet pressure	bar	2.5
C_P, inlet	Heat capacity Air 758C		1.147
T_Amb Turb	turbine outlet temperature - Actual	C	660.2
m_Amb Turb	turbine outlet flow rate	kg/s	115.00
P_Amb Turb	turbine outlet pressure	bar	1.43
Power			
	Turbine power req	kW	3.59
	Turbine power req	kJ/kg	12908.55
Turbine - MVC			
γ	specific heat ratio of air		1.33
T_Amb Turb	turbine inlet temperature	C	660.23
m_Amb Turb	Air flow into Air Turbine	kg/hr	115.00
P_Amb Turb	turbine inlet pressure	bar	1.43
C_P, inlet	Heat capacity Air 660C		1.127
T_Combine Turb	turbine outlet temperature - Actual	C	604.7
m_Amb Turb	turbine outlet flow rate	kg/s	115.00
P_Amb Turb	turbine outlet pressure	bar	1.005008
Power			
	Turbine power req	kW	2.00
	Turbine power req	kJ/kg	7200.00

Table A.5: Air Turbocharger & Heat Exchanger 100L/hr

Temperature K	C_p kJ/kg.K	Temperature C	c_p *(T_1-115)
400	1.013	127	12.156
450	1.020	177	63.24
500	1.029	227	115.248
550	1.040	277	168.48
600	1.051	327	222.812
650	1.063	377	278.506
700	1.075	427	335.4
750	1.087	477	393.494

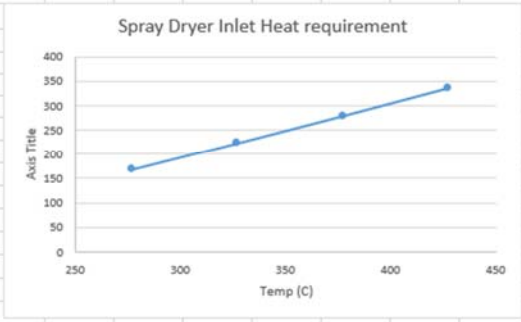

Table A.6: Spray Dryer Inlet Heat Requirement

APPENDIX B

Table B.1: Pilot Plant Daily Power Draw

	HP Pump RO (kW)	Well Pump (kW)	Feed (kW)	Irrigation (kW)	Brine (kW)	Hammer Mill (kW)	Process (kW)	Maximum Draw (kW)
12:00:00 AM	0.105	0.042	0.25		0.82	0.75	0.1	2.067
1:00:00 AM	0.105	0.042	0.25		0.82	0.75	0.1	2.067
2:00:00 AM	0.105	0.042	0.25		0.82	0.75	0.1	2.067
3:00:00 AM	0.105	0.042	0.25	0.44	0.82	0.75	0.1	2.507
4:00:00 AM	0.105	0.042	0.25	0.44	0.82	0.75	0.1	2.507
5:00:00 AM	0.105	0.042	0.25		0.82	0.75	0.1	2.067
6:00:00 AM	0.105	0.042	0.25		0.82	0.75	0.1	2.067
7:00:00 AM	0.105	0.042	0.25		0.82	0.75	0.1	2.067
8:00:00 AM	0.105	0.042	0.25		0.82	0.75	0.1	2.067
9:00:00 AM	0.105	0.042	0.25		0.82	0.75	0.1	2.067
10:00:00 AM	0.105	0.042	0.25		0.82	0.75	0.1	2.067
11:00:00 AM	0.105	0.042	0.25		0.82	0.75	0.1	2.067
12:00:00 PM	0.105	0.042	0.25		0.82	0.75	0.1	2.067
1:00:00 PM	0.105	0.042	0.25		0.82	0.75	0.1	2.067
2:00:00 PM	0.105	0.042	0.25		0.82	0.75	0.1	2.067
3:00:00 PM	0.105	0.042	0.25		0.82	0.75	0.1	2.067
4:00:00 PM	0.105	0.042	0.25		0.82	0.75	0.1	2.067
5:00:00 PM	0.105	0.042	0.25		0.82	0.75	0.1	2.067
6:00:00 PM	0.105	0.042	0.25		0.82	0.75	0.1	2.067
7:00:00 PM	0.105	0.042	0.25		0.82	0.75	0.1	2.067
8:00:00 PM	0.105	0.042	0.25		0.82	0.75	0.1	2.067
9:00:00 PM	0.105	0.042	0.25		0.82	0.75	0.1	2.067
10:00:00 PM	0.105	0.042	0.25		0.82	0.75	0.1	2.067
11:00:00 PM	0.105	0.042	0.25		0.82	0.75	0.1	2.067
	2.52	1.008	6	0.88	19.68	18	2.4	**50.49**
							Average:	2.103666667

APPENDIX C

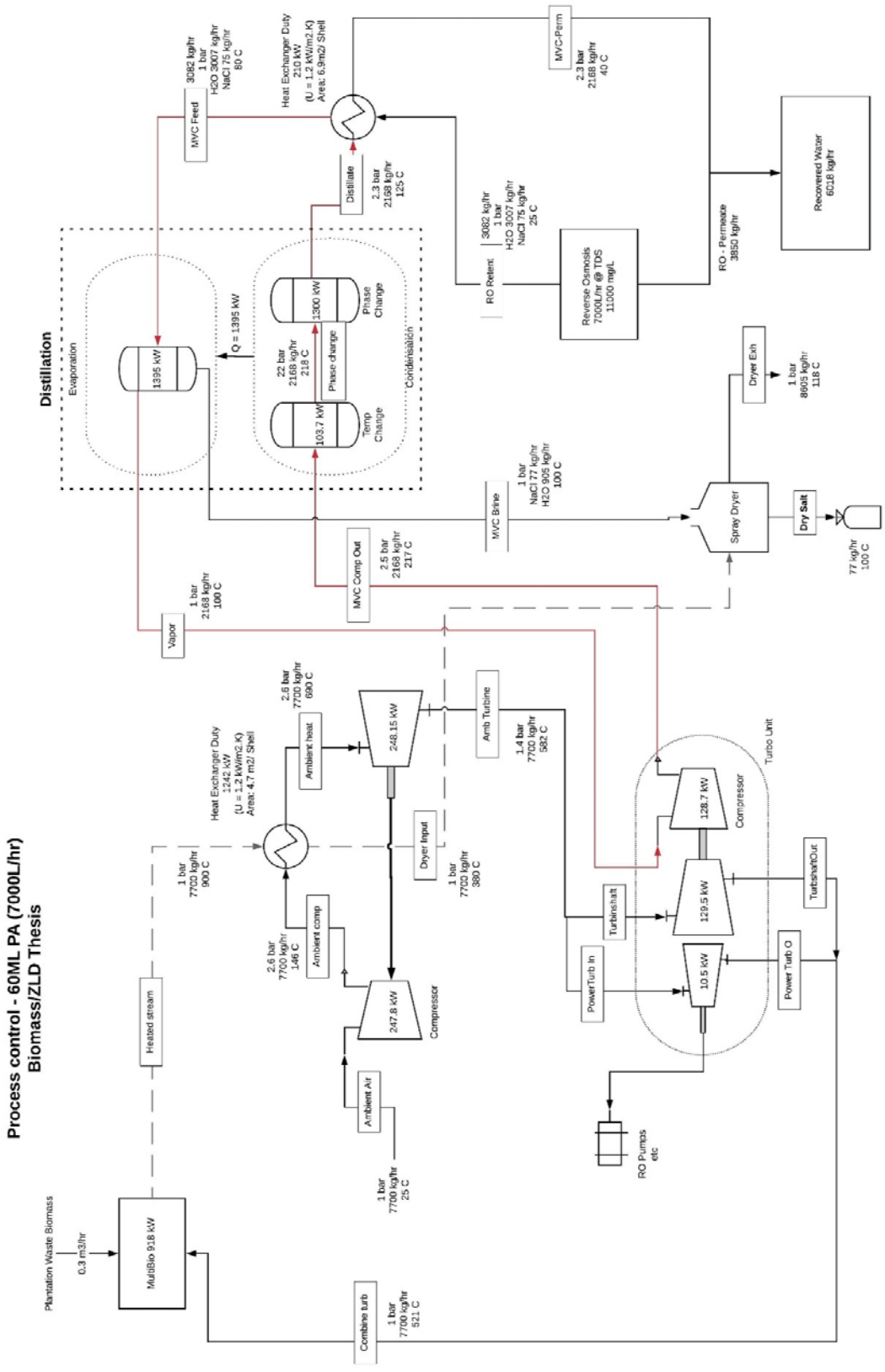

Figure C.1: 60ML Process Control Diagram

APPENDIX D

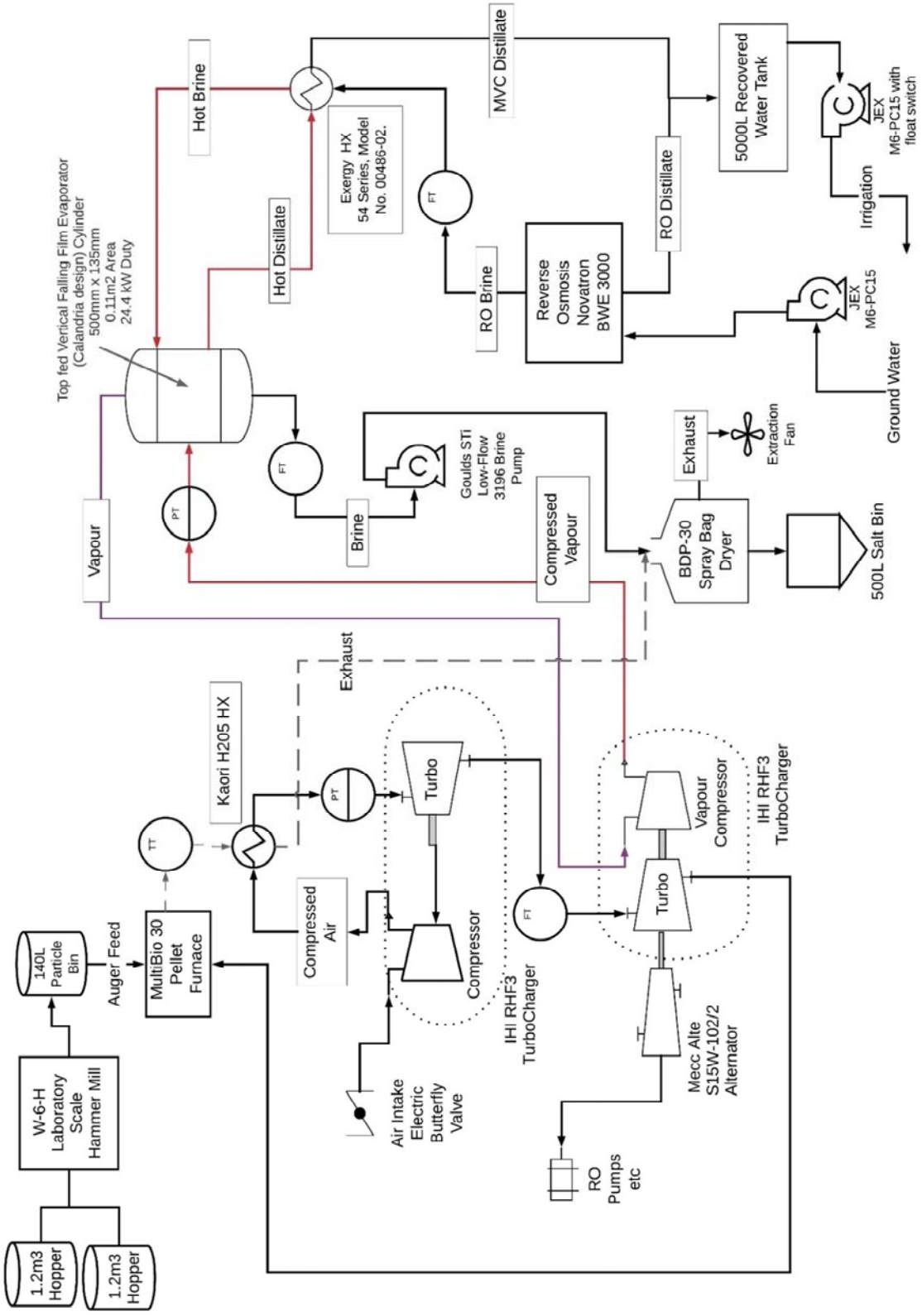

Figure D.1: 120L/hr Pilot Plant Component Flow Diagram

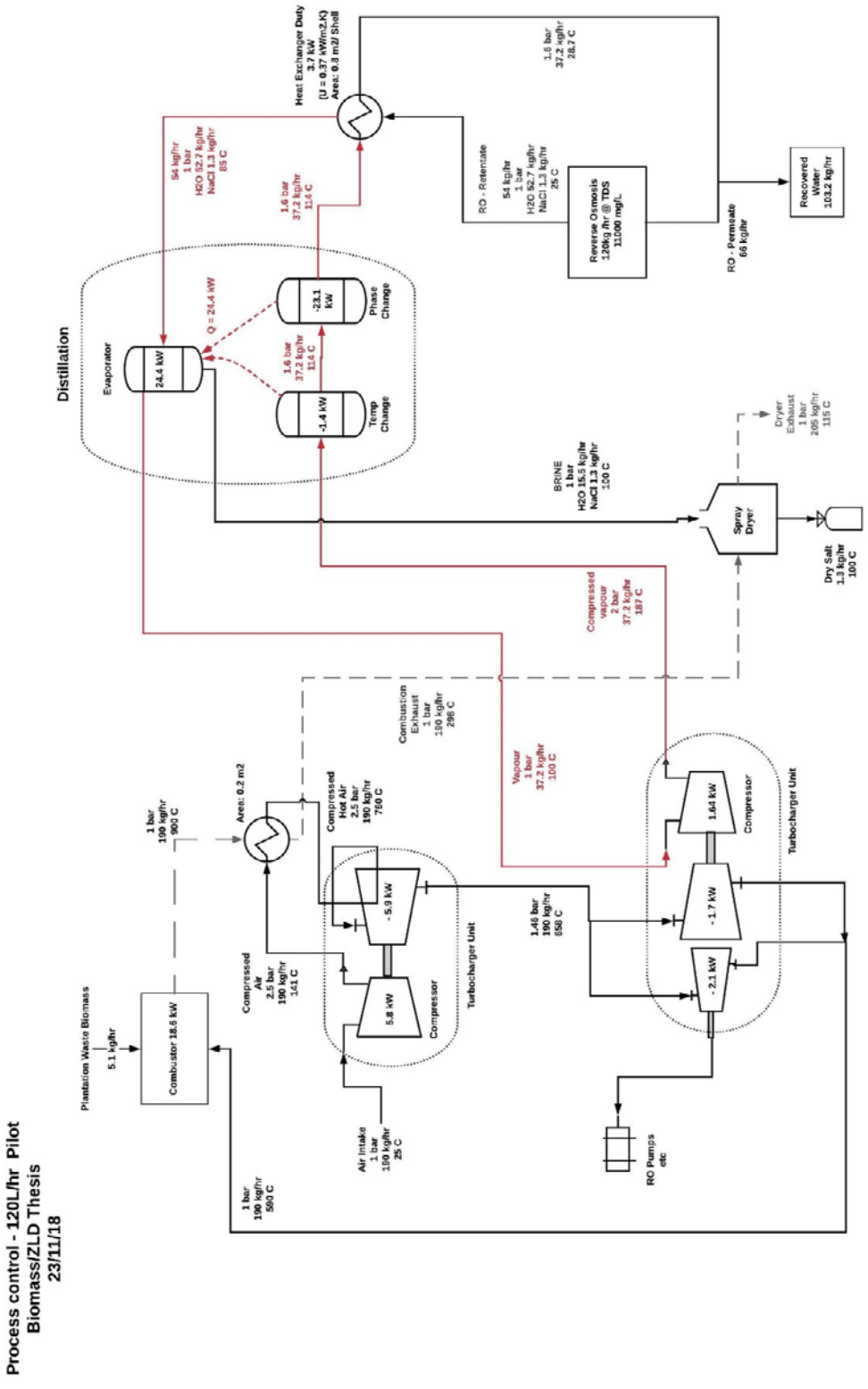

Figure D.2: 120L/hr Pilot Plant Flow Diagram